Universidad Autónoma de Madrid

Departamento de Bioquímica

Pathophysiology of hypoxia: Molecular mechanisms involved in pulmonary hypertension and renal carcinoma.

Tesis doctoral

David Labrousse Arias

Madrid, 2017

Departamento de Bioquímica

Facultad de Medicina

Universidad Autónoma de Madrid

Pathophysiology of hypoxia: Molecular mechanisms involved in pulmonary hypertension and renal carcinoma.

Memoria presentada por el licenciado en Biotecnología:

David Labrousse Arias

para optar al título de Doctor por la Universidad Autónoma de Madrid.

Director de la Tesis: María José Calzada García

Este trabajo se realizó en el Servicio de Inmunología del Hospital Universitario de la Princesa.

Madrid, 2017

María José Calzada García, Doctora en Ciencias Biológicas y Profesora del Departamento de Medicina de la Facultad de Medicina de la Universidad Autónoma de Madrid,

CERTIFICA:

Que David Labrousse Arias, licenciado en Biotecnología por la Universidad de León, ha realizado bajo mi dirección el trabajo de investigación correspondiente a su Tesis Doctoral con el título:

Pathophysiology of hypoxia: Molecular mechanisms involved in pulmonary hypertension and renal carcinoma.

Revisado este trabajo, el que suscribe considera el trabajo realizado satisfactorio y autoriza su presentación para ser evaluado por el tribunal correspondiente.

Y para que así conste y a los efectos oportunos, firma el presente certificado en Madrid a 3 de Marzo de 2017.

Fdo. Dra. María José Calzada García

Que la fuerza te acompañe.

AGRADECIMIENTOS

La ciencia es un trabajo de equipo, por lo tanto, cualquier proyecto, o como en este caso, una tesis doctoral no puede llevase a cabo sin una compleja red de pequeños esfuerzos de un montón de amigos, compañeros y colaboradores. No es postureo, es una realidad, las publicaciones, que son el verdadero motor de la ciencia tienen cientos de momentos en los que se podrían echar a perder, pero siempre hay alguien que da un empujón o una idea clave para que sigan adelante.

Siguiendo con este planteamiento, mi equipo científico comienza por mi jefa, María José Calzada. Es obvio, pero hay que decirlo, muchísimas gracias. Ella me contrató para realizar este trabajo de tesis doctoral, confió en mí y me dio la oportunidad de convertirme en doctor aquí en Madrid, una ciudad estupenda donde tengo gran parte de mi familia y amigos. Ha sido un gusto tenerla como jefa, siempre me ha ayudado en todo y me ha dado muchísima libertad a la hora de enfrentar los proyectos.

Al margen de mi equipo personal, pero esencial, está Francisco Sánchez Madrid, jefe del servicio de Inmunología del Hospital Universitario de la Princesa, donde he realizado todo mi trabajo, un sitio en el que me he sentido como en casa y se me ha tratado estupendamente. Le agradezco enormemente toda ayuda, medios y apoyo recibido para poder desarrollarme sin ataduras. A su lado está nuestra gran secretaría, María Ángeles Vallejo que siempre se ha encargado de que no me faltase de nada.

Quiero darle las gracias de todo corazón a mi compañera, mi flor, una pasada de científica y de mujer, imposible cuantificar su ayuda y apoyo. Ahora de camino a Viena, somos un combo perfecto.

Ahora llega la hora de los profesores y equipo consejero, en primer lugar, tengo que resaltar a Miguel Vicente de “El Norte” al que tengo mucho afecto y le estoy muy agradecido por todos los consejos científicos, así como de todos los chismes y reactivos molones que me ha dado a lo largo de estos años para hacer mis experimentos. Quiero hacer una mención especial para Hortensia de la Fuente por sus consejos y ayuda incondicional hasta horas insospechadas. A Raquel Pimpollo, Alicia Izquierdo y Elena Ramos por ser mis primeras maestras en el mundo del Western blot y técnicas de “High Tech”.

A mis demás compañeros “Hightekianos”, Capitán Hipoxia y Toño, a todos mis pollitos, en especial a Raquel, Javi y el Gallego, todos unos buenos motivados sacando muchísimo trabajo adelante. A mi amigo Japo, que siempre está dispuesto a darte una chapa sobre ciencia y ayudarte con lo que sea. A “el equipo princess”: a los freaks de mis compañeros Álvaro, Rafa, Javi y

Eugenio, nunca me habría imaginado que en el trabajo se pudiera discutir a gusto de cosas tan importantes como la verosimilitud de Harry Potter o el trasfondo de Kylo Ren. A los no frikis también, Rocío y Noelia que aparte de aguantarnos, que no es poco, nos hemos echado buenas risas y cañas para superar largos días de laboratorio. Agradezco también a todo el equipo de novatos que montamos el "Show de los Becarios", creo que hicimos un buen trabajo.

Me parece fundamental darle las gracias a todos los colaboradores que han formado parte de mis publicaciones, en especial a Emma Martínez, Mar y a Julián Aragonés, Ángel Cogolludo y Jeffrey Isenberg. Gracias también a Jeff y a la Dr Rinaman por acogerme en USA.

Por último, agradecer a mi familia y a mis amigos "el equipo original", que, aunque no tienen mucho que ver con mi tesis, también se lo merecen, en especial a mi abuela Paloma.

SUMMARY

SUMMARY

Hypoxia is a well-studied prototype and a paradigm of responses that involve the organism as a whole with different consequences on health and disease. Prolonged generalized hypoxia is the cause of hypoxic pulmonary arterial hypertension (PAH). Conversely hypoxia can also be a consequence during uncontrolled growth of tumors with aberrant blood vessels and thus an insufficient oxygen supply. In this work, hypoxia was treated from two points of view, as the cause in hypoxic PAH or as the consequence of cancer in clear cell renal cell carcinoma (ccRCC).

Hypoxic conditions stimulate pulmonary vasoconstriction and vascular remodeling, both pathognomonic changes in PAH. The secreted protein thrombospondin-1 (TSP1) promotes PAH, but it is largely unknown how hypoxia regulates TSP1 in the lung and whether this contributes to pathological events in PAH. Using a murine model of constitutive hypoxia, gene silencing and luciferase reporter experiments in cells, we found that hypoxia induced pulmonary TSP1 in a HIF2α-dependent manner. Additionally, we found that TSP1 induced migration in pulmonary fibroblasts and PASMC, and increased permeability in PAEC through effects on the cell-matrix and cell-cell interactions. In fibroblasts, TSP1 induced differentiation into a SMC-like phenotype, while in PASMC, TSP1 seems to have a role in the regulation of the potassium channel Kv1.5. In addition, we found in end-stage PAH patients, both TSP1 and HIF2α protein expression increased in pulmonary arteries compared to non-PAH controls. This provides genetic evidence that HIF2α-induced TSP1 contributes to vascular response and remodeling during PAH.

VCAM-1 is an adhesion molecule assigned to the activated endothelium mediating immune cells adhesion and extravasation. However, its expression in renal carcinomas inversely correlates with tumor malignancy. Our studies in ccRCC demonstrated that loss of VHL, hypoxia or PHD inactivation decreased VCAM-1 levels through a transcriptional mechanism that was independent of the hypoxia-induced transcription factor HIF and dependent on the NF-κB signaling pathway. VCAM-1 decreased levels in ccRCC might be relevant to tumor cell immune evasion since this molecule elicited immune cell binding specifically mediated by its interaction with the α4β1 integrin expressed in the immune cells. Furthermore, this interaction made ccRCC cells more sensitive to the cytotoxic effects mediated by activated monocytic cells. Remarkably, in ccRCC human samples with VHL non-missense mutations we observed a negative correlation between VCAM-1 levels and ccRCC stage and microvascular invasion pointing out the clinical value of VCAM-1 levels as a marker of ccRCC progression.

RESUMEN

RESUMEN

La hipoxia es un proceso bien estudiado y un paradigma de respuestas que involucran al organismo como un todo con diferentes consecuencias sobre la salud y la enfermedad. La hipoxia generalizada prolongada es la causa de la hipertensión arterial pulmonar (HAP) inducida por hipoxia. Por el contrario, la hipoxia también puede ser una consecuencia durante el crecimiento descontrolado de tumores con vasos sanguíneos aberrantes y, por tanto, un suministro insuficiente de oxígeno. En este trabajo, la hipoxia se ha tratado desde dos puntos de vista, como causa en HAP hipóxica o como consecuencia en el carcinoma renal de célula clara (ccRCC).

La hipoxia estimula la vasoconstricción pulmonar y el remodelado vascular, cambios patognomónicos en la HAP. La proteína secretada trombospondina-1 (TSP1) promueve la HAP, pero se desconoce cómo la hipoxia regula su expresión en pulmón y si esto contribuye a los eventos patológicos en la HAP. Usando un modelo murino de hipoxia constitutiva, silenciamiento génico y experimentos reporteros, encontramos que la hipoxia inducía TSP1 en pulmón de manera dependiente de HIF2α. Además, se encontró que TSP1 inducía la migración de fibroblastos pulmonares y PASMC, y aumentaba la permeabilidad en PAEC, a través de efectos sobre las interacciones célula-matriz y célula-célula. En los fibroblastos, TSP1 indujo la diferenciación a un fenotipo de tipo SMC y en PASMC TSP1 parece tener un papel en la regulación del canal de potasio Kv1.5. Además, en pacientes en estado terminal de HAP se encontraron altos niveles de TSP1 y HIF2α comparados con controles sanos. Estos resultados proporcionan evidencias genéticas de que la TSP1 inducida por hipoxia contribuye a la respuesta vascular y al remodelado durante la HAP.

VCAM-1 es una molécula de adhesión asignada al endotelio activado que media la adhesión y la extravasación de las células inmunes. Sin embargo, su expresión en carcinoma renal se correlaciona inversamente con tumores malignos. Nuestros estudios en ccRCC demostraron que la pérdida de VHL, la hipoxia o la inactivación de las PHDs disminuían los niveles de VCAM-1 a través de un mecanismo de transcripción que era independiente del factor de transcripción HIF y dependiente de la vía de señalización NF-κB. Los niveles disminuidos de VCAM-1 en ccRCC podrían ser relevantes para la evasión inmune de células tumorales, ya que la interacción de esta molécula con su receptor, la integrina α4β1 expresada en células inmunes, provocó la unión de las células inmunes con las células ccRCC. Además, esta interacción hizo que las células ccRCC fueran más sensibles a los efectos citotóxicos mediados por células monocíticas activadas. Es destacable que en muestras humanas de ccRCC con mutaciones sin sentido en *vhl* se observó una correlación negativa entre los niveles de VCAM-1 y el estadio de ccRCC y la invasión microvascular señalando el valor clínico de los niveles de VCAM-1 como marcador de progresión de ccRCC.

INDEX

INDEX

ABBREVIATIONS

ABBREVIATIONS

5-HT: Serotonin or 5-hydroxytryptamine

Ach: Acetyl choline

Akt (PKB): Protein kinase B

ANOVA: Analysis of variance

ARD: Ankyrin repeat domain

ARD1: Acetyl-transferase named arrest-defective 1

ARNT: Aryl receptor nuclear translocator

ATF4: Activating transcription factor 4

ATP: Adenosine triphosphate

BAFF: B-cell activating factor

bHLH: Basic-helix-loop-helix

BIMEL: Bcl2-interacting mediator of cell death extra long

BKca: Big potassium channel

C-TAD: C-terminal transactivation domain

cAMP: Cyclic adenosine monophosphate

CB: Carotid body

CBP: Creb binding protein

ccRCC: Clear cell renal cell carcinoma

CDK8: Cell division protein kinase 8

cGMP: Cyclic guanosine monophosphate

CLARITY: Clear Lipid-exchanged Acrylamide-hybridized Rigid Imaging

CNN-1: Calponin 1

CO: Cardiac output

COPD: chronic obstructive pulmonary disease

CTEPH: Chronic thromboembolic pulmonary hypertension

Cul2: Cullin 2

DAPI: 4',6-diamidino-2-phenylindole

DMOG: Dimethyloxalylglycine

DNA: Deoxyribonucleic acid

DPO1: Diphenylphosphine oxide

E-box: Enhancer box

EC: Endothelial cells

EGF: Epidermal growth factor

EGTA: Ethylene glycol-bis(β-aminoethyl ether)-N,N,N',N'-tetraacetic acid)

eNOS: Endothelial nitric oxide synthase

EPAS: Endothelial PAS

EPO: Erythropoietin

ERK: Extracellular signal–regulated kinase

ET-1: Endothelin 1

ETC: Electron transport chain

F-Actin: Filamentous actin

FA: Focal adhesion

FAK: Focal adhesion kinase

FIH: Factor inhibiting HIF1α

FITC: Fluorescein isothiocyanate

FoxM1: Forkhead box M1

GF: Growth Factor

GFR: Growth Factor Receptor

GLUT-1*:* Glucose transporter 1

HGB: Haemangioblastomas

HIF: Hypoxia inducible factor

hnRNA: Heterogeneous nuclear RNA

Hp: Hypoxia

hPAEC: human pulmonary artery endothelial cells

HPV: Hypoxic pulmonary vasoconstriction

HRE: Hypoxia response elements

HUVEC: Human umbilical vein endothelial cells

ICAM-1: Intercellular adhesion molecule 1

IF: Immunofluorescence

Ig: Immunoglobulin

IGF2: Insulin-like growth factor 2

IKK: Inhibitor of NF-κB kinase

IL-1β: Interleukin 1 beta

IL1: Interleukin 1

Kca: Calcium-activated potassium channels

Km: Michaelis-Menten constant

Kv: Potassium voltage dependent channels

LTβ: Lymphotoxin beta

MAC-1: Macrophage-1 antigen

MAPK: Mitogen-activated protein kinase

MEK: Mitogen-activated protein kinase kinase

mFIB: Mouse lung fibroblast

MLC: Myosin light-chain

MLCK: Myosin light-chain kinase

mPASMC: Mouse pulmonary artery smooth muscle cells

mRNA: Messenger ribonucleic acid

mTOR: Mammalian target of rapamycin

N-TAD: N-terminal transactivation domain

NADH: Nicotinamide adenine dinucleotide

NDUFA4L2: NADH dehydrogenase (ubiquinone) 1 alpha subcomplex, 4-like 2

NF-κB: Nuclear Factor Kappa-Light-Chain-Enhancer of Activated B Cells

NIK: NF-κB-inducing kinase

NO: Nitric Oxide

NRE: NF-κB response elements

NSCC: Non-selective cationic channels

Nx: Normoxia

Oct4: Octamer binding factor 4

ODDD: Oxygen-dependent

degradation domains

p53: Tumor protein p53

PA: Pulmonary artery

PAEC: Pulmonary artery endothelial cells

PAFIB: Pulmonary artery fibroblast

PAH: Pulmonary artery hypertension

PAI-1: Plasminogen activator inhibitor 1

PAPm: Pulmonary artery pressure mean

PAPsys: Systolic pulmonary artery pressure

PAS: Pax/Aryl hydrocarbon receptor/Sim

PASMC: Pulmonary artery smooth muscle cells

PCC: Pheochromocytomas

PGI2: Prostaglandin 2

PH: Pulmonary Hypertension

PHD: Prolyl hydroxylase domain protein

PI3K: Phosphatidylinositol-4,5-bisphosphate 3-kinase

PKA: Protein kinase A

PKG: Protein kinase G

PKM2: Pyruvate kinase M2 isoform

PTEN: Phosphatase and tensin homolog

PVR: Pulmonary vascular resistance

RA: Right atrium

RCC: Renal cell carcinoma

ROS: Reactive oxygen species

RT-Q-PCR: Real time quantitave Polymerase chain reaction

RV: Right ventricle

Scr: Scrambled

SEM: Standard error of the mean

siRNA: Silencing RNA

SIRT6: Sirtuin 6

SMA: Smooth muscle actin

SMC: Smooth muscle cells

SU: Sugen 5416 (Semaxanib)

TGB-β: Tumor growth factor beta

TLR: Toll like receptor

TNFα: Tumor necrosis factor alpha

TSP1: Thrombospondin 1

TSR: Thrombospondin type I repeat or Properdin like domain

TXA2: Thromboxane 2

VCAM-1: Vascular cell adhesion molecule 1

VDCC: Voltage-dependent calcium channels

VEC complex: VHL enlongin cullin complex

VEGF: Vascular endothelial growth factor

VEGFR: Vascular endothelial growth factor receptor

VHL: Von Hippel Lindau

VLA-4: Very late activation antigen 4

WHO: World Health Organization

β2AR: β2-subtype adrenergic receptor

FIGURES AND TABLES

FIGURES AND TABLES

1. INTRODUCTION

2. RESULTS

2.1 HYPOXIA AND PULMONARY HYPERTENSION: HYPOXIC REGULATION OF TSP1 AND ITS EMERGING ROLE IN PULMONARY HYPERTENSION

2.2 HYPOXIA AND CANCER: IMPACT OF HYPOXIA AND VHL LOSS ON THE REGULATION OF VCAM-1 AND ITS EFFECTS ON THE IMMUNE EVASION OF RCC

3. DISCUSION

4. TABLES

INTRODUCTION

INTRODUCTION

HYPOXIA, GENERAL LINES AND MECHANISM OF CONTROL

The term hypoxia is defined as a deficiency in the amount of oxygen that reaches the tissues of the body. It differs from hypoxemia, which means an inadequate amount of oxygen traveling in the blood. Hypoxia may affect the whole body, when is generalized, or a specific organ or tissue, then is considered tissue hypoxia or local hypoxia. Generalized hypoxia may occur under different conditions, these including high altitude, when people breathe air with displaced oxygen due to a chemical process or treatment, due to respiratory problems, deficiencies in blood flow or insufficient hemoglobin (known as anemia), all of them leading to a decrease in the partial pressure of oxygen and hypoxemia. Conversely, local hypoxia occurs when a tissue is not properly perfused, generally due to blood irrigation problems. The most common cases are hemorrhages or vascular obstructions, such cerebral ischemia, myocardial stroke or in inflammatory foci. In addition, local hypoxia is present in the core of solid tumors, being this considered a hallmark of tumor progression (Figure 1). Hypoxia can also be acute or chronic, with acute meaning a rapid onset, and chronic meaning that hypoxia has been ongoing for long time. Although hypoxia is considered a physiopathological event, low oxygen levels are a common feature under physiological conditions such as embryonic development [1], physical exercise [2] or in specific microenvironments such as the stem cell niche [3].

In mammals, the oxygen passively diffuses from the breathed air to the arterial blood. This process takes place in the lung alveoli, the minimal structure for gases interchange, according to a pressure gradient. Once in the blood, oxygen is transported by the hemoglobin in red blood cells and delivered to the tissues, where it reaches the cells by passive diffusion. Cells use the oxygen to generate energy in form of adenosine triphosphate (ATP) by the oxidative phosphorylation in the mitochondria. During the aerobic respiration, the mitochondria generates ATP by oxidizing glucose products, pyruvate and NADH. When oxygen is limited, the glycolytic products are metabolized by anaerobic fermentation, an independent and less efficient mitochondrial process. Furthermore, during hypoxia, hydrogen is shifted to pyruvic acid producing lactic acid, switching the cell to an anaerobic metabolism. This response is mainly mediated by the hypoxic inducible factors (HIFs), which also regulates several cellular mechanisms to hypoxic adaptation as angiogenesis in order to improve blood flow and oxygen support (Figure 1).

Systemic Response to Hypoxia

As oxygen is absolutely essential for complex organisms, they have developed different

physiological responses that permit adaptation to a hypoxic environment. The Carotid body through the release of neurotransmitters increases respiration and cardiac rate. The medulla oblongata in the brain measures the partial pressure of CO_2 and H^+ and integrates signals from carotid body and other parts of the body increasing respiration and cardiac rate. The pulmonary arteries suffer a vasoconstriction to redirect blood flow to alveoli with higher oxygen content. Conversely a systemic vasodilatation occurs to help blood flow to reach the whole body. In addition, the kidneys response increasing erythropoietin (EPO) levels (Figure 1).

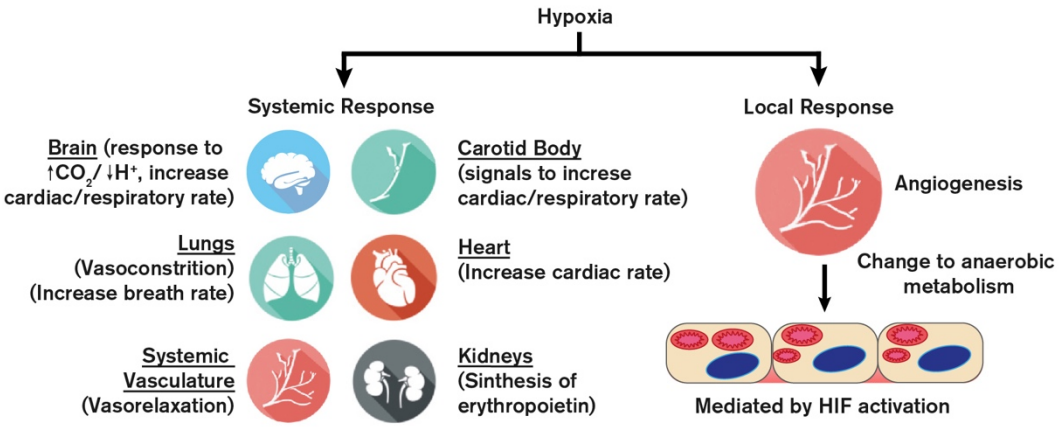

Figure 1: Scheme of systemic and local responses to hypoxia.

Carotid Body Response

Carotid body (CB) is a small arterial chemoreceptor located at the bifurcation of the carotid artery. Its function is to detect changes in blood oxygen levels and activate the respiratory center to allow the correct adaptive ventilatory response. The CB is composed of functional units named glomeruli, which are clusters of cells separated by a profuse network of small capillaries and connective tissue. It is thought that mitochondria produce reactive oxygen species (ROS) and reduced pyridine nucleotides under hypoxia. These molecules lead to cell depolarization, calcium entry, and neurotransmitters release, which activate the afferent fibers of the sinus nerve. [4-6]. This ion cascade ends releasing dopamine to the next afferent nerve producing an increase in respiration and cardiac rate (Figure 1).

Erythropoietin production

Erythropoietin (EPO) is produced by interstitial fibroblast in the kidney in close association with peritubular capillary and proximal convoluted tubule and in perisinusoidal cells in the liver. While liver production predominates in the fetal and perinatal period, kidneys are the main physiologic site of EPO synthesis during adulthood. Under hypoxia these organs increase the levels of EPO

[7, 8]. The increase on EPO levels contributes to heighten the levels of red blood cells aimed to compensate the decrease of oxygen in the tissues [9] (Figure 1).

Vascular adaptation to hypoxia

In response to hypoxia most of the vessels of the body have a vasodilatory response aimed to increase oxygen supply. Conversely, the lungs response to hypoxia with vasoconstriction, also called hypoxic pulmonary vasoconstriction (HPV) (Figure 1). It is thought that the first signals for general hypoxic vasodilation and hypoxic pulmonary vasoconstriction could be the same, and that their effect depends on the cellular type and localization. Nevertheless, the effects are completely opposed [10, 11]. **Vasodilation** is the process of blood vessels widening which increases perfusion by decreasing vascular resistance. It is leaded by the relaxation of the smooth muscle cells (SMC) within the tunica media of the vessels walls of arteries, arterioles and large veins. The vascular tone depends on the intracellular calcium ion concentration, which is closely linked with phosphorylation of the light chain of the contractile protein myosin. Therefore, vasodilation occurs after lowering intracellular calcium concentration or by dephosphorylation of myosin in SMC [12, 13]. Although hypoxic vasodilation very first events are endothelium-independent [14], endothelial cells regulate vascular tone in prolonged hypoxia as well as in physiological conditions. There are two main endothelial-dependent vasodilation pathways: via cGMP and via cAMP. This two molecules can modulate several targets including multiple calcium, potassium and ATPase channels, myosin light-chain kinase (MLCK) or Rho kinase, among others. The response varies between different cell types and species. One main example of each pathway is described below:

1. Via cGMP: E.g. Nitric oxide (NO) activates soluble guanylate cyclase, which catalyzes the formation of cyclic guanosine monophosphate (cGMP), this activates protein kinase G (PKG) causing the reuptake of calcium and the opening of calcium-activated potassium channels (Kca) as big potassium channel (BKca). The opening of Kca channels causes membrane hyperpolarization and the close of voltage-dependent calcium channels (VDCC) [15, 16], which in turn decreases the intracellular calcium concentration [17]. In these conditions, MLCK can no longer phosphorylate the myosin molecule, thereby stopping the crossbridge cycle and leading to relaxation of the SMC.

2. Via cAMP: Direct modulation of MLC phosphorylation. Some vasodilators as prostaglandins (e. g. PGI2) trigger the activation of adenylate cyclase, increasing cyclic adenosine monophosphate (cAMP), which activates protein kinase A (PKA) that subsequently inhibits MLCK by phosphorylation [18]. Dephosphorylated myosin light chain (MLC) cannot continue the crossbridge cycle and therefore SMC falls into relaxation [19, 20].

Hypoxic pulmonary vasoconstriction (HPV), also known as the von Euler–Liljestrand mechanism, is a physiological phenomenon that happens in pulmonary arteries under hypoxia. HPV achieves to redirect blood flow to alveoli with more oxygen, improving gaseous exchange. HPV is activated at a partial pressure of oxygen (PO_2) of 100 mmHg (13.3 kPa), which is equivalent to an altitude of approximately 3700 meters. Pulmonary arterial smooth muscle cells (PASMC) contract in response to hypoxia at a PO_2 of 25–50 mmHg (3.33–6.66 kPa) [21] in an endothelium-independent manner [22]. Intracellular calcium increases by the influx of extracellular calcium and the release of intracellularly stored calcium from the endoplasmic reticulum and mitochondria [23]. There are multiple components generally accepted in the calcium enhancement mechanism; L-type calcium channels, potassium voltage dependent channels (Kv), non-selective cationic channels (NSCC) (e.g. TRP channels) and Rho-kinase involved that could be activated sequentially or in parallel during HPV [23-25]. When hypoxia is maintained for long periods (hours, days or months), as it occurs at high altitude or during respiratory diseases, these including chronic obstructive pulmonary disease (COPD), sleep apnea, fibrosis, or failure of ventilation due to neurological diseases, HPV produces vascular remodeling processes with subsequent pulmonary arterial hypertension and finally right heart hypertrophy and cor pulmonale [24].

Cellular response to hypoxia: Oxygen sensing machinery

Oxygen supply is essential for aerobic organisms to generate energy. In order to overcome the insufficient oxygen availability, mammals have also developed cellular adaptive responses to match oxygen supply with metabolic, bioenergetics, and redox demands. Cells may stop cell cycle, decrease energy consumption and generate survival and proangiogenic factors. All these actions are orchestrated by cellular pathways like mammalian target of rapamycin (mTOR), unfolded protein response or gene regulation by HIFs, which were initially described as regulators of EPO production and nowadays they are considered the most important genetic factors in response to hypoxia.

Hypoxia inducible factors

HIFs are a family α/β-heterodimeric transcription factors that regulate the expression of hundreds of genes in a tissue context-dependent manner. These transcription factors are heterodimers composed of a constitutively expressed beta subunit (HIFβ), also known as aryl receptor nuclear translocator (ARNT) and an oxygen-regulated α subunit (HIFα). In mammals, there are three different alpha isoforms of HIFα: HIF1α /MOP1, HIF2α/EPAS (endothelial PAS)/MOP2 and HIF3α (IPAS), being HIF1α and 2α the most studied isoforms. Both subunits belong to the basic-helix-loop-helix (bHLH) family of transcription factors containing a Pax/Aryl hydrocarbon

receptor/Sim (PAS) domain [26-29]. HIF1α and HIF2α subunits also carry N- and C-terminal transactivation domains (N-TAD and C-TAD) that are required for the activation of HIF target genes. The C-TAD domain interacts with coactivators such as CBP/p300 to activate gene transcription [30]. An oxygen-dependent degradation domains (ODDD) within these alpha subunits confer oxygen-regulated turnover as it contains the key asparagine (N) and proline (P) residues targeted for hydroxylation in normoxic conditions [31-35]. HIFα subunits heterodimerize with HIFβ by their bHLH and PAS domains [36]. Transcriptionally active HIF heterodimers get into the nucleus and bind to hypoxia response elements (HREs) in the chromatin, (Figure 2). These HRE are DNA consensus sequences containing a conserved core with G/ACGTG, which is similar to the Enhancer box (E-box) to induce adaptive hypoxic genes [37]. Comparatively much less is known about HIF3α, although is also regulated by oxygen [38]. HIF3α is considered a negative regulator of hypoxia-inducible genes [39].

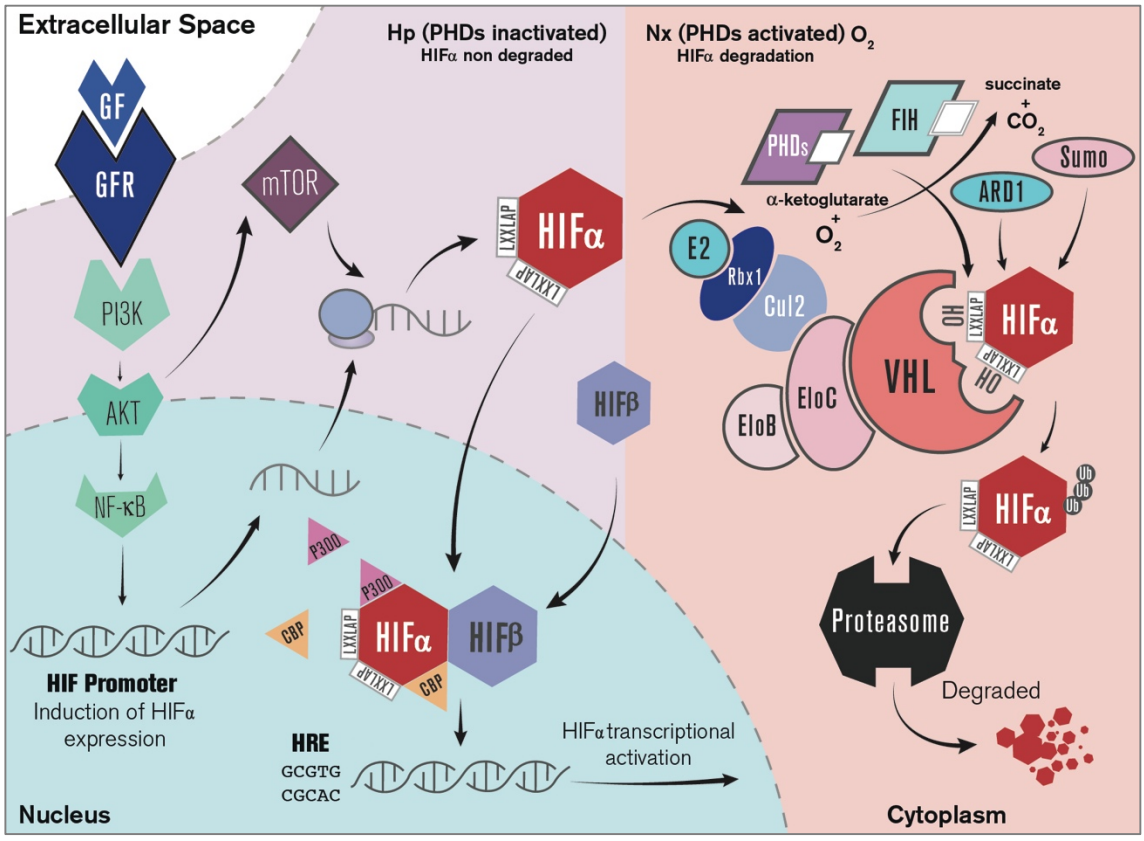

Figure 2: Simplified scheme of signaling networks in the regulation of HIF. Classical and some alternative regulations of HIF under normoxia or hypoxia are represented.

Isoform-specific genetic regulation of HIFα

Despite HIF1α and HIF2α recognize the same HRE sequences, they can induce equal or differential gene expression in a context-dependent manner. Different cell type, severity, association with regulatory proteins, duration and variety of stimulation as well as the presence of functional VHL could shift the transcriptional regulation between HIF1α and HIF2α [37, 40, 41]. HIF1α is ubiquitously expressed while HIF2α is predominantly expressed in the lung, endothelium, and carotid body [42-44]. Several pieces of evidence support a temporal organization of HIF1α and HIF2α-dependent responses. Under acute hypoxia transactivation of target genes is primarily mediated by HIF1α, while during longer hypoxic insults HIF2α becomes more relevant [40, 45]. HIF1α is the main activator of glycolytic genes, allowing cells to adapt to low oxygen by switching the oxidative phosphorylation to anaerobic glycolysis (also known as Warburg Effect) [46-50]. At the same time, HIF1α down-regulates oxidative phosphorylation through a range of actions on mitochondrial metabolism and biogenesis. For instance, the activity of mitochondrial complex I is inhibited by HIF1α-mediated activation of NDUFA4L2 [51]. Meanwhile, HIF2α plays preferably a role in the expression of genes involved in pluripotent stem cell maintenance [52, 53], and angiogenesis [54]. Therefore, the effects of HIFα are complex and involves the activation of several adaptive pathways that may in turn require the expression of a specific set of genes [45, 55-57] (Figure 3).

Hypoxic inducible factors regulation

As the main orchestrators in the response to hypoxia, the expression of HIFs is tightly regulated. In normoxic conditions, two proline residues found at aminoacid positions 402 and 564 in HIF1α and, 405 and 531 in HIF2α, located within the oxygen-dependent degradation domain (ODDD) [58, 59] are hydroxylated by a family of oxygen–dependent dioxygenases termed PHD (for prolyl hydroxylase domain containing proteins) [60, 61]. Prolyl hydroxylation promotes HIFα interaction with the von Hippel-Lindau protein (VHL) [62], which promotes polyubiquitination and thereby targeting the HIFα protein for degradation by the 26S subunit of the proteasome [63, 64]. Under hypoxia, PHD activity is significantly decreased, HIFα is not degraded and therefore heterodimerizes with HIFβ promoting the expression of hypoxic genes [37, 39, 57, 65] (Figure 3).

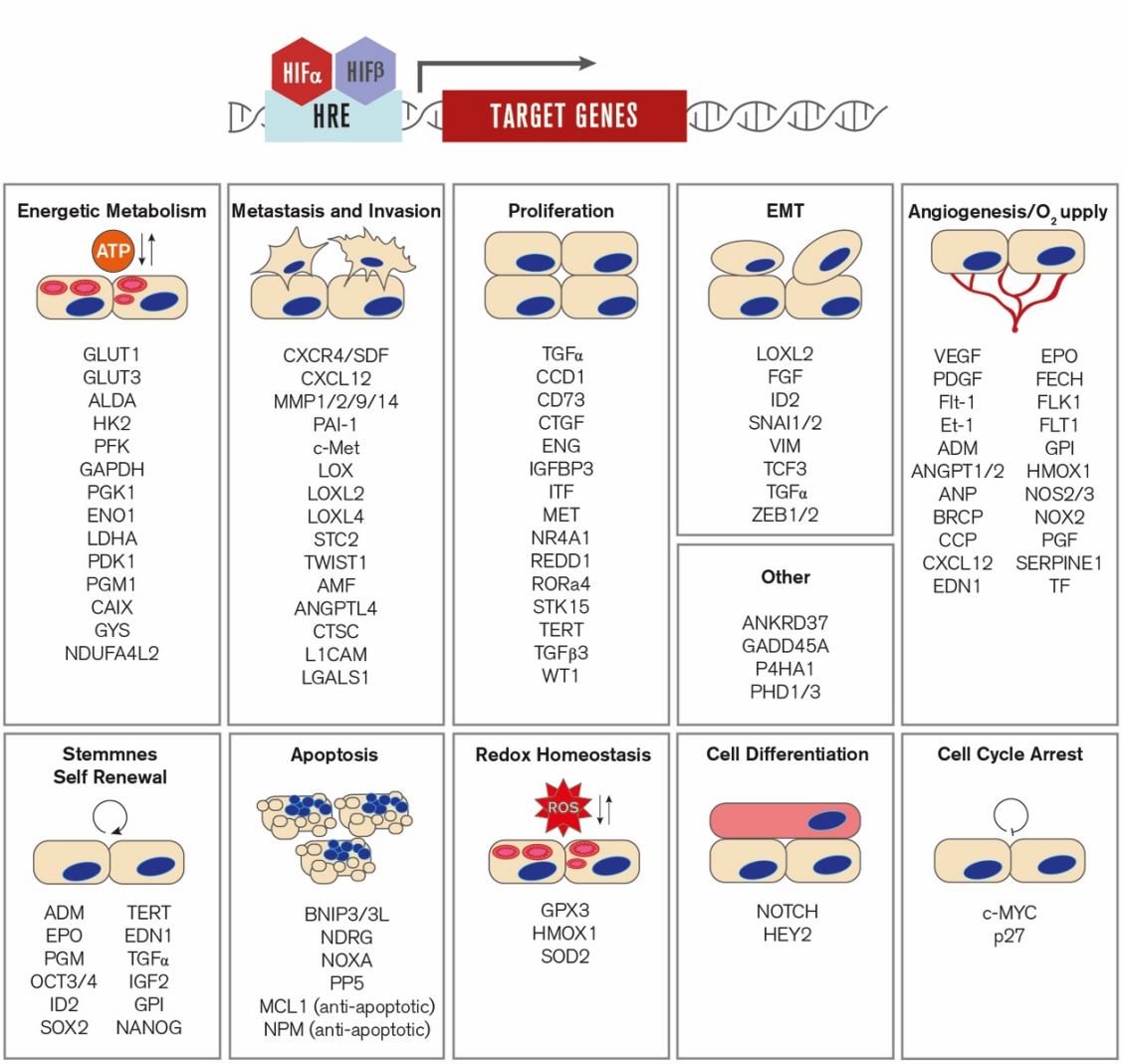

Figure 3: HIF target genes in several adaptive pathways. Figure modified from Dengler *et al* 2014 [37].

Von Hippel Lindau protein

VHL is a tumor suppression protein encoded by the gen *vhl*. It was described in 1894 by Treacher Collins, although its name was given by the german ophthalmologist Eugene von Hippel and the Swedish pathologist Arvid Lindau, who studied retinal and cerebellar disease lesions one decade later [66]. Two isoforms with functional activity have been reported, with 213 or 160 aminoacids length each, and molecular weights of 30 and 19 kDa respectively [67]. Mutations in the germline of the *vhl* gene are the basis of familial Von Hippel Lindau disease, a dominantly inherited cancer syndrome predisposing to a variety of tumors as kidney, pancreas, brain or eye. One mutation alone is not sufficient to alter VHL function, but when the second allele of *vhl* is mutated it may promote carcinomas. Germline mutations of the VHL gene are now identified in more than 95% of the patients with clinical manifestations of the disease [68]. The largest group of mutations accounting for about 50% of cases is represented by missense mutations. In about 30% of the

cases, deletions that remove one or more exons of VHL are observed and usually arise from *Arthrobacter luteus (Alu)* restriction endonuclease-mediated recombination [69]. Remaining mutations consist in nonsense mutations, splicing sites mutations, microinsertions or microdeletions leading to truncated proteins [62]. Therefore, nature of the mutation in the *vhl* gene leads to phenotypic manifestations in the pattern of cancer that develops. Nonsense mutations or deletion have been linked to type 1 disease, which is the most frequent form of all and is mostly characterized by the development of haemangioblastomas (HGB) and renal cell carcinomas (RCC), with a low risk of pheochromocytomas (PCC). Type 2 VHL has been linked to missense mutations and it has been further subdivided based on the risk to develop RCC. Type 2A families are affected by the presence of HGB and PCC with a low risk of RCC; type 2B by the presence of HGB, PCC and high risk of RCC; and type 2C only by the presence of PCC [70]. Patients with type 3 disease are affected by Chuvash polycythaemia, a heritable disease linked to homozygous or compound heterozygous VHL mutations [71]. These patients are characterized by elevated hematocrit and increased serum levels of erythropoietin and vascular endothelial growth factor (VEGF), but do not develop any of the other usual features of VHL disease. In types 1, 2A, 2B and 3 the mutant VHL is defective in HIF regulation, while type 2C mutant are defective in protein kinase C regulation and fibronectin assembly [62].

VHL protein is composed by an α domain implicated in the formation of a multi-subunit complex and a β domain that mediates substrate recognition. VHL forms part of an ubiquitin-ligase E3 complex known as the VEC complex, together with Elongin B, Elongin C, Cullin2 (Cul2) and Rbx1 (also known as ROC1/Hrt1). Elongin C is in the core of the complex, binding VHL, Cul2 and Elongin B [72]. Cul2 acts as a bridge associating Rbx1 to Elongin C. VHL interacts with Elongin C through amino acids 157-170 in the α domain and with HIF1α through amino acids 67-117 in the β domain, mutations in these regions are extremely relevant for VHL syndrome [73]. This VHL-E3 complex works as polyubiquitination machine, once a protein is ubiquitinated, it is degraded by proteasome [72, 74, 75] (Figure 2, right side). Although VHL main role is to label proteins for degradation, as HIFα and other targets like MAPK1 [76], in few special cases it has been observed that VHL has an opposite role increasing half-life of proteins such as the Bcl2-interacting mediator of cell death extra long, (BIMEL) [77], p53 [78] and Jade-1 [79, 80]. Moreover, it has been recently published that VHL can protect HIF1α from SART1-mediated degradation in clear-cell renal cell carcinoma (ccRCC) [81]. In addition to protein degradation and stabilization functions, VHL has been shown to play an important role in the maintenance of cell morphology [82, 83] through HIF-dependent or HIF-independent mechanisms [84-86].

Inactivation of VHL impairs HIFα degradation and this promotes inappropriate activation of downstream target genes that directly contribute to tumorigenesis. Consistent with the notion that

regulation of HIFα is the key in the tumor suppressor function of VHL, a large proportion of VHL mutations-associated diseases have been predicted and demonstrated to significantly impair the interaction between VHL and HIF [66, 87, 88]. However, in the absence of VHL, the stabilization of HIF is not the unique mechanism to promote tumor growth. VHL is closely involved with the regulation of energy and homeostasis during tumor progression, maintenance of the epithelial phenotype of renal tubular cells, and regulation of extracellular matrix degradation and homeostasis [89-91]. Studies of HIF-independent functions of VHL in cancer have shown that VHL expression abolishes the activation of the canonical Nuclear Factor Kappa-light-chain-enhancer of activated B cells (NF-κB) pathway and the induction of anti-apoptotic genes in those cells [92-94]. Cummins *et al* have demonstrated that VHL interacts with IKKs in a PHD-dependent manner [95]. Taking into account the multiple loose ends and the increasing complexity of NF-κB pathway, the molecular mechanisms underlying VHL-mediated suppression of NF-κB need to be more deeply studied.

Prolyl hydroxylase domain proteins

PHDs are a family of prolyl hydroxylase domain proteins, which main role is to hydroxylate prolines residues. These enzymes require iron, α-ketoglutarate (2-oxoglutarate), ascorbate and molecular oxygen for their catalytic activity. There are three isoforms of PHDs: PHD1, PHD2 and PHD3, also known as HIFαP4Hs (HPHs)3, HIFαP4Hs (HPHs)2 and HIFαP4Hs (HPHs)1 or EGLN2, EGLN1 and EGLN3 respectively. Although PHD2 has a dominant role controlling the levels of HIF1α [96], all PHD isoforms contribute to the regulation of HIF in a cell-specific way [61]. During the prolyl hydroxylation reaction, α-ketoglutarate is oxidatively decarboxylated to produce succinate and CO_2 i.e. PHDs incorporates one atom of oxygen from dioxygen molecule (O_2) into the hydroxylated proline and the other into the succinate [97]. Ascorbate (vitamin C) recovers active PHD state through the reduction of the inactive iron (III) to the active iron (II) [98, 99]. They mainly hydroxylate prolines in LXXLAP protein motifs as in HIFα [58], although, they can also hydroxylate prolines in alternative protein motifs [100-102].

PHDs also interact with key components of the NFκB pathway. For instance, PHD1 hydroxylates IκB kinases (IKKs) under normoxia [95]; PHD2 controls TNF-α effects by positively regulating NF-κB signaling [103]; and PHD3 serves as a co-activator of NF-κB signaling activity [104]. PHDs also interact with other factors such as the activating transcription factor 4 (ATF4) [105]. ATF-4 was shown to interact with PHD3, but not with PHD1 or PHD2. Like HIFα, ATF4 is stabilized by PHD inhibitors, hypoxia, and proteasome inhibitors. The interaction was mapped to a portion of the zipper II domain, which contains five proline residues, although none are within an LXXLAP motif. As well as ATF4, β2-subtype adrenergic receptor (β2AR) is hydroxylated by

PHD3 in prolines that are not located in LXXLAP motif. Hydroxylation of proline residues in β2AR promotes the binding of pVHL-E3 ligase, and consequently degradation by the proteasoma [102]. Because of their oxygen dependence, and the fact that they have a Km value for oxygen greater than the concentration of molecular oxygen in tissues [106], which allows the enzymatic activity to report on oxygen concentrations along the physiological range, PHDs have been proposed to be "oxygen sensors". However, studies inhibiting components of the electron transport chain (ETC) have shown that mitochondria stimulate the production of cellular ROS, which inhibit PHD activity and HIFα degradation [107-109]. Therefore, the mitochondria can also participate in oxygen sensing, although the notion of mitochondria as "oxygen sensor" is still controversial, and many questions remain still unanswered.

Alternative mechanisms in the regulation of HIF

Although the Hypoxia/VHL/PHDs axis is considered the canonical pathway in HIF regulation, there are a number of alternative mechanisms that can regulate HIF. These mechanisms can regulate its transactivation or their interaction with other transcription factors or cofactors. They can also affect HIF protein stabilization by post-translational modifications as in the canonical pathway or even control HIF abundance through post-transcriptional or transcriptional regulation. Alternative post-translational regulations include modifications that affect HIF transactivation activity, as that mediated by factor inhibiting HIF1α (FIH1), an asparaginyl hydroxylase that hydroxylates the asparagine Asn803 or Asn847 within the C-TADs of HIF1α or HIF2α respectively, thereby disrupting the interaction with the coactivator CBP/p300 and the transactivation potential of these factors [110, 111]. Acetylation of HIF by the acetyl-transferase named arrest-defective-1 (ARD1) or SUMOylation are post-translational modifications that affect HIF protein stability [112, 113] (Figure 2, right side). In addition, changes on HIF phosphorylation have been shown to regulate both, transactivation and HIFα stability [114-117].

Functional analysis revealed that there is an interplay between HIFs and other transcription factors that cooperate to fine-tune the expression of HIF target genes [37, 41]. These cofactors include members of the p160 family of coactivators [118], the pyruvate kinase M2 isoform (PKM2) [101, 119], mediator-associated kinase (CDK8) [120] or Sirtuin-6 (SIRT6) [121]. Other stimulus may also induce HIF1α mRNA levels through transcriptional mechanisms. For instance, transcription factors such NF-κB and Egr1 act upon their respective binding sites on the HIF1α promoter [122, 123]. HIF transcripts can also be subjected to regulation at the levels of pre-mRNA splicing and maturation, as well as mRNA export to the cytoplasm, stability, and translation [124]. Therefore, there are many regulatory pathways. Additionally, under normoxic conditions several cytokines and growth factors, like IGF2, IL-1β, TNF-α and EGF among others, can affect HIF through post-

transcriptional mechanisms. The signaling pathways involved in HIF induction by these factors include PI3K, MAPK and MEK [125-127]. Moreover, other oncogenes and tumor suppressor genes including *PTEN*, *mTOR*, *Ras*, *Akt* and *p53* also regulate HIF activity through different mechanisms [128-130], revealing the importance of HIF in tumor growth and development (Figure 2).

HYPOXIA AND DISEASE

Hypoxia is a well-studied prototype and a paradigm of responses that involve the organism as a whole with different consequences on health and disease. Prolonged generalized hypoxia is the cause of hypoxic pulmonary arterial hypertension (PAH). Conversely hypoxia can also occur as a consequence of numerous pathologies, these including pathologies of the respiratory system such as chronic obstructive pulmonary disease (COPD) or pulmonary fibrosis, pathologies produced by ischemic processes such as myocardial infarction or cerebral stroke, but also uncontrolled growth of tumors causes aberrant blood vessels and thus an insufficient oxygen supply. In this thesis, hypoxia will be treated from two points of view, as the cause or as the consequence of a pathological process. Although there are many pathological conditions in which hypoxia have been involved, we will focus on the role of hypoxia in PAH, and in ccRCC, being hypoxia the cause or the consequence of these pathologies.

Pulmonary Arterial Hypertension

PAH or just pulmonary hypertension (PH) is characterized by a progressive elevation of pulmonary arterial pressure (PAP $\geq$ 25mmHg at rest) due to changes in the structure and function of pulmonary arteries (PA), ultimately producing right ventricular failure and death (Figure 4). Initially described by Dr. Ernst von Romberg in 1891 [131]. PAH symptoms include as shortness of breath, fatigue, non-productive cough, weakness, angina pectoris, syncope and peripheral edema [132]. The World Health Organization (WHO) has classified PH in five groups; the first includes idiopathic and hereditable PAH, induced by drugs and toxins or associated with other diseases. The other four groups correspond to PAH due to left heart disease; lung disease and/or hypoxemia; chronic thromboembolic pulmonary hypertension (CTEPH) and other PA obstruction; and PH with unclear and/or multifactorial mechanism [132]. Moreover, the New York Heart Association (NYAH) and the WHO classify PH into four functional classes that share a similar degree of exercise limitation, symptoms and prognosis. [133-135]. Epidemiologic studies report a greater incidence of the disease in females, and depending on the disease classification the female-to-male ratio can be as great as 4:1 [136]. PAH class I has a prevalence of 15-60 cases per million population and an incidence of 5-10 cases per million per year in Europe. In some cases, a genetic mutation has been linked to human disease [137]. Still, in most

instances the causative events remain unknown and this likely contributes to the delay in therapeutic progress. Elevated pulmonary pressure results from a decrease in arterial lumen through the combination of increased contractility of pulmonary arteries, endothelial dysfunction, proliferation and remodeling of PA cells, and thrombosis.

In PAH, **vasoconstriction** is originated by a decrease in the production of vasodilators/growth inhibitors such as NO and PGI2, while there is an increase in the production of vasoconstrictor/pro-mitogens such as endothelin-1 (ET-1), thromboxane-2 (TXA2) and serotonin or 5-hydroxytryptamine (5-HT) [138, 139]. This miss-regulation of endothelial cells is called endothelial dysfunction and may have implications in all the pathologic events of PAH. It is also crucial the regulation of K^+/Ca^{2+} channels [140, 141]. Several studies have reported the involvement of Kv channels in controlling membrane potential of PASMC and PA tone [142]. It has been also described that Kv1.5 has an important role in the development of PAH as a result of mutation or downregulation of the channel [143, 144]. Moreover, acute hypoxia causes pulmonary vasoconstriction in some degree by inhibiting Kv activity in PASMC [145], caused in part by AMPK-mediated phosphorylation and inhibition of Kv1.5 [25]. However, the link between long-term hypoxia and the repression of this channel remains poorly understood.

Remodeling of PA is considered one of the most important hallmarks in PAH. The three main cellular types of the PA, endothelial (PAEC) in the tunica intima or endothelium, PASMC in the tunica media, and fibroblast (PAFIB) in the tunica adventitia contribute to this process. PAEC overgrowth cause neointimal formation, plexiform lesions and endothelial dysfunction [146]. PASMC show aberrant proliferation leading to tunica media thickening. They also miss-regulate and inhibit the activity of ion channels losing the control of contraction and relaxation. PAFIB in turn suffer a process of differentiation to SMC-like phenotype contributing to the thickening of the media layer, [147, 148]. They release growth factors and interleukins, generating more overgrowth and inflammation [149, 150]. They also exacerbate the synthesis of extracellular matrix, releasing huge amounts of collagen, fibronectin and elastin [151]. Moreover, PAEC, PASMC and PAFIB can migrate through the arterial layers disrupting arterial functions and promoting remodeling [23, 139].

Thrombosis is a complex process characterized by the interaction of ECs with both, soluble elements (plasma coagulation proteins) and cellular elements of blood such as platelets. In PAH, the balance between thrombotic and antithrombotic is lost, generating thrombosis in small arteries and increasing arterial pressure. Therefore, thrombosis occurs in PAH by a hypercoagulant phenotype characterized by increased levels of plasminogen activator inhibitor-1 (PAI-1), von

Willebrand factor, TXA2 and 5-HT, and decreased levels of tissue plasminogen activator (t-PA), thrombomodulin, NO and PGI2 [152].

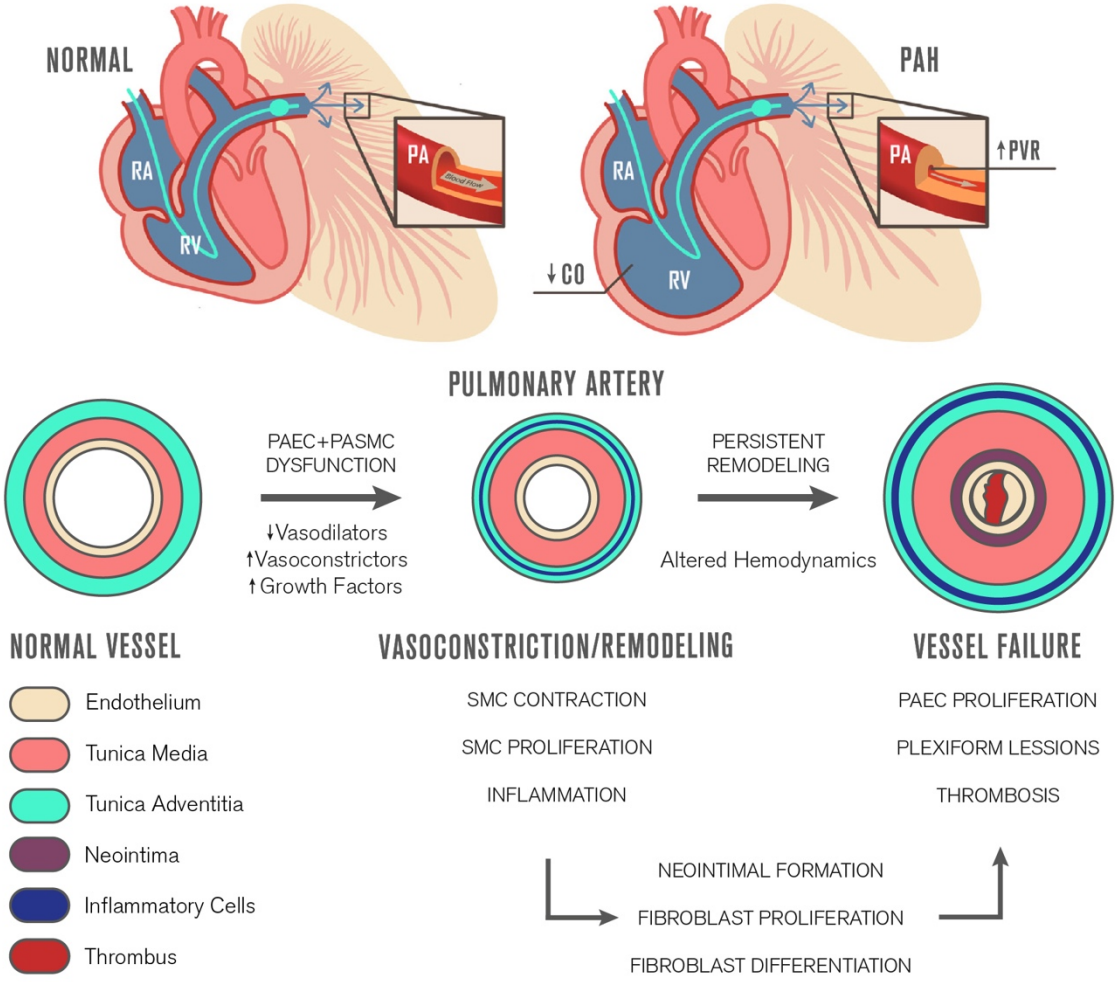

Figure 4: Graphical abstract of cellular events in PAH. Small PAs are progressively narrowed, leading to an increase in pulmonary vascular resistance (PVR) and the PA pressures. The progressive increase in PVR and pulmonary pressures subsequently lead to reduced cardiac output (CO) and right heart failure. RA (right atrium); and RV (right ventricle). Figure modified from Lai *et al* 2014 [153].

Studies in animal models and human subjects have identified a number of signaling mechanisms that are dysregulated in the setting of PAH including hyperactive vasoconstriction [154] and loss of vasodilation in general and NO-mediated vasodilation in particular [155, 156]. Hypoxia stimulates pulmonary vasoconstriction and, if chronic, causes hypertrophy of the tunica media of PAs [157]. In a feed-forward manner, vascular deterioration due to decreased blood flow through the lungs further exacerbates tissue hypoxia [158]. Most responses to hypoxia are mediated through the induction of the HIF pathway. Although HIF2α is abundantly expressed in the lung

[159], studies in mutant mice suggest that both HIF1α and HIF2α are involved in the hypoxic adaptive process in the lung vasculature [160-163].In heterozygous *hif1α*$^{+/-}$ mice, hypoxia-induced vascular remodeling is decreased [160]. Likewise, heterozygous *hif2α*$^{+/-}$ mice did not develop pulmonary hypertension following prolonged hypoxia [161]. Furthermore, dysregulation of the HIF pathway has been reported to promote pulmonary hypertension both in mouse models and human patients with HIF2α mutations [164, 165]. However, the molecular changes triggered by HIF are incompletely understood. Now is being appreciated the role of thrombospondin-1 (TSP1), a matricellular protein reported to be important in the maintenance of vascular homeostasis [166, 167], in the development of PAH. It has been shown that hypoxia induces vascular cell expression of TSP1 [168] and it has been found high levels of TSP1 in PAH patients [169-172]. Nonetheless, it is largely unknown how hypoxia regulates TSP1 in the lung, whether this occurs in a HIF-dependent manner, and if this regulation contributes to pulmonary vascular dysfunction and PAH.

Thrombospondin-1

TSP1 belongs to the family of thrombospondins, a family of highly conserved, oligomeric and multi-domain matricellular glycoproteins [173]. These proteins are non-structural proteins dynamically expressed and present in the extracellular matrix during specific developmental or pathological events. They generally have regulatory roles binding to other extracellular matrix proteins, cell surface receptors or signaling proteins [174]. This family consists of 5 members that are subdivided into 2 subgroups according to the state of oligomerization and molecular structure [173]. TSP1 and TSP2, forms part of the group 1. These two members of the thrombospondin family are organized in homotrimers and contain in their C-terminal end a highly conserved 650 amino acid sequence which includes type 2 or EGF repeats and type 3 repeats or calcium-binding domain conforming what has been termed the "identity domain" [175]. In the N-terminal end these proteins have an oligomerization domain, a procollagen (Willebrand type C domain) and a type 1 repeats domain or properdin like domain (TSR) which are specific of group 1 [175, 176].

Thrombospondin-1 (TSP1) is a homotrimer of about 450 KDa expressed during the development of tissues and organs [175]. It was first described in 1971 by Baenziger et *al*. [177] under the name Thrombin-sensitive protein, since it was released by platelets when these were stimulated by thrombin [177, 178]. TSP1 regulates multiple cellular events involved in tissue repair including hemostasis, cell adhesion, migration, proliferation, extracellular matrix expression and organization, and regulation of growth factor activity [173, 175]. This is possible due to its multi-domain structure which interacts with several cell receptors and matrix proteins. E.g. TSP1 binds and activates transforming growth factor beta (TGF-β) through TSR repeats domain, this domain

also binds to CD36, VEGF or heparin sulfate. N-terminal end interacts with heparin and α3β1, α6β1, α4β1 modulating angiogenesis and C-ternimal end binds to CD47 regulating vascular homeostasis [174]. In addition to physiologic repair, TSP1 is also expressed at elevated levels in many tissues undergoing fibroproliferative remodeling. The blockade of specific actions of TSP1 or loss of TSP1 expression can attenuate pathologic tissue remodeling [179-181]. TSP1 was the first anti-angiogenic factor described [182] and acts directly on endothelial cells through its interaction with the CD36 surface receptor [183].Transgenic mice deficient for TSP1 are viable and display a mild and variable lordotic curvature of the spine that is apparent from birth, an increase in the number of circulating white blood cells, with monocytes and eosinophils having the largest percent increases, and a reduction of TGF-β activation [184].

TSP1 is also considered for its role in vascular health and disease. In the systemic vasculature, TSP1 modulates vascular response and at pathologic levels promotes vascular dysfunction [185, 186]. In cells and animal models, over-active TSP1 signaling inhibits vasodilation in part by limiting nitric oxide production and signaling [170, 171]. In addition, TSP1 is reported to be involved in arteriosclerosis-associated vascular remodeling [187]. In the lung, TSP1 has been reported to be important in the maintenance of homeostasis [166, 167] and to inhibit growth of lung cancer [188, 189]. Beyond these functions, a role for TSP1 in promoting pulmonary vasculopathy is now being especially relevant. Previous reports have found that *tsp1*$^{-/-}$ mice are protected from hypoxia-mediated PAH [169, 190]. In addition, TSP1 is upregulated in lungs from PAH patients compared to non-PAH controls [169-172]. However, the molecular mechanisms by which hypoxia regulates TSP1 in the lung and its implication in PAH events are still unknown.

Hypoxia and cancer

Hypoxia is a hallmark of almost all kind of solid tumors as brain, prostate, kidney, breast, cervical or colon, among others. As a consequence of the abnormal and aberrant process of neoplastic growth in tumorigenesis, the proliferating cancer cells have not a well stablished vascular network that support oxygen and nutrient supply. Under such conditions tumor cells activate cellular responses to improve cell survival; increase angiogenesis, improve glycolytic flux to enhance energy production, and regulate autophagy or apoptosis. Furthermore, clinical studies reveal that solid tumors have also been shown to harbor hypoxic areas, maintaining survival of cancer cells via the HIFα pathway, this being associated with bad outcome and prognosis [129, 130]. It is well established that HIFs play an important role in tumor progression. Previous studies have reported that HIF1α, HIF2α and HIF3α are overexpressed in human cancers and their expression levels correlate patient mortality [129, 130]. Studies with knockout mice for HIF1α or HIF2α revealed differences in their contribution to promote tumor growth [191, 192]. In this respect, HIF1α and

HIF2α demonstrated opposite effects in ccRCC, while HIF2α drives tumor progression, HIF1α, whose expression is frequently lost, inhibits growth and predicts for better patient prognosis [193-195]. Thus, the relative importance of HIFα in tumor growth probably depends on the type of tumor. Investigating specific functions of HIF1α and HIF2α in ccRCC, there were identified different target genes differently activated either by HIF1α or HIF2α with opposing effects on tumor growth [196, 197].

Clear cell Renal Cell Carcinoma

Kidney cancer is among the top ten most common cancers in the world. The most frequent type of renal neoplasm is RCC, which accounts for 85% of all renal malignancies. It is estimated that 320,000 new cases will be diagnosed in 2016, with an approximated number of deaths around 140,000 worldwide [198]**.** RCC is the most common malignant tumor of adult kidney, being tumor resection the only effective treatment [199], due to its resistance to chemotherapy [200] and radiotherapy [201]. ccRCC is a subtype of RCC that comprises 75-88% of cases [202]. Somatic gene mutations in *vhl* is the main cause in most primary sporadic ccRCCs [203], see steps of the ccRCC development in Figure 5. Moreover, VHL loss in animal models has clearly implicated this gene as a gatekeeper gene in the pathogenesis of ccRCC [66, 204].

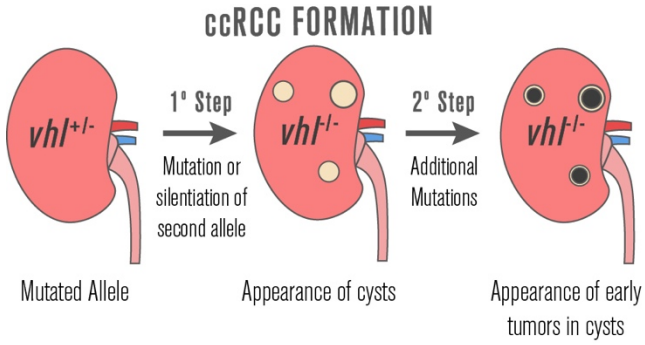

Figure 5: Scheme of ccRCC tumor formation. Mutations in the second allele of *vhl* facilitate the appearance of cysts. Additional mutations promote the formation of tumors.

ccRCC is characterized by the accumulation of glycogen, phospholipids and neutral lipids [205], a well-defined plasma, they are also highly vascularized tumors with high expression of proangiogenic factors due to the loss of VHL and the presence of hypoxic foci. Both situations produce an accumulation of HIF favoring the increase in hypoxic response genes. VEGF is one of the most relevant gene induced in ccRCC and its inhibition have been used as a therapeutic approach to repress angiogenesis [206]. However, VEGF inhibition has not been enough to stop tumor growth, suggesting that there must be additional mechanisms involved. In this regard, HIF-independent VHL functions have been shown to contribute to tumor growth [66, 76, 207, 208].

Therefore, it is conceivable that new additional pathways still unknown might also contribute to the growth of these tumors. Previous results have identified that Vascular Cell Adhesion Molecule (VCAM-1) is regulated by VHL in ccRCC cell lines and may help to explain why these tumors are highly invasive [209-211].

Vascular Cell Adhesion Molecule-1

VCAM-1 or cluster of differentiation 106 (CD106) is a cell adhesion protein that belongs to the immunoglobulin (Ig) superfamily of proteins [212] and was first described as a cytokine-inducible endothelial adhesion molecule [213, 214]. Generally, VCAM-1 is expressed on the luminal and lateral side of endothelial cells under inflammatory conditions, mediating rolling and adhesion of various subsets of leukocytes as a prerequisite for their recruitment from blood into tissues. [215, 216]. The integrin α4β1 (very late activation antigen-4, VLA-4) was identified as the ligand for VCAM-1 mediating the adhesion of leukocytes to endothelium [217-219] (Figure 6).

Figure 6: Monocyte recruitment by activated endothelium. Under inflammatory conditions endothelial cells express and show ICAM-1 and VCAM-1 to the lumen and capture monocyte trough Mac1 and VLA4 respectively.

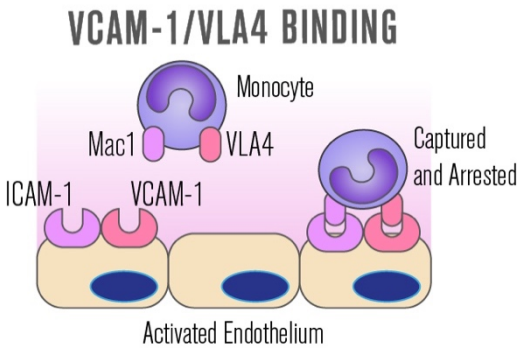

VCAM-1 is localized in lipid-raft-like platforms with the tetraspanins CD9, CD81, and CD151, referred as tetraspanin-enriched microdomains, suggested to support VCAM-1 surface expression and function [220-222]. Two alternative VCAM-1 splicing variants in humans have been identified, consisting of seven (7d) or six (6d) Ig-like domains, with domains one and four revealed as binding sites for VLA-4 [223]. VCAM-1 can also be cleaved from the endothelial surface to a soluble (s)VCAM-1, which is increased in various diseases [224]. In addition to its extracellular interaction, VCAM-1 intracellular terminus is connected to the actin cytoskeleton via Ezrin and Moesin clustering in a docking structure that anchor and partially embrace leukocytes [221, 225].

Although VCAM-1 expression has been mostly assigned to activated endothelium, it is also expressed on follicular dendritic cells, macrophages in the spleen and thymus, and Kupffer cells in the liver under non-inflamed conditions [226]. Because of its wide distribution in human tissues

and organs, VCAM-1 participates in many pathophysiological situations like autoimmune diseases, cardiovascular disease, or infections [227]. Furthermore, it has been reported that tumor cells as melanoma, osteosarcoma or kidney and naturally blood borne tumors like leukemia and lymphoma cell lines are positive for VLA-4, and its interaction with VCAM-1 on endothelium is crucial for metastasis [228, 229]. Others tumors show a high level of expressed VCAM-1, however, it does not give any advantage concerning the endothelial adhesion, invasion or transendothelial migration of tumor cells. Instead, it allows a strong adhesion and interaction with VLA-4 of monocytes and tumor-associated macrophages generating prosurvival signals to the tumor cells [230, 231]. On the other hand, there are tumors that show a downregulation of VCAM-1, these include melanoma and carcinoma, [232], suggesting a tumor protecting mechanism by attenuating the immune response for immune infiltration. [233].

VCAM-1 is also expressed in renal epithelium [234] and it has been considered as a predictor of cancer-free survival in ccRCC [209-211], however the mechanisms underlying VCAM-1 regulation in these tumors and why this ccRCC with high levels of VCAM-1 have a better prognosis are yet unknown. VCAM-1 expression is stimulated under inflammatory conditions by a multitude of signals like cytokines as tumor necrosis factor alpha (TNFα), ROS, high concentrations of glucose, (toll like receptor) TLR agonists, or shear stress [222, 235]. It is well established that NF-κB is one of the main regulator of VCAM-1 in many different cell types [236] and that NF-κB is activated by TNF-α, a cytokine produced by activated leukocytes and many other cell types that is involved in systemic inflammation [237].

Nuclear Factor Kappa-Light-Chain-Enhancer of Activated B Cells

Hypoxia stimulates a complex cell signaling network in cancer cells, some of them regulated by HIF, as previously shown. In addition, there are other pathways that interact with each other causing positive and negative feedback loops and enhancing or diminishing hypoxic effects. NF-κB is a family of transcription factors implicated in processes such as inflammation, apoptosis, proliferation, and development which are ubiquitously expressed in mammalian cells. NF-κB subfamily is composed by five members; p65 (RelA), c-Rel, RelB, p105/p50 (NF-κB-1) and p100/p52 (NF-κB-2) that share a conserved N-terminal REL homology domain (RHD). This domain is responsible of dimerization, nuclear translocation and DNA binding. DNA binding occurs in special conserved sequences called κB elements or NF-κB response elements (NRE). In addition, RelA, c-Rel and RelB contain C-TAD that are important for transcriptional activation [238, 239]. IκB family (most known IκBα, IκBβ, IκBε) have an ankyrin repeat domain (ARD) that binds to the RHD of NF-κB family. IκB proteins function as NF-κB inhibitors sequestering NF-κB in the cytosol. IκB kinases (IKK) phosphorylate IκB upon cell stimulation, which leads

to their ubiquitination and proteasomal degradation. Degradation and processing of the precursors p105 and p100 generate the proteins p50 and p52 respectively, which form dimeric complexes with RelA, c-Rel and RelB. These complexes go into the nucleus and activate genes under κB elements. [238, 239]. NF-κB activation is controlled in a cell/tissue specific way by two major pathways depending on the stimulus and the members of the NF-κB family that are being expressed. These two pathways are generally described as canonical and non-canonical NF-κB pathways, although in some cases it is difficult to determine which is acting due to the crosstalk between them [240] (Figure 7).

In the **canonical** pathway, signaling cascades are induced upon stimulation by pro-inflammatory cytokines (for instance; TNFα, IL1), pathogen-associated molecular patterns (PAMPs) from bacteria and viruses, B- or T-cell antigen receptor (BCR or TCR) agonists, chemicals or radiation. Its activation culminates with the activation of the IKK complex formed by IKKα IKKβ and IKKγ (NEMO). When the IKK complex is activated, IKKβ phosphorylates IκBα, leading to its K-48-linked ubiquitination and proteasomal degradation [241]. This enables the NF-κB dimers (the most abundant being p65–p50) to accumulate, bind to NREs, and activate NF-κB target genes [242, 243].

In the **noncanonical** NF-κB pathway, NF-κB2 p100/RelB complexes are inactive in the cytoplasm. Signaling is restricted to a subset of TNF family members such as lymphotoxin (LTβ), B-cell activating factor (BAFF) and CD40L, although there are numerous cases in which canonical NF-κB activator can induce RelB-p52 translocation into the nucleus and gene transcription [238, 239]. This signaling activates the kinase NF-κB-inducing kinase (NIK), which in turn activates IKKα complexes that phosphorylate C-terminal residues in NF-κB2 p100. Phosphorylation of NF-κB2 p100 leads to its ubiquitination and proteasomal processing to NF-κB2 p52. This creates transcriptionally competent NF-κB p52/RelB complexes that translocate into the nucleus and induce target gene expression (Figure 7). As we have mentioned before, it is well established that NF- B is one of the main regulator of VCAM-1 in many different cell types [236]. NF- B is activated by the TNF-α [237], and despite it is thought that it can only induce NF- B through the canonical pathway, there are numerous reports showing that TNF-α can induce both, canonical and non-canonical NF- B pathways [244-247]. Previous studies demonstrate that VHL loss induces heightened activity of NF- B classical pathway [93, 94], in addition, NF-κB activation is a critical component in the transcriptional response to hypoxia [125]. However, the molecular mechanisms underlying VHL-mediated suppression of NF-κB have not been completely elucidated.

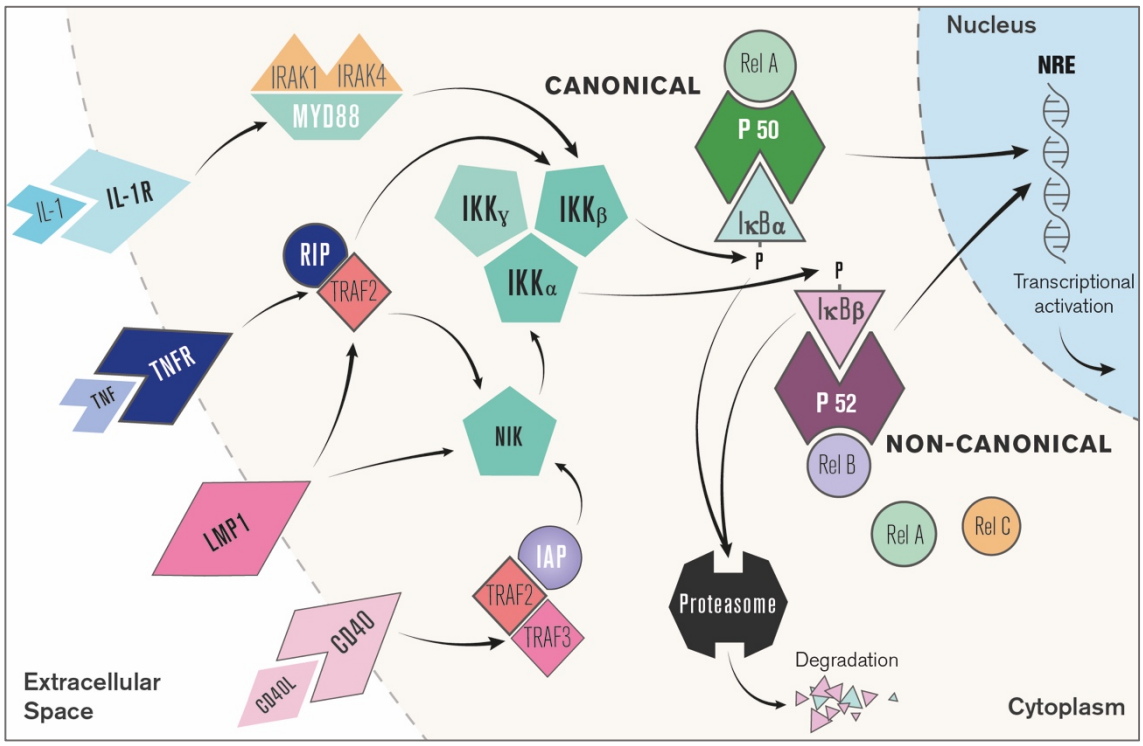

Figure 7: Molecular model of NF-κB activation pathways. Several stimuli trigger different pathways that induce IKKs. Activation of IKKs promote the phosphorylation of IκB and its subsequent degradation by the proteasoma. This liberates P50 or P52 allowing dimerization with Rel proteins and transactivation. Note different pathways for canonical or non-canonical pathways.

OBJECTIVES

OBJECTIVES

In this thesis, hypoxia will be treated from two points of view, as the cause or as the consequence of a pathological process. Although there are many pathological conditions in which hypoxia is involved, we will focus on the role of hypoxia in pulmonary arterial hypertension PAH as the cause of the disease, and in clear-cell renal carcinoma (ccRCC) as a consequence. Taking into account all the previously mentioned in the introduction of this thesis these are the objectives proposed in each section:

1. Hypoxia, TSP1 and PAH.

Based on the role of TSP1 in vascular homeostasis and its recent implication in hypoxic PAH, we postulate that TSP1 could be activated through a hypoxia-mediated mechanism and its regulation may have a special relevance during PAH events. Therefore, we propose the following aims in this matter:

1.1 Analyze the cellular source involved in the induction of TSP1 in the lung under hypoxia

1.2 Elucidate the mechanisms by which hypoxia induces TSP1 levels in the lung

1.3 Study the contribution of TSP1 to functional aspects and cellular events during PAH.

1.3.1 Effects of TSP1 on vascular remodeling

1.3.2 Effects of TSP1 on endothelial dysfunction and cell contractility

2. Hypoxia, ccRCC and VCAM-1

Taking into account all the previous background, we hypothesized that decreased levels of VCAM-1 in ccRCC, which has been clearly related with a worst prognosis, might be due to the effects of VHL loss or hypoxia. In addition, given that NF-κB activation is a critical component in the transcriptional response to hypoxia, and on the other hand it is a transcriptional regulator of VCAM-1, it is plausible that the regulation of this pathway by VHL or hypoxia modulates the levels of VCAM-1 in these tumors. In order to challenge our hypothesis our aims were:

2.1. Elucidate the mechanism by which hypoxia and VHL loss regulate VCAM-1.

2.2. Study the contribution and functional effects of VCAM-1 in these tumors.

MATERIALS AND METHODS

MATERIALS AND METHODS

Animals.

Age matched male C57BL/6 WT and *tsp1*$^{-/-}$ mice (stock numbers 000664, 006141 respectively) were obtained from the Jackson Laboratory (Bar Harbor, ME). Vhlfl/fl-UBC-Cre-ERT2, HIF2αfl/fl-UBC-Cre-ERT2 and HIF1αfl/fl-UBC-Cre-ERT2 mice were used to generate VHL (*vhl*$^{-/-}$), or HIF2α (*hif2α*$^{-/-}$) knockout mice respectively or double VHL/HIF2α, VHL/HIF1α knockout mice (*vhl*$^{-/-}$*/hif2α*$^{-/-}$, *vhl*$^{-/-}$*/hif1α*$^{-/-}$ respectively). The gene deletion procedure employed to generate these animals was previously described [248, 249]. To induce hypoxia in vivo, mice were placed in an airtight chamber with inflow and outflow valves, and infused with a mixture of 10% O2 and 90% N2 (Carburos Metálicos). When mice were exposed to hypoxia in combination with Semaxanib (SU5416), a potent and selective VEGFR(Flk-1/KDR) inhibitor, animals were injected subcutaneously with SU5416 (20 mg/kg) or vehicle (DMSO) once a week. All mice in this work were sacrificed by first administering inhalation general anaesthesia (isoflurane 1.5%) followed by cervical dislocation. All studies were performed under the supervision of the Head of Animal Welfare and Health with a protocol approved by the Committee for Research and Ethics of the Universidad Autonoma of Madrid in accordance with Spanish and European guidelines (Directive 2010/63/EU of the European Parliament).

Reagents.

Table 1: Most important reagents employed in this work.

Reagents				
Reagent	**Manufacturer**	**#Catalog**	**Use /Description**	**[C]**
TSP1	Athens	16-20-201319	TSP1 extracted from human platelets.	20 mg/mL
TNF-α	RyD	210-TA-005 RD	Recombinant human TNF-α from *E.coli* used to activate NFkB	20 ng/mL
IFN-γ	RyD	285-IF-100	Recombinant human IFN-γ from E.coli used to activate human monocytes.	100 U/ml

SM7368	Sigma Aldrich	380623-76-7	TNF-α inhibitor.	20 µM
LSKL	AnaSpec	AS-60877	TSP1 inhibitor.	1 µM
SB 431542	RyD	1614/1	TGFβ inhibitor.	10 µM
DMOG	Sigma Aldrich	89464-63-1	Prolyl hydroxylases Inhibitor	1 mM
DAPI	Sigma Aldrich	28718-90-3	Cell permeable fluorescent minor groove-binding probe for DNA.	1/1000
Alexa Fluor® Phalloidin 568	Thermo Fisher Scientific.	A12380	Phalloidin is a toxin which binds and stabilizes F-Actin. Label F-Acting in Alexa Fluor 568.	1/200
Alexa Fluor® Phalloidin 647	Thermo Fisher Scientific	A22287	Phalloidin is a toxin which binds and stabilizes F-Actin. Label F-Acting in Alexa Fluor 647.	1/100
DPO1 (diphenyl phosphine oxide-1)	Sigma Aldrich	43077-30-1	Inhibits Kv1.5 channels.	1-2 µM
XE-991	Sigma Aldrich	122955-42-4	Inhibits Kv7 channels.	0.3 µM
Ionomycin	Sigma Aldrich	407952	Calcium Salt.	1 µM
LPS	Sigma Aldrich	297-473-0	Stimulates cells of the innate immune system by (TLR4)	2 µg/mL
cd14-Beads	Miltenyi	130-050-201	Beads coated with cd14 to isolate human monocytes.	20 µL/10^7 total cells
FITC-dextran (70 kDa)	Sigma Aldrich	FD70S-100MG	Dextran labeled with FITC used in perfusion studies in cell monolayers	10 mg/mL
Calcein-AM	Sigma Aldrich	148504-34-1	It is a fluorescent dye with excitation and emission wavelengths of 495/515 nm, respectively.	2.5 mM
Fluo4-AM	Thermo Fisher Scientific	F14201	Fluorescent Calcium Probe with excitation and emission wavelengths of 494/506 nm, respectively.	1 µM
SU 5416 Semaxanib	Sigma Aldrich	S8442	SU 5416 is a VEGFR inhibitor used to exacerbate PAH remodeling in animal models.	20 mg/kg

Antibodies.

Table 2: All the antibodies employed.

Primary Antibodies						
Antibody	**Host**	**Used for**	**Manufacturer**	**#Catalog**	**Technique**	**[C]**
TSP1 Ab11 (Cocktail)	Mouse	Human, Mouse	Neomarkers	MS-1066-P1	WB	1/500
TSP1 Ab6.1	Mouse	Human, Mouse	Thermo Fisher Scientific	MA5-13398	IF	1/100
anti-α-Tubulin	Mouse	Human, Mouse	Sigma Aldrich	T6199	WB	1/2000
anti-β-Actin	Mouse	Human, Mouse	Sigma Aldrich	A5441	WB	1/2000
anti-Vinculin hVIN-1	Mouse	**Mouse**	Sigma Aldrich	V9131	IF	1/400
rabbit anti-ZO-1	Rabbit	Mouse	Thermo Fisher Scientific	40-2300	IF	1/200
anti-HIF1α	Mouse	Human	RyD	mab1536	WB	1/500
anti-HIF1α C-term	Rabbit	Human	Cayman Chemical Company	*10006421*	WB	1/500
anti-HIF2α Ab199	Rabbit	Human Mouse	Abcam	ab73895	WB	1/500
anti-VCAM-1 H-276	Mouse	Human	SantaCruz Biotechnology	sc-8304	WB	1/1000
anti-VHL (VHL40)	Mouse	Human	SantaCruz Biotechnology	sc-135657	WB	1/500
anti-NIK	Rabbit	Human	SantaCruz Biotechnology	sc-7211	WB	1/500
anti-NF-κB p65 (C-20)	Rabbit	Human	SantaCruz Biotechnology	sc-372	WB	1/500

anti-NF-κB p52 (k-279	Rabbit	Human	SantaCruz Biotechnology	sc-298	WB	1/500
anti-NF-κB p50 (E-10	Mouse	Human	SantaCruz Biotechnology	sc-8414	WB	1/500
anti-NF-κB Rel B (D-4)	Mouse	Human	SantaCruz Biotechnology	sc-48366	WB	1/500
anti-IKKα (3G12)	Mouse	Human	Cell Signaling Technology	682	WB	1/500
anti-SMA (clone 1A4),	Mouse	Human Mouse	(Dako, Carpinteria, CA)	M0851	IF	1/400
anti-SMA-cy3	Mouse	Human Mouse	Sigma Aldrich	C6198	IF	1/400
(CNN1) EP798Y	Rabbit	Human Mouse	Abcam	ab46794	IF	1/400
Secondary Antibodies						
Antibody	**Host species**	**Specificity**	**Manufacturer**	**Catalog Number**	**Use**	**[C]**
GAM-488	Goat	Mouse IgG	Thermo Fisher Scientific	A11029	IF	1/200
GAM-568	Goat	Mouse IgG	Thermo Fisher Scientific	A-11031	IF	1/200
GAR-488	Goat	Rabbit IgG	Thermo Fisher Scientific	A-11034	IF	1/200
GAR-568	Goat	Rabbit IgG	Thermo Fisher Scientific	A-11036	IF	1/200
RAM-HRP	Rabbit	Mouse IgG	Dako Diagnosticos SA	P0260	WB	1/1000
DAR-HRP	Donkey	Rabbit IgG	GE Healthcare	NA934V	WB	1/2000

Cell culture.

Primary Cells

Primary murine pulmonary artery vascular smooth muscle cells (**mPASMCs**) were obtained from 8-10 weeks-old male C57BL/6 WT and *tsp1*$^{-/-}$ mice. Mice were sacrificed as previously described and flushed with sterile PBS to remove blood, and lungs were then extracted under sterile conditions. Pulmonary arteries were carefully dissected and the adventitia was removed under a dissecting microscope. Arteries were then cut into rings (1.8–2 mm length) and explanted in a 35 mm culture dish in Dulbecco's Modified Eagle's Medium (DMEM) with 20% FBS, penicillin (100 units/mL), streptomycin (100 units/mL), amphotericin B (100 µg/mL), HEPES (200 µg/mL) and Heparin 500x (1 ml/500 mL media). After 3 days, cells were maintained in media with 10% FBS at 37ºC and 10% CO_2. The cells migrated from the explants within 6-9 days and grew to confluence in approximately 2 weeks. Cell purity was confirmed by immunostaining with mouse anti-SMA and rabbit anti-Calponin-1 (CNN1) antibodies.

Primary pulmonary-derived fibroblasts (**mFIB**) were isolated by enzymatic digestion with collagenase A from chlostridium histolyticum (Sigma-Aldrich). Briefly, mice were sacrificed as above and lungs were perfused with PBS, extracted, cut into small pieces and then incubated with 3 mL of 2 mg/mL collagenase solution for 30 min. After digestion cells were washed twice in DMEN with 10% FBS and then cultured in DMEM supplemented with 20% FBS, penicillin (100 units/mL), streptomycin (100 units/mL) and 1% HEPES buffer. Cells were grown for two days and then cultured for an additional three days in minimum media with 5% FBS to minimize contaminating endothelial or smooth muscle cells. Following, these cells were maintained in media with 10% FBS at 37ºC and 5% CO_2.

Human pulmonary arterial endothelial cells (**hPAEC**), smooth muscle cells (**hPASMC**) and human umbilical vein endothelial cells (**HUVEC**) were obtained from ATCC (PCS-100-022, PCS-100-023 or CRL-1730 respectively) and were cultured following manufacturer´s recommended specifications. Human pulmonary arterial fibroblast (**hPAFIB**) were obtained from ScienceCell (#3120) and were cultured following manufacturer´s recommended specifications.

Myeloid cell isolation and culture. Peripheral blood mononuclear cells were purified by Ficoll gradient centrifugation from pooled human buffy coats obtained from the Hospital Universitario de la Princesa (Madrid, Spain). Myeloid cells were isolated from mononuclear cell populations by positive selection for CD14 by magnetic beads immune selection according to the manufacturer's directions (Miltenyi Biotech, Auburn, CA). All studies with human cells were

conducted with the approval of the Human Subjects Institutional Review Board of the Hospital Universitario de la Princesa.

Cellular Lines

Renal carcinoma cell lines **786-O** (CRL-1932), **Caki-1** (HTB-46), **Caki-2** (HTB-47) and **ACHN** (CRL-1611) were from the American Type Culture Collection (ATCC: Rockville, MD, USA), and the RCC4 cell line was kindly provided by Dr. W. Kaelin (Dana-Farber Cancer Institute, Boston, MA). Cells were cultured in DMEM (Dulbeco's modified Eagle's medium) containing 10% (v/v) FBS (fetal bovine serum), 100 units/ml penicillin/100µg/ml streptomycin (antibiotics). Chinesse Hamster Ovary cells, **CHO.K1** (ATCC, #CCl-61) were cultured in 1% glucose DMEN, 10% FBS and antibiotics. 786-O and RCC4 cells were stably transfected with the vectors pRc/CMV or HA-VHL-pRc/CMV, in the text named as pRv or VHL (30 kDa) respectively, provided by Dr. W. Kaelin through Addgene (plasmids # 20814 and 19999 respectively). Transfected cells were selected with 1 mg/ml G418 sulfate. Additionally, we used 786-O expressing the naturally occurring type 2C VHL mutant L188V or a non neddylateable version of VHL termed RRR (in which lysines (K) 159, 171, and 196, have been substituted by an arginine (R), with K159 being an essential residue for neddylation. As a control for this mutant we used 786-O cells transfected with another version of VHL (KRR) that carries mutations only at Lys171 and Lys196 (which do not interfere with the normal VHL function) [250]. These mutants were kindly provided by Dr. Michael Ohh (University of Toronto, Canada). Cells were maintained in culture at 37ºC in the presence of 5% CO_2 and 21% O_2 (normoxia) and grown in DMEM containing 10% (v/v) FBS and antibiotics. For hypoxic experiments, cells were incubated at 37ºC in an *Invivo$_2$ 400* hypoxia workstation (Ruskinn Technology, West Yorkshire) in the presence of 5% CO_2 and 0.5-1 % oxygen for the times indicated.

HIF reporter in vitro assay.

Tsp1 Hypoxia Response Elements (HRE1: GGCGGCTGACGTCCCATCCCGAAGA and HRE2: CCAAGGCTGCGTGGGCGGGCACCGA) were introduced in the luciferase reporter plasmid pGL4.23 vector (Promega) between Kpn1 and Hind3, generating pGL4.23-HRE1 and pGL4.23-HRE2 with three copies in tandem. As an HRE validated control the HIF-responsive firefly luciferase reporter, expressing the luciferase gene under the control of nine tandem copies of the VEGF hypoxia response element (9xHRE) [251] was used. Renilla, pRL-SV40 Vector (Promega) was used as an internal control. In addition, to test HIF functional activity, we used retroviral vectors pRV-GFP encoding HIF mutated constitutive active forms, HIF2α $(P\text{-}A)^2$ or HIF1α $(P\text{-}A)^2$ or a mutation lacking transcriptional activity HIF1α$(P\text{-}A)^2$bHLH [193]. CHO.K1

were cultured in p24 plate at the 75% optimum confluence, and then cells were transiently transfected with the pRV vectors (0,25 µg), luciferase vectors (0,25 µg) and Renilla (0,05 µg) using 2,5 µg of the transfection reagent jetPEI (Polyplus) per well. After 24 h reporter activity was determined using the Dual-Luciferase Reporter Assay System (Promega) according to the manufacturer's instructions. Firefy luciferase activity was normalized based on the Renilla luciferase activity and Luciferase activity was measured using a Glomax Multidetection (Promega).

Human tissues

Control non-PAH and **end-stage PAH lungs** were obtained immediately following explantation under ongoing University of Pittsburgh IRB protocols (970946 and PRO14010265). Informed consent was given for the use of human samples and the study conformed to the principles outlined in the Declaration of Helsinki. Under sterile conditions and employing magnification, distal 5th order PAs were dissected for further processing using a minimal "touch" technique to prevent tissue injury.

Tumor samples were collected from non-selected patients who underwent nephrectomy at Yokohama City University Hospital and its affiliated hospitals. All specimens were snap-frozen with liquid nitrogen and stored at −80 ◦C until nucleic acid extraction. All tumors were confirmed to have occurred sporadically according to the patients'medical records. The histopathology of the tumors was classified according to the classifications recommended by the Union Internationale Contre le Cancer (UICC) and the American Joint Committee on Cancer [252]. Tumor stage and grade were determined after surgical treatment according to the tumor–node–metastasis (TNM) classification [252]. Written informed patient consent was obtained for studying gene expression profiles and the study protocol was approved by the institutional ethics committee.

Immunofluorescence.

Cells were seeded onto fibronectin coated 13-mm glass coverslips (5 µg/mL fibronectin) and then incubated in normoxia or hypoxia (1% O_2) for 24 h. Afterwards cells were fixed with 4% paraformaldehyde in PBS and permeabilized with 0.5% Triton in PBS with 1% BSA, 100 µg/mL gammaglobulin and 0.05% azide. Cells were blocked for 30 min with 5% BSA in PBS with 100 µg/mL gammaglobulin and 0.05% azide and stained with the indicated primary antibodies followed by Alexa Fluor 488 or 568 labeled secondary antibodies and Phalloidin-conjugated Alexa 568 or 647. DAPI to stain cell nuclei was used. Cells were mounted in Prolong Gold (Invitrogen) and imaged with a Leica fluorescence microscope (Leica DMR 020-525.024

fluorescence microscope). Images were taken with camera Leica Microsystems CMS GmbH, D-35578 Wetzlar, DFC360 Fx (115470000) and the following objetives: Leica HCX PL APO 40x/1.25-0.75 OIL, Leica HCX PL APO 63x1.32-o,6 oil or dry objective Leica N PLAN 10X/0.25. Imaging software used was Leica Application Suit (LAS v4.1). Focal adhesion (FA) contacts were quantified with ImageJ following the protocol described by Horzum U. et al. [253].

Protein expression by Western blot analysis.

Lysates of snap frozen lung tissues (murine and human), isolated primary cells (human and murine) and human RCC cell lines were prepared in RIPA buffer (50 mM TRIS (pH 7.5), 1% NP-40, 1 mM EDTA, 125 mM NaCl, 0.25% sodium deoxycholate, 1mM sodium orthovanadate, 1 mM sodium fluoride and 1X phosphatase/protease inhibitors cocktail (Roche Applied Science, Hercules, CA). Lysates were centrifuged at 17,000x*g* for 20 min. A bicinchoninic acid assay (BioRad, Life Sciences Research, Hercules, CA) was used to quantify total protein. Lysates (30 µg/lane) mixed with 1X reducing Laemmli buffer (Bio-rad) were boiled at 95°C for 5 min, electrophoretically separated onto SDS-page gels and transferred onto nitrocellulose membranes (BioRad). Blots were probed with primary antibody to the respective proteins and afterwards with HRP-conjugated secondary antibodies. Proteins were visualized with HRP substrate (Luminata Forte, Millipore) on ImageQuant LAS 4000 (GE Healthcare Life Sciences). Alternatively, human samples were blocked in Odyssey blocking buffer (LI-COR Biosciences, Lincoln, NE), incubated overnight at 4°C with primary fluorescent labeled antibodies and visualized on an Odyssey Imaging System (Licor). The intensity of the bands was quantified using ImageQuant 5.2 or ImageJ (NIH, Bethesda, MD).

Real Time quantitative PCR analysis.

Analysis of mRNA to determine gene expression levels or analysis of heterogeneous nuclear RNA to determine transcriptional state of genes was performed by quantitative reverse transcription polymerase chain reaction (RT-Q-PCR). Cells were grown to 95% confluence in 60 mm culture dishes, and the total RNA was isolated from cells using the Trizol RNA Isolation System (Invitrogen). RNA (1 µg/sample) was reverse-transcribed to cDNA with Improm II RT (Promega, Madison, WI) in a final volume of 20 µl. For RT-Q-PCR 1 µl of cDNA was amplified with the specific primers pairs and polymerase chain reaction amplifications were performed using Power SYBR green PCR Master Mix (Applied Biosystems). The data were analyzed using StepOne Plus Software (Applied Biosystems, Carlsbad, CA). The primer pairs used to analyze *tsp1* were designed to amplify exon 2 and 3 of the tsp1 sequence, which is missing in *tsp1*$^{-/-}$ mice. Primers used for the analysis of heterogeneous nuclear RNA (hnRNA) of VCAM-1, mRNA

before splicing modification were designed for exon 3 and intron 3-4. All values were controlled with *β-Actin* gene expression levels.

Table 3: Primer pairs of genes analyzed by RT-Q-PCR

Oligos	Species	5´- 3´ Forward Sequence	5´- 3´ Reverse Sequence
β-Actin	Human Mouse	CGATGCCTGAGGCTCTTT	TGGATGCCACAGGATTCCA
tsp1	Mouse	GGTGTCCTGTTCCTGTTGCA	CCGTTATCTCCCCCAGACTCT
tsp1	Human	ACTGGGTTGTACGCCATCAGG	CTACAGCGAGTCCAGGATCAC
Kv1.5	Mouse	CTGGGTCAGCAAGAGCCATT	TCAGGCAGAGTCTCCAAGCA
Hif1α	Human	AGCCGAGGAAGAACTATGA ACATAA	GTGGCCTGTGCAGTGCAA
Hif2α	Human	CTCATCCCTGCGACCATGA	TTCCCAAAACCAGAGCCATT
Vhl	Human	CGCCGCATCCACAGCTA	TGTGTCCCTGCATCTCTGAAGA
vcam-1	Human	GTTCCTAGCGTGTACCC	GCTGACCAAGACGGTTG
vcam-1	Human (hnRNA)	CCACAGTAAGGCAGGCTGTAAA	GCAGCTTTGTGGATGGATTCA
vcam-1	Human Clinical Samples	CAAAGGCAGAGTACGCAAACAC	CTGGCTCAAGCATGTCATATTCAC
glut-1	Human	TCAACCGCAACGAGGAGAA	CTGTCCCGCGCAGCTT
phd1	Human	GCGCTGCATCACCTGTATCTAT	CCGCCATGCACCTTAACG
phd2	Human	CCCTCATGAAGTACAACCAGCAT	CATCTGCATCAAAATACCAAACAGT
phd3	Human Mouse	TGCATCACCTGCATCTACTATCTG	TACATGGTGGGATCCTGCG

For the analysis of VCAM-1 in human clinical samples the probe (5-6FAM-CAGAGATACAACCGTCTTGGTCAGCCCTTTAMRA-3) was used. PCR amplification was done using the iCycler iQ Real-time quantitative PCR Detection System (Bio-Rad Laboratories, Hercules, CA). The amount of product was measured by interpolation from a standard curve. In each experiment, at least two independent RT-Q-PCRs were done to obtain the mean expression signal values. Values were controlled with *β-Actin* gene expression levels.

siRNA-mediated gene silencing.

siRNA experiments were carried out with specific pools of siRNAs directed against human *tsp1* (sc-36665), *vcam-1* (sc-29519), *vhl* (sc-36816), *hif1α* (sc-35561), *hif2α* (sc-35316), *phd1* (sc-45616), *phd2* (sc-45537), *phd3* (sc-45799), *nik* (sc-36065), *ikkα* (sc-29365), *p52* (sc-29409) *and p50* (sc-29407) or with a non-targeted pool of control Scr siRNAs (sc-37007) from Santa Cruz Biotechnology (Santa Cruz, Heidelberg, GE). Cells were transfected with Lipofectamine 2000 (11668019, Invitrogen), according to the manufacturer's instruction. Two days after transfection silencing efficiency was analyzed and cells were used for experiments.

Cell migration.

Cells were serum starved for 3 h and then allowed to migrate across Transwell filters (6.5-mm diameter, 8 μm pore size, Costar Corning, NY) for 7 h at 37ºC and 5% CO_2 under normoxia or hypoxia (1% O_2). As a chemoatractant DMEM with 20% FBS was added into the lower chamber while basal media was used as a negative control. Non-migrating cells on the upper surface of the membrane were gently removed with Q-tips, while the migrating cells on the lower surface were fixed, stained with Diff-Quick (International Reagent, Kobe, Japan) and counted under the microscope (Leica DMR 020-525.024 fluorescence microscope) with a dry objective Leica N PLAN 10X/0.25.

Transwell permeability assays.

Transendothelial flux of FITC-dextran (molecular mass of 70 kDa; Sigma) was used as an index of endothelial paracellular permeability. hPAEC were seeded at passage five-eight at a density of 2-3 × 10^4 cells/cm^2 on Transwell polycarbonate filters, 6.5-mm diameter, 0.4 μm pore size (Costar Corning, NY). FITC-dextran (10 mg/mL) in cell medium was added to the upper chambers of the Transwell system and the monolayers were then exposed for 6-7 h to normoxia or hypoxia (1% O_2). Transfer of FITC-dextran across hPAEC monolayers was quantified after 1h in 100-μL taken from the lower chamber. As a permeability control, we treated hPAEC monolayers with 1mM

EGTA, which alters intercellular junctions increasing the FITC-dextran flux across the cell monolayer. The fluorescence was measured with a spectrophotometer (FLUOstar Omega, BMG Labtech) using 480 and 515 nm as the excitation and emission wavelengths, respectively. The absolute quantities of FITC-dextran in experimental samples were determined using a standardization curve.

Vascular contractility.

Murine pulmonary arteries were carefully dissected free of surrounding tissue, cut into rings (1.8-2 mm length) and maintained for 16 hours under normoxic or hypoxic (1% O_2) conditions in basal medium (DMEN with penicillin (100 units/mL) and streptomycin (100 units/mL)). Afterwards vessel segments were mounted on a wire myograph in the presence of Krebs physiological solution. To maintain normoxic or hypoxic conditions, buffer solutions were continuously aerated with 21% O_2, 5% CO_2 and 74% N_2 (pO2=17–19kPa) or with 95% N_2 and 5% CO_2 (pO_2=2.6–3.3kPa) respectively, and stretched to a transmural pressure equivalent to 30 mHg. Contractility was recorded by an isometric force transducer and a displacement device coupled to a digitalization and data acquisition system (PowerLab). To confirm smooth muscle viability arteries were first stimulated by raising the K^+ concentration of the buffer to 80 mmol/L and then allowed to recover. Arteries were then stimulated with serotonin (5-HT, 10 μM) and treated with a concentration-response curve of the endothelium-dependent and independent vasodilators acetylcholine (Ach, 0.001-10 μmol/L) or sodium nitroprusside (SNP, 0.01-1000 nmol/L). In other experiments vessels were pre-treated with XE991 (0.3 μmol/L) or diphenyl phosphine oxide-*1,* DPO1 (1 μmol/L), to inhibit Kv7 and Kv1.5 channels respectively.

Life cell calcium measurement:

Calcium was measured in mPASMC 10 days after cell harvesting from age matched male WT and *tsp1*$^{-/-}$ mice. Cells were seeded on Lab-Tek 4 wells (Chambered Coverglass, Thermo Scientific). When cells reached 70% confluence they were incubated for 16 h in normoxic or hypoxic (1% O_2) conditions. They were then washed with 4,5 g/L glucose supplemented Hank's Balanced Salt Solution (HBSS) and incubated at 37ºC, 5% CO_2 for 30 min with the cytosolic calcium probe Fluo-4 AM at 1 μmol/L in HBSS glucose. After incubation, the wells were washed and incubated for additional 30 min. Next, cells were time lapse photographed with a Leica SP5 Confocal Microscope every 7 seconds using a Leica dry objective HC PL APO 20X/0,75 CS2 and illuminated with a 488nm-Ar laser using spectral filtering and hybrid (HyD) detectors. To interrogate the role of potassium Kv1.5 channels in this process cells were treated with DPO1 (2 μmol/L). Images were collected using Leica TCS software, and the increase in the fluorescence

peak was quantified using ImageJ (NIH, Bethesda, MD). As a control of calcium measurement, we quantified the fluorescence of cells treated with Ionomycin (1 µmol/L).

Flow cytometry analysis.

VCAM-1 levels on the cell surface were measured by flow cytometry. 786-O cells and their counterparts stably expressing VHL were cultured under normoxia or hypoxia (0.5% O_2) for 24 h. Afterwards cells were washed and resuspended in PBS at $1x10^6$ cells/ml, then incubated with anti-VCAM-1 antibody for 1h at 4ºC. After this time non-bound antibody was washed out and the cells were incubated with Alexa Fluor 488 goat anti-mouse secondary antibody for 30 min at 4ºC. VCAM-1 expression was quantified using a FACS®Calibur flow cytometer (Becton Dickinson).

Co-culture adhesion experiments.

786-O cells stably transfected with VHL or empty vector (pRv) and with siScr or siVCAM-1 were grown at confluence in a 24-multiwell plate ($30x10^3$ cells/well). When indicated, cells were grown under hypoxia (0.5% O2) for 24 h previous to adhesion experiments. THP-1 or U937 monocytic cell lines from the American Type Culture Collection (ATCC, Rockville, MD, USA) were labelled with the fluorescent dye calcein AM 2.5 mM in serum-free medium for 20 min at 37ºC. Then cells were washed and resuspended in adhesion buffer (HEPES-buffered Hanks' balanced salt solution containing 1% bovine serum albumin, 2 mM MgCl2, 2 mM CaCl2, and 0.2 mM MnCl2) and added (60x103 cells/well) on top of the ccRCC monolayer and both cell lines were allowed to interact for 20 min at 37ºC. When indicated, cells were incubated with anti-α4 (HP2/1) [254], anti-β1 (VJ1/14) [255] or anti-αL (TS1/11) [256] blocking antibodies, kindly provided by Dr Sanchez-Madrid (Universidad Autónoma of Madrid, Madrid, Spain). After 15 min at 37ºC membranes were washed with adhesion buffer. Afterwards unbound THP-1 or U937 monocytic cells were gently removed and bound monocytes were fixed with 3% paraformaldehyde and counted under a fluorescence microscope (Leica DMR 020-525.024 fluorescence microscope). Images were taken with camera Leica Microsystems CMS GmbH, D-35578 Wetzlar, DFC360 Fx (115470000), objective Leica HCX PL APO 100x/1.40-0.7 OIL CS and the imaging software used was Leica Application Suit (LAS v4.1).

Cytotoxicity assays.

These assays were performed with the xCELLigence System (Roche) that measures electrical impedance across micro-electrodes integrated in the bottom of tissue culture plates. This provides quantitative information about the status of the adherent cells, including viability. Co-cultures of ccRCC (2500 cells) with M1 differentiated monocytic cells (activated with 100 U/ml INF-γ and 2 µg/mL LPS, in a proportion of 1/60 respectively were monitored for 96 h with measures every 5 min. Cellular index normalized with RTCA Software (Roche, Applied Science, Germany), was expressed as percentage of living cells.

Passive CLARITY.

Detailed protocol (modified from Dr Rinaman´s lab. [257]) used to clarify mice lungs,

Table 4: Reagents for CLARITY.

Reagent:	Source/Product #
40 % Acrylamide solution	BioRad, 161-0140
10X Phosphate-buffered saline, pH 7.4	Invitrogen, GIBCO 10010
2,2-Azobis[2-(2-imidazolin-2-yl)propane] dihydrochloride (VA-044 initiator)	Wako, 27776-21-2
Paraformaldehyde aqueous solution, 16 %	Electron Microscopy Sciences, 15710-S
Boric acid	Sigma–Aldrich, B3637
Sodium dodecyl sulphate (SDS)	Promega, H5114
2,20-Thiodiethanol	Sigma–Aldrich, 166782
Mineral oil	Fisher Scientific # S25439A

Solutions:

1. Hydrogel solution: Paraformaldehyde (PF)- acrylamide. (Post-fixation solution) 1X (PBS, pH 7.4; prepared by diluting 10X PBS 1:10 in dH2O) containing 4.0 % PF (vol/vol), 4.0 % acrylamide (vol/vol), and 0.25 % VA-044 initiator (wt/vol). Briefly, PF, acrylamide and VA-044 were stirred into 1X PBS at room temperature to dissolve, then immediately chilled on ice

and kept cold until used within 1–2 h. Additional solution (30 ml/lung) was reserved for post-fixation and hydrogel polymerization.

2. Tissue clearing solution: 0.2 M boric acid (pH 8.5) containing 4.0 % sodium dodecyl sulphate (SDS).
3. Rinsing buffer for immunofluorescent labeling (IFL): 0.5M boric acid (pH 8.5) containing 0.1 % triton- X100.
4. Antibody diluent for IFL: 0.5 M boric acid containing 0.1 % triton-X100 and 1.0 % normal donkey serum.
5. Refractive index matching (RIM) medium: 2,20-Thiodiethanol (TDE) diluted to concentrations of 20, 40 and 60 % in 1X PBS. (*RIM has to be conducted at RT without shaking).*

Protocol:

Animals were sacrificed by first administering inhalation general anaesthesia (pentobarbital sodium, 130mg/kg) followed by cervical dislocation. Mice were perfused transcardially with 10-30 ml of ice-cold 1XPBS, and then transcardially and intratracheally with 50-100 ml of ice-cold hydrogel solution. Lungs were extracted and placed into 50 ml Falcon conical tubes containing 30 ml of post-fixation hydrogel solution and stored overnight at 4ºC. To minimize exposure of hydrogel-immersed lungs to oxygen, a 1 cm-thick layer of mineral oil was gently laid over the top of the hydrogel solution before the tubes were tightly capped. The day after, hydrogel was polymerized at 37ºC for 3h in a water bath without shaking. Then, the excess of hydrogel of the organs was removed in order to make an easier clarification. At this point the organs can be cut into pieces for faster clarification, although tissues in this work were integrally clarified.

Tissue samples were submerged into 40 ml of tissue clearing solution in 50 ml Falcon conical tubes and placed onto a rotating platform at 37ºC to enable passive clearing. Clearing solution was replaced every day during the first week and subsequently three times a week until the tissue was visibly cleared. Tissues can be stored in clearing solution for up to 9 months at RT. Then, cleared samples were transferred into a 20 ml glass scintillation vial to perform IFL. First, samples were rinsed to remove residual SDS, then they were incubated for 72 h with the indicated primary antibodies (antibodies were diluted in IFL antibody diluent) and then rinsed with four changes of rinsing buffer along 24 h. Afterwards they were incubated for 72 h with the appropriated secondary antibody. Samples were finally rinsed and washed with 1XPBS for 24 h. Antibody incubations and rinses were conducted onto a rotating platform in a 37 °C incubator.

Cleared tissue needs to be submerged in TDE solutions at progressively higher concentrations to achieve the correct refractive index matching (RIM). To that end, clarified organs were

sequentially submerged in 20%, 40% and 60% TDE solution for 4-12h each (time depends on tissue size). The tissues were washed (3xtimes) with fresh 60% TDE solution at RT for late imaging of IFL. (*The 60 % concentration of TDE has a refractive index of 1.45* [258] *matching the refractive index of clarified tissues. This is very important for immersion objectives, even though in this work images were taken with a dry objective).* At the end, samples were placed into 30 mm MatTeK Botton Glass (MATTEK corporation Massachusetts USA), and covered with 60% TDE solution for imaging. Images were obtained with a Leica SP5 Confocal Microscope using a Leica dry objective N PLAN 10X/0.25, illuminated with a 561 nm dioded-pumped solid state laser using hybrid (HyD) detector. Images were collected using Leica LAS 4.0 image collection software and 3D reconstruction and videos were made using IMARIS software.

Statistical analysis.

The data are presented as the mean ± standard error of the mean (SEM) for all the studies. ANOVA followed by Bonferroni's post hoc test was used when comparing three or more groups and two-tailed Student's t-test was used to compare two groups, according with the conditions of normality and homoscedasticity. Shapiro-Wilk normality test and Brown–Forsythe test were used to analyze these conditions. In case the assumptions of normality and homoscedasticity were not accomplished we used non-parametrical statistic tests; Mann Whitney test to compare two groups and Kruskal-Wallis followed by Dunn's post hoc test to compare three or more groups. P value of less than 0.05 was considered significant. Additionally, we used a trend test in those experiments where we wanted to show changes along the time, P-trend less than 0.05 was considered significant.

RESULTS

RESULTS

1. HYPOXIA AND PULMONARY HYPERTENSION: HYPOXIC REGULATION OF TSP1 AND ITS EMERGING TOLE IN PULMONARY HYPERTENSION.

1.01 Hypoxia-mediated induction of pulmonary TSP1 parallels stabilization of HIF2α.

Previously we showed that chronic hypoxia increases TSP1 expression in the lung [169]. Extending these results, we found that WT mice subjected to hypoxia (10% O_2) for 7h or 24h experience an increase in pulmonary TSP1 mRNA levels concurrent with induction of *phd3*, a known hypoxia sensitive gene [259] (Figure 8). Analysis of TSP1 mRNA levels in *tsp1*$^{-/-}$ mice showed no detectable levels of TSP1 message but demonstrated significant induction of *phd3* under hypoxia (Figure 8). Analysis of protein levels in WT mice under hypoxia demonstrated a rapid time-dependent increase in TSP1 that was matched by parallel increase in the levels of HIF2α (Figure 9). As expected, *tsp1*$^{-/-}$ mice lungs showed no evidence of protein post-hypoxia (Figure 9).

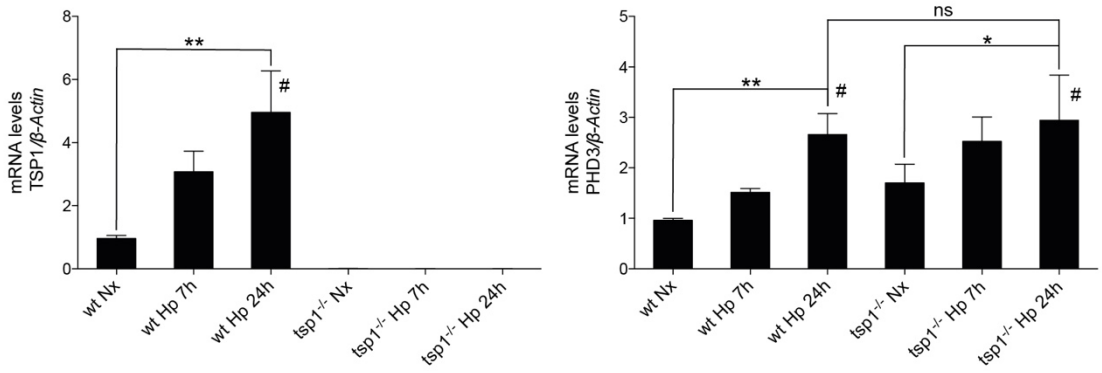

Figure 8: Hypoxia-mediated induction of TSP1 mRNA in mice lungs. Quantitative RT-Q-PCR analysis was performed to determine TSP1 mRNA expression levels in lung samples from WT and *tsp1*$^{-/-}$ mice exposed to normoxia (Nx) or hypoxia (Hp) -10% O_2- for the indicated time points. mRNA levels are expressed as fold change over WT in normoxic conditions and controlled with *β-Actin* as the housekeeping gene. The hypoxia reporter gene *phd3* was analyzed in the same samples as a control of hypoxic stress. Statistical analysis between different conditions was made using two-way ANOVA test followed by Bonferroni's post hoc test, * P<0.05, **P<0.01; # P-trend<0.05. Results are expressed as means ± SEM. (n=4), ns (not significant).

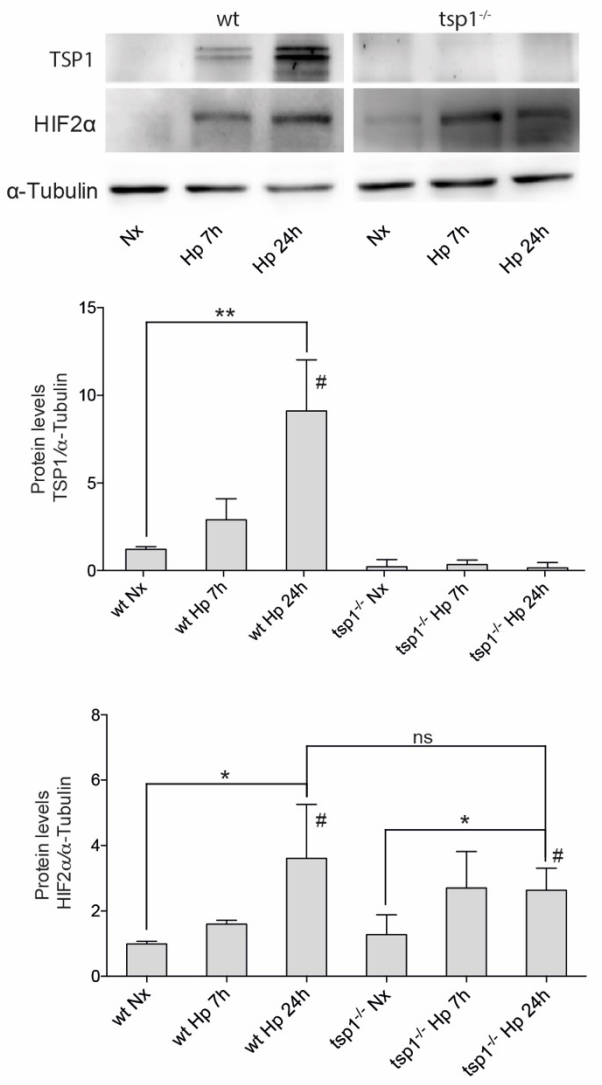

Figure 9: Hypoxia-mediated induction of TSP1 protein in mice lungs. Protein levels in lung samples from WT and *tsp1*$^{-/-}$ mice challenged with normoxia (Nx) or hypoxia (Hp) were detected via Western blot probed against TSP1, HIF2α and α-Tubulin as a loading control. Quantification of TSP1 and HIF2α bands was done by densitometry and controlled with α-Tubulin. Protein levels are expressed as fold change over WT in normoxic conditions. Statistical comparisons between different conditions were made using a Kruskal-Wallis followed by Dunn's post hoc test, * P<0.05. **P<0.01. # P-trend<0.05. Results are expressed as means ± SEM. (n=4), ns (not significant).

1.02 Hypoxia upregulates TSP1 in pulmonary vascular and non-vascular cells.

TSP1 is produced and secreted by systemic arterial VSMC [260], fibroblasts and endothelial cells [261]. However, it is not known if PASMC cells and PAEC, and pulmonary-derived fibroblasts produce TSP1 and whether this process is modulated by changes in oxygen tension. To test this, we isolated pulmonary fibroblasts (mFIB) and pulmonary arterial smooth muscle cells (mPASMC) harvested from murine (WT and *tsp1*$^{-/-}$) lungs and PAs respectively and confirmed

their linage by staining with specific markers for SMC, like smooth muscle actin (SMA) and calponin 1 (CNN-1) (Figure 10).

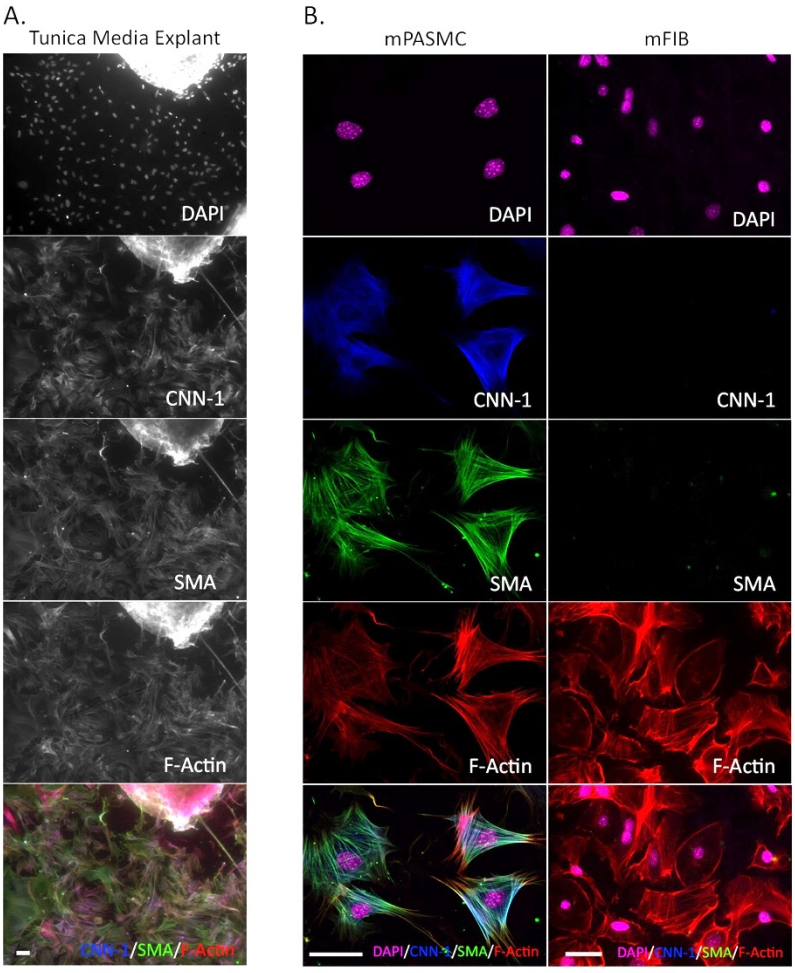

Figure 10: Characterization of mPASMC and mFIB. A. Staining of tunica media explant of murine PA and **(B)** mPASMC and lung derived fibroblast (mFIB) 7 days after extraction. Visualization of DAPI (purple), CNN-1 (blue), SMA (green) and F-Actin (red). Cells were grown on fibronectin (5 µg/ml)-coated coverslips. Images shown are representative of three experiments. Bars, 50 µm.

Then we challenged them with hypoxia (1% O_2) for 24h. Our results demonstrated that hypoxia significantly increased TSP1 mRNA levels in mFIB and stimulated a modest but not significant increase in mPASMC (Figure 11A). Accordingly, TSP1 protein levels were significantly increased in mFIB and mPASMC cell types after a hypoxic challenge (Figure 11B). To more precisely define the hypoxic induction of pulmonary TSP1, we employed fluorescent imaging of normoxic and hypoxic cells. Immunofluorescence imaging confirmed increased TSP1 levels in hypoxic mFIB and mPASMC that was localized to the peri-nuclear cytoplasm (Figure11C). The

same set of experiments were performed in human pulmonary endothelial cells (hPAEC). TSP1 mRNA and protein levels were upregulated under hypoxic conditions and the same peri-nuclear cytoplasm staining of TSP1 was found (Figure 12).

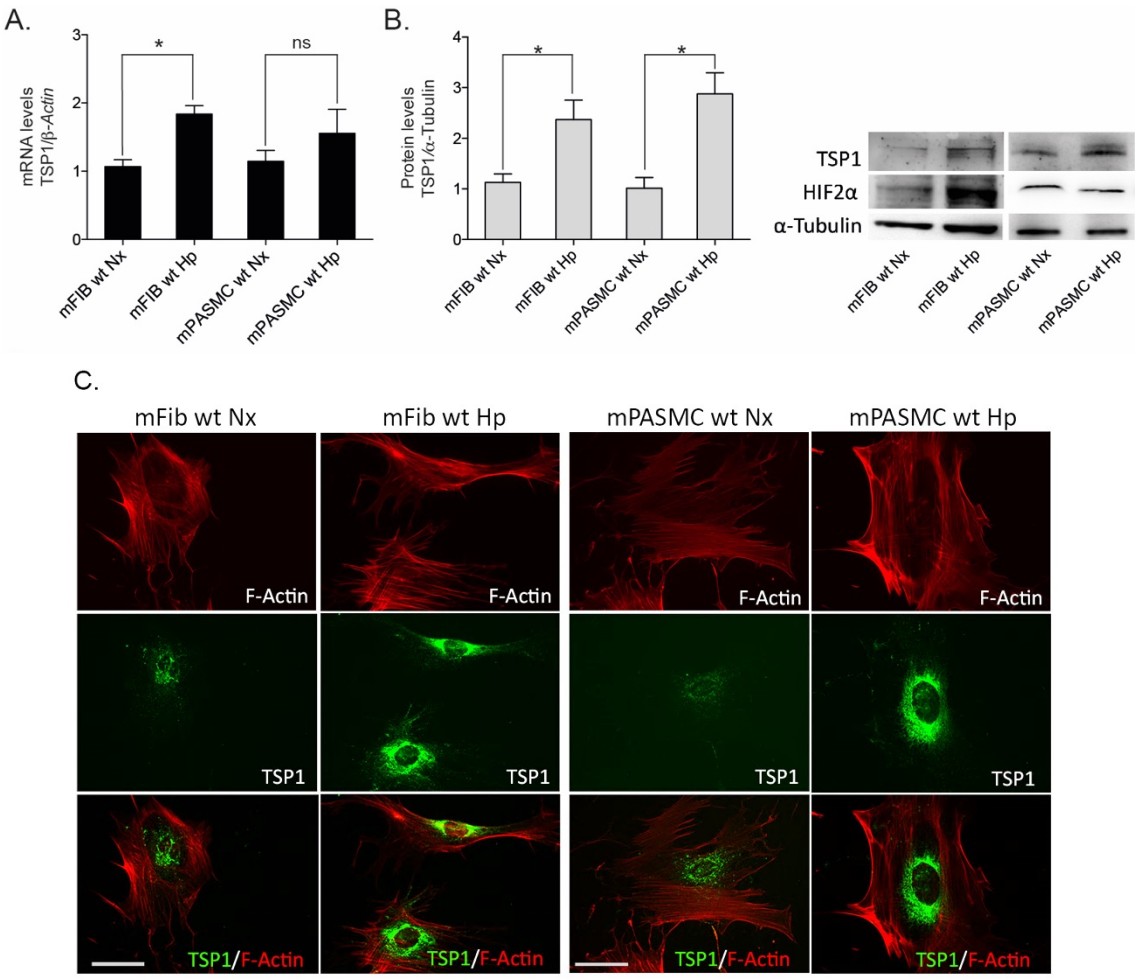

Figure 11: Hypoxia upregulates TSP1 in mouse pulmonary vascular and non-vascular cells. A. mFIB and mPASMC from WT were exposed to normoxia (Nx) or hypoxia (Hp) -1% O2- for 24 h and changes in mRNA levels determined by RT-Q-PCR. TSP1 mRNA levels are expressed as fold change over normoxic conditions and controlled with *β-Actin* as the housekeeping gene. Average ± SEM of n=3 performed is shown. * $p<0.05$. Student´s T-test, ns (not significant). **B.** Protein levels from mFIB, and mPASMC exposed to normoxia (Nx) or hypoxia (Hp) -1% O2- for 24 h were detected by Western blot probed against TSP1, HIF2α and α-Tubulin as a loading control. Densitometric analysis was performed to quantify TSP1 bands and levels were controlled with α-Tubulin and expressed as fold change over Nx. Average ± SEM of n=3 performed is shown. * $p<0.05$. Student´s T-test, ns (not significant). **C.** Visualization of TSP1 (green) and F-Actin (red) in mFIB, mPASMC grown on fibronectin (5 µg/ml)-coated coverslips. Images shown are representative of three experiments. Bars, 50 µm.

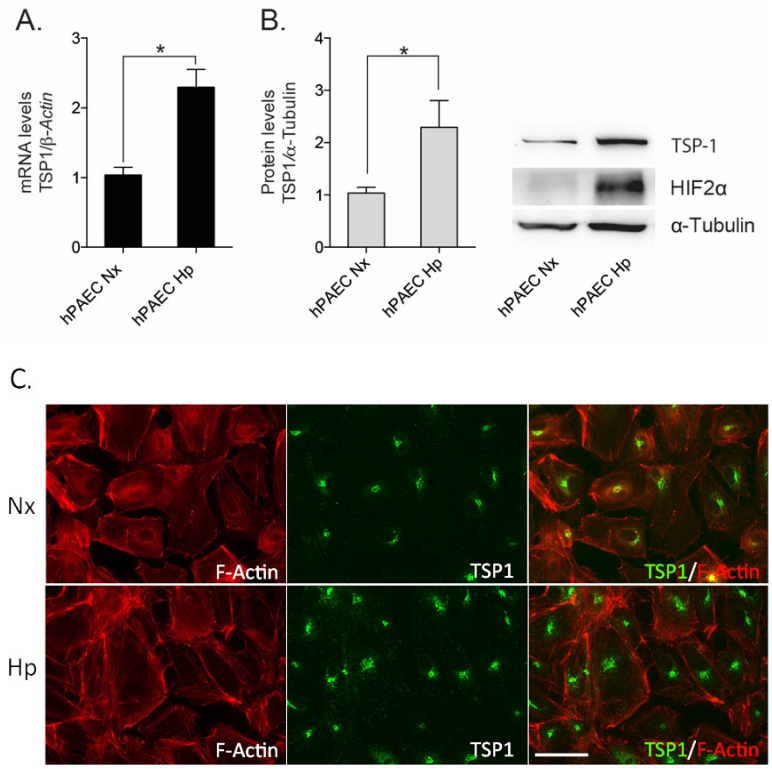

Figure 12: Hypoxia upregulates TSP1 in human hPAEC. A. hPAEC were exposed to normoxia (Nx) or hypoxia (Hp) -1% O2- for 24 h and changes in mRNA levels determined by RT-Q-PCR. TSP1 mRNA levels are expressed as fold change over normoxic conditions and controlled with *β-Actin* as the housekeeping gene. Average ± SEM of n=3 performed is shown. * $p<0.05$. Student´s T-test, ns (not significant). **B.** Protein levels from hPAEC exposed to normoxia (Nx) or hypoxia (Hp) -1% O2- for 24 h were detected by Western blot probed against TSP1, HIF2α and α-Tubulin as a loading control. Densitometric analysis was performed to quantify TSP1 bands and levels were controlled with α-Tubulin and expressed as fold change over Nx. Average ± SEM of n=3 performed is shown. * $p<0.05$. Student´s T-test, ns (not significant). **C.** Visualization of TSP1 (green) and F-Actin (red) in hPAEC grown on fibronectin (5 µg/ml)-coated coverslips. Images shown are representative of three experiments. Bars, 50 µm.

1.03 HIF2α regulates TSP1 levels in mouse lung.

From the above studies, it was apparent that hypoxia rapidly upregulated TSP1 transcript in the lung. Nonetheless, it remained unknown at what level HIF controlled TSP1 expression. Since both HIF1α and HIF2α null mice are resistant to pulmonary hypertension [160, 161] as well as the *tsp1*$^{-/-}$ mice [169, 190], we wondered whether HIFα activation was sufficient to produce TSP1 induction in the lung. To this aim we generated mice deficient in the von Hippel Lindau protein (VHL). Mice lacking the VHL gene (*vhl*$^{-/-}$) no longer process HIFα protein for degradation under normoxia [63, 248], and therefore phenocopy hypoxic WT mice. Pulmonary TSP1 mRNA and protein levels in normoxic *vhl*$^{-/-}$ mice were significantly increased compared to the levels in normoxic WT mice (Figures 13A, B). To assess whether HIF1α or HIF2α were required for

hypoxia-mediated induction of pulmonary TSP1 we generated mice in which both VHL and HIF2α or VHL and HIF1α were simultaneously inactivated (*vhl*$^{-/-}$*/hif2α*$^{-/-}$, *vhl*$^{-/-}$*/hif1α*$^{-/-}$ *respectively*) and analyzed pulmonary TSP1 levels. In contrast to the induction observed in *vhl*$^{-/-}$ mice, pulmonary TSP1 mRNA and protein levels in *vhl*$^{-/-}$*/hif2α*$^{-/-}$ double knockout mice were decreased (Figures 13A, B), while in *vhl*$^{-/-}$*/hif1α*$^{-/-}$ TSP1 mRNA levels remained induced (Figure 6A). To confirm the role of HIF2α in regulating pulmonary TSP1, we exposed *hif2α*$^{-/-}$ mice to chronic hypoxia. As in double knockout mice, hypoxia did not upregulate pulmonary TSP1 in *hif2α*$^{-/-}$ mice (Figure 13B).

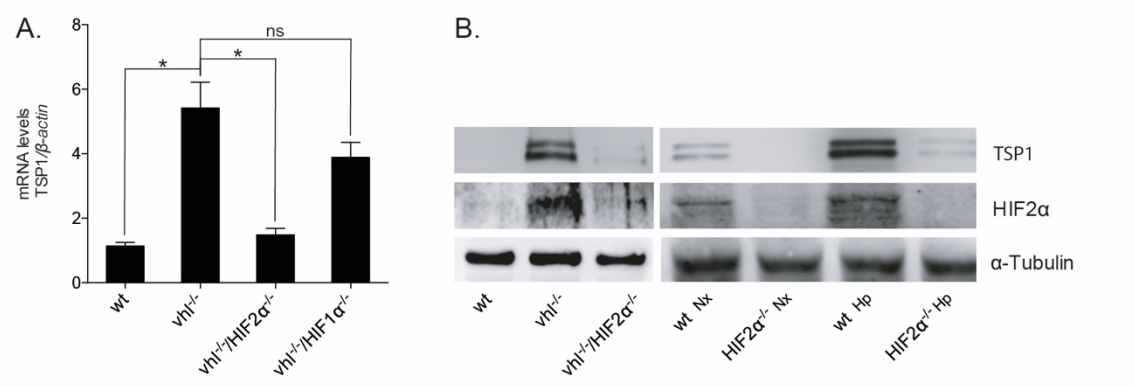

Figure 13: HIF2α regulates TSP1 levels in the mice lung. A. Quantitative RT-Q-PCR analysis was performed to determine TSP1 mRNA expression levels in lung samples from WT, VHL deficient (*vhl*$^{-/-}$), VHL/HIF2α (*vhl*$^{-/-}$*/hif2α*$^{-/-}$) and VHL/HIF1α (*vhl*$^{-/-}$*/hif1α*$^{-/-}$) double deficient mice. mRNA levels are expressed as fold change over WT and controlled with *β-Actin* as the housekeeping gene. Average ± SEM of n=4 performed is shown. Statistical comparisons between different conditions were made using Kruskal-Wallis followed by a Dunn's post hoc test, * P<0.05, ns (not significant). **B.** Protein levels in lung samples from WT, *vhl*$^{-/-}$, *vhl*$^{-/-}$*/hif2α*$^{-/-}$ and *hif2α*$^{-/-}$ mice under normoxia (Nx) or hypoxia (Hp) -10% O_2- for 3 days were analyzed by Western blot. Representative images of three experiments are shown.

To further extend these results to human lung, we analyzed TSP1 levels in hPAEC following HIF1α or HIF2α interference. Interestingly, hypoxia-mediated induction of TSP1 mRNA was downregulated in hPAEC treated with the HIF2α siRNA (Figure 14). When protein levels were analyzed in hPAEC, we observed no increase in TSP1 levels in hypoxia following HIF2α suppression (Figure 14).

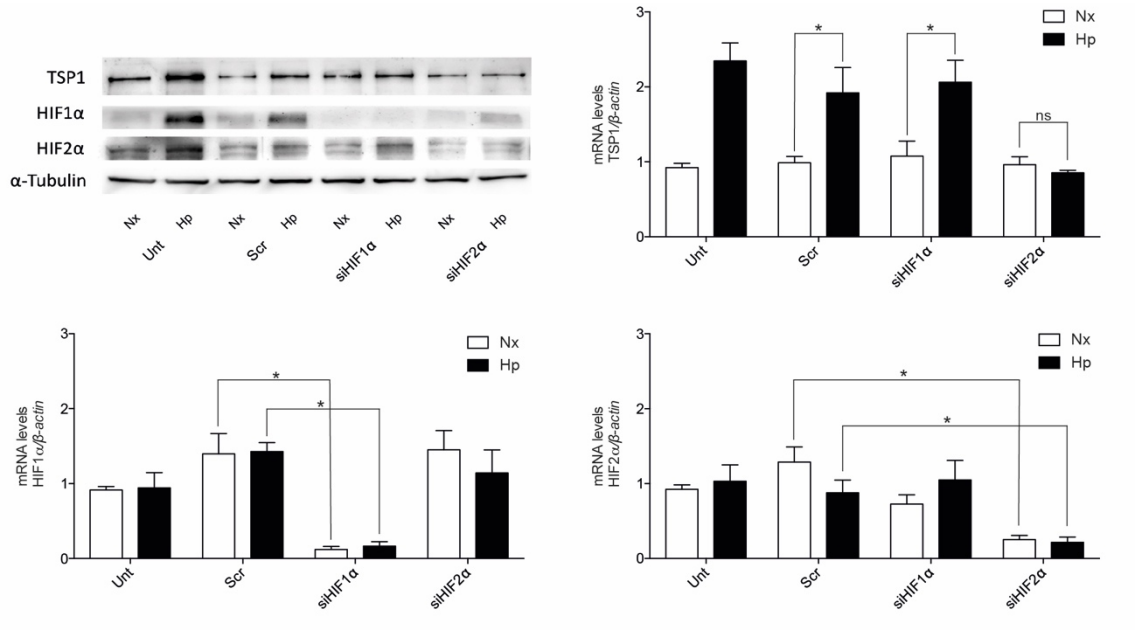

Figure 14: HIF2α regulates TSP1 levels in hPAEC. Protein and mRNA levels of TSP1, HIF1α, HIF2α from hPAEC untreated or transfected with scrambled (Scr), HIF1α or HIF2α siRNA and then exposed to Nx or Hp -1% O_2- for 24h. Western blot is controlled with α-Tubulin. Representative images of four experiments are shown. mRNA expression levels are expressed as fold change over normoxic conditions and controlled with *β-Actin* as the housekeeping gene. Average ± SEM of n=4 performed is shown. Statistical comparisons between different conditions were made using two-way ANOVA followed Bonferroni´s post hoc test, * P<0.05 was considered significant. n=4. ns (not significant).

1.04 TSP1 protein levels are increased in PAs of PAH-patients.

Extending cell and animal studies, we performed Western blot analysis of 5th order PAs from individuals with (n=15) and without PAH (n=8). Paralleling results obtained in mice, we found upregulation of pulmonary TSP1 protein in PA samples from PAH compared to non-PAH individuals. Interestingly though, HIF2α as well as HIF1α protein levels were increased in PA samples from PAH (Figure 15).

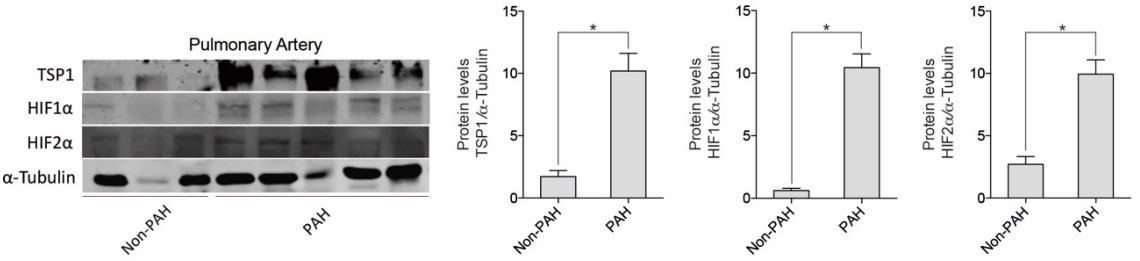

Figure 15: Analysis of TSP1 levels in PAs of PAH-patients. Western blot analysis of lysates of 5th order PAs from non-PAH and PAH human lungs was performed against TSP1, HIF1α, HIF2α and α-Tubulin as loading control. Representative blots and densitometry (average ± SEM) are presented as the mean ratio of

target protein to α-Tubulin respectively (n=8 normal and 15 PAH samples), Mann-Whitney test corrected by Bonferroni´s post hoc test was performed, * $p<0.05$.

1.05 The proximal promoter region of *tsp1* contains functional Hypoxia Response Elements (HREs).

We analyzed the proximal promoter region of *tsp1*and identified two putative HREs between positions -1120 to -1196 (site 1) and -249 to -225 (site 2) relative to the transcription starting site. These sites contained the core RCGTG/C sequence and were selected based on the highest score corresponding to potential HRE sites published in the literature [262]. Further, these sites corresponded with open chromatin and transcription factors binding site clusters that are highly conserved among different mammalian species (Figure 16).

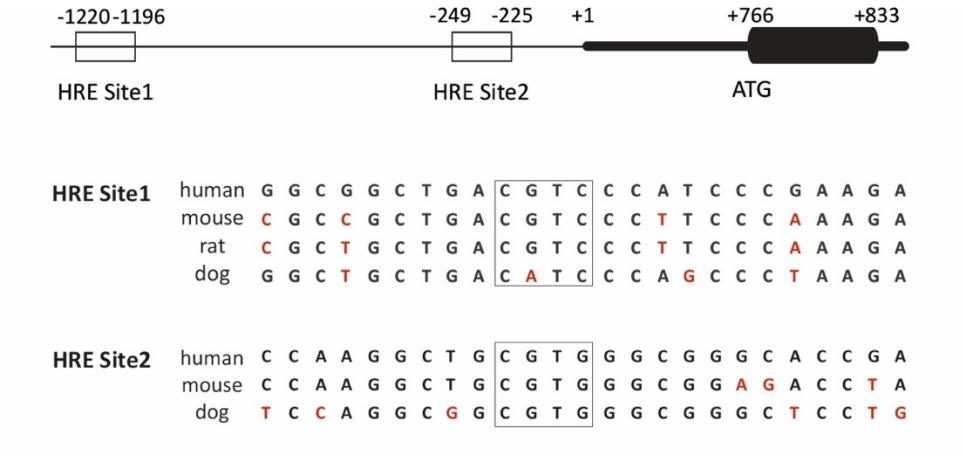

Figure 16: Localization of HREs in the proximal promoter sequence of *tsp1*. Blast sequence alignment of the *tsp1* proximal promoter sequence of different mammalian species containing conserved HRE sites (Site 1 and Site 2), boxes mark core sequences of HRE sites.

To establish a possible direct interaction of HIF with these putative *tsp1* HRE regulatory sites, we performed luciferase reporter assays. We inserted *tsp1* HRE site 1 or HRE site 2 with three copies in tandem in the luciferase reporter plasmid pGL4.23. CHO.K1 cells were co-transfected with these HREs and the constitutive active forms of HIF1α or HIF2α, (HIF1α $(P\text{-}A)^2$ or HIF2α $(P\text{-}A)^2$ respectively) [193]. Reporter activity demonstrated a HIF2α-mediated significant induction (4- and 18-fold in HRE site 1 and HRE site 2 respectively) (Figure 17A). These results clearly indicate that HIF2α interacts with both HRE, and on the other hand this interaction reports functional activity. It is worth mentioning that HIF2α displayed a higher reporter activity on *tsp1* HRE site 2 compared to HRE site 1. To validate these vectors, we employed as a control the luciferase vector p3EGR.Luc bearing a well know functional HRE of VEGF [251] (Figure 17B).

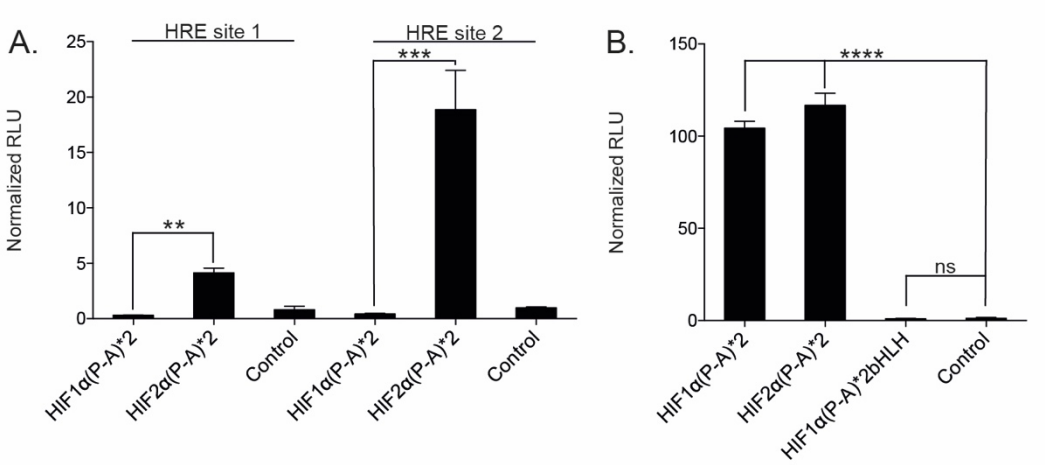

Figure 17: HIF2α functionally binds to HREs of the *tsp1* proximal promoter sequence. A. Luciferase reporter activity assay of *tsp1* HREs. Equal numbers of CHO.K1 cells were plated in 24 wells plate ($5x10^5$ cells per well) and co-transfected with PGL4.23-3xHRE1 (HRE site 1) or PGL4.23-3xHRE2 (HRE site 2) and with pRV-GFP-HIF1α(P-A)^2 (HIF1α(P-A)*2) or pRV-GFP-HIF2α(P-A)^2 (HIF2α(P-A)*2) or pRV-GFP empty vector as control. pRL-SV40 (*Renilla*) was included in all transfections as a luciferase internal control. 24 hours after co-transfection cells were lysed and analyzed for luciferase activity. Results are expressed as means ± SEM of relative light units (RLU) normalized to control. Statistical comparisons between different conditions were made using Kruskal-Wallis, followed by a Dunn's post hoc test, **P<0.01, ***P<0.001, n=8. **B.** HIF1α and HIF2α functionally binds to hypoxia response elements of the VEGF promoter. Luciferase reporter activity assay of VEGF HRE. CHO.K1 cells were seeded into a 24 wells plate at equal cell number (5x105 cells per well) and co-transfected with p3EGRLuc-9xHRE.VEGF and with pRV-GFP-HIF1α(P-A)2 (HIF1α(P-A)*2) or pRV-GFP-HIF2α(P-A)2 (HIF2α(P-A)*2) or pRV-GFP-HIF1α(P-A)2bHLH (HIF1α(P-A)*2bHLH), the latest with an additional mutation that inhibits its transcriptional activity, or pRV-GFP empty vector as control. pRL-SV40 (Renilla) was included in all transfections as a luciferase internal control. Luciferase activity was analyzed 24 hours after co-transfection. Results are expressed as means ± SEM of relative light units (RLU) normalized to control. n=3.

1.06 TSP1 stimulates de-adhesion to promote hypoxia-mediated migration of pulmonary-derived fibroblasts and PASMC.

In pulmonary vasculature activation, subsequent migration of fibroblasts and myofibroblasts into the medial layer of vessels have been suggested to contribute to vessel remodeling [263, 264]. Although TSP1 is known to promote migration of cells under normoxia [265, 266], it is unknown if TSP1 controls the migratory activity of mFIB and mPASMC under either normoxia or hypoxia. To assess this, we tested *in vitro* cell migration with the classic transwell assay. mFIB and mPASMC harvested from WT and *tsp1*$^{-/-}$ mice were incubated under normoxia or hypoxia (1% O_2) for 7 h and migration determined. In response to normoxia both WT and *tsp1*$^{-/-}$ mPASMC and mFIB displayed similar migratory capacity (Figures 18). In contrast, under hypoxic conditions WT mFIB displayed significantly greater migratory response compared to *tsp1*$^{-/-}$ cells

Also, hypoxia increased migration in mPASMC from WT but not from *tsp1*$^{-/-}$ mice (Figure 18).

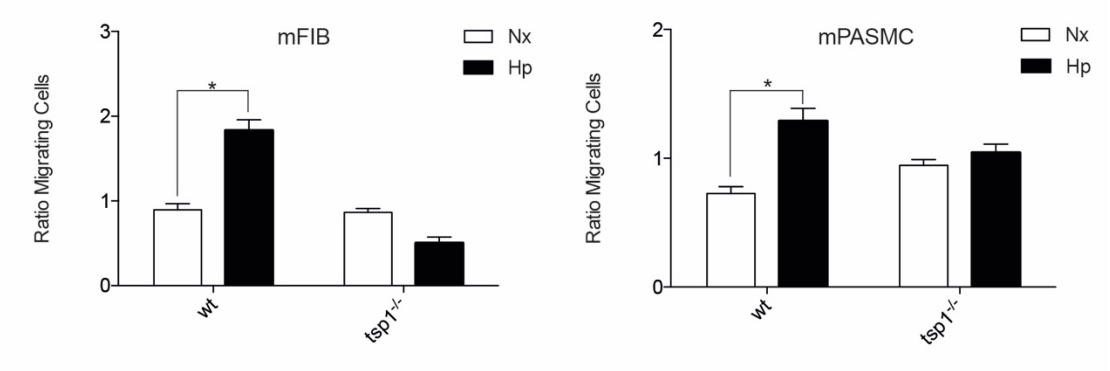

Figure 18: Analisis of TSP1 effects on migration of mFIB and mPASMC. Migration of mFIB **(A)** and mPASMC **(B)** from WT and *tsp1*$^{-/-}$ mice was assessed in transwell assays. Cells (12 x 103 cells/well) were serum-starved for 3 h and then allowed to migrate for 7 h at 37ºC and 5% CO2 under normoxia (Nx) or hypoxia (Hp) -1% O2-. As chemoattractant, DMEM with 20% FBS was added into the lower chamber, and basal media was used as a negative control. Number of cells migrated are represented as fold ± SEM over WT under normoxic conditions. Statistical comparisons between different conditions were made using a Kruskal-Wallis followed by Dunn's post hoc test, * P<0.05. was considered significant, n=4, ns (not significant).

Focal adhesion (FA) disassembly promotes cell motility [267]. Interestingly TSP1 is an intermediate of cell adhesion and stimulates disassembly of FA contacts [268, 269]. Consistent with this, hypoxic WT mFIB and mPASMC exhibited reduced adhesion to fibronectin substrate, which correlated with a decrease in FA contacts, compared to cells from *tsp1*$^{-/-}$ mice (Figure 19).

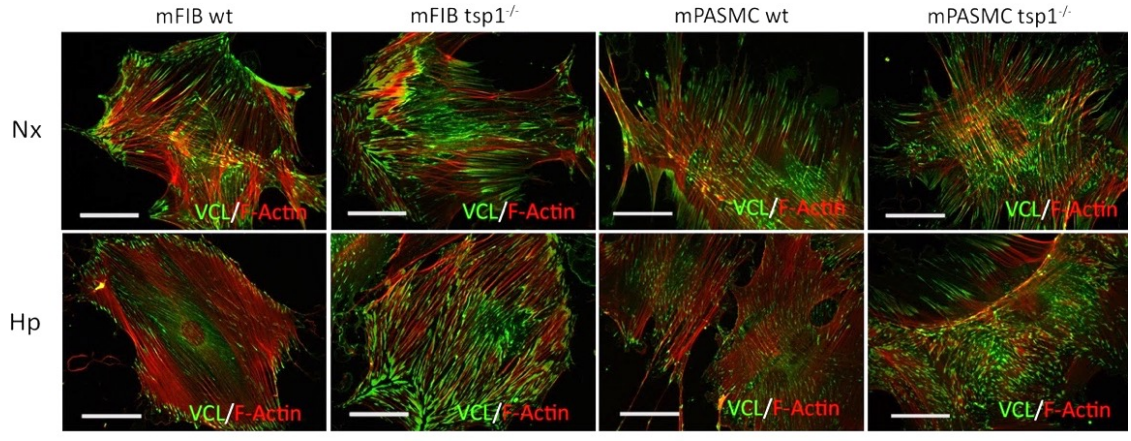

Figure 19: Effect of TSP1 on the adhesive capacity of mFIB and mPASMC. Visualization of cell adhesion plaques. mFIB and mPASMC grown on fibronectin (5 µg/ml)-coated coverslips were cultured under normoxia or hypoxia (1% O2) for 24 h, then fixed, permeabilized and incubated with monoclonal antibody to Vinculin (VCL), visualized with Alexa 488 (green), together with phalloidin 568 (red) to stain actin filaments (F-Actin). Images shown are representative of three experiments and at least 30 cells per condition. Bars, 50 µm.

Quantification of the percentage of total FA contacts per cell area, the average area of an individual FA contacts and the number of FA contacts per cell area, all demonstrated decreased adhesiveness of WT mFIB and mPASMC under hypoxic conditions, consistent with their demonstrated increased migratory capacity (Table 5).

Table 5: FAs quantification of WT and *tsp1*$^{-/-}$ mFIB and mPASMC under normoxia and hypoxia (Corresponding to Figure 19).

	Total % of FAs/cell area	**Mean FA area (μm^2)**	**FAs/cell area (μm^2)**
mFIB			
wt Nx	19,95 ± 1,57	7,06 ± 0,30	2,61 x 10^{-2} ± 2,99 x 10^{-3}
wt Hp	13,36 ± 1,23	5,94 ± 0,24	2,00 x 10^{-2} ± 1,69 x 10^{-3}
tsp1$^{-/-}$ Nx	22,90 ± 1,84	7,36 ± 0,29	3,46 x 10^{-2} ± 2,37 x 10^{-3}
tsp1$^{-/-}$ Hp	22,55 ± 1,51 *	7,48 ± 0,31 *	3,13 x 10^{-2} ± 2,02 x 10^{-3} *
mPASMC			
wt Nx	18,75 ± 1,65	6,64 ± 0,23	2,86 x 10^{-2} ± 1,88 x 10^{-3}
wt Hp	15,29 ± 1,20	5,87 ± 0,16	2,53 x 10^{-2} ± 1,55 x 10^{-3}
tsp1$^{-/-}$ Nx	22,05 ± 1,30	7,20 ± 0,17	3,04 x 10^{-2} ± 1,37 x 10^{-3}
tsp1$^{-/-}$ Hp	24,91 ± 1,60 *	7,17 ± 0,17 *	3,45 x 10^{-2} ± 1,79 x 10^{-3} *

The data are presented as average ± SEM. Total % of FAs/cell area = Sum of all FAs area in one cell divided by the total area of the cell. Mean FA area = Area of a single FA. FAs/cell area = Number of FAs in one cell divided by the total area of the cell. Number of experiments = 3. Number of cell analysed = 50-60 per treatment condition, number of FAs analysed = 400-1500 per cell. Two-way ANOVA followed by Bonferroni´s test was used. * Significance vs. WT Hp, P<0.001.

1.07 Hypoxia-mediated increase of TSP1 destabilizes PAEC junctions and increases paracellular permeability.

The above results indicated that TSP1 induces FA disassembly in mFIB and mPASMC. Related to this prior, reports have shown that TSP1 also regulates intercellular junctions in PAEC [270]. Junctions between endothelial cells are essential for the correct function of the endothelium, which has two main roles; shield the underlying vascular layers from the blood, and receive and send cell signaling. The resulting loss of endothelial barrier integrity may provide a surreptitious avenue for proliferative mediators to come in direct contact with the subendothelium, leading to cell proliferation in the medial and adventitial vascular layers [271]. Moreover, after the initial

damage, endothelial cells start to growth abnormally by monoclonal endothelial expansion creating the plexiform lesions, this contributing to endothelial dysfunction. [146]. Therefore, we aimed to determine whether the hypoxia-mediated induction of TSP1 could also influence endothelial cell function. To this aim we transfected hPAEC with a control or siRNA against TSP1 and then cultured them in normoxia or hypoxia and conducted permeability studies in the absence or presence of exogenous TSP1.

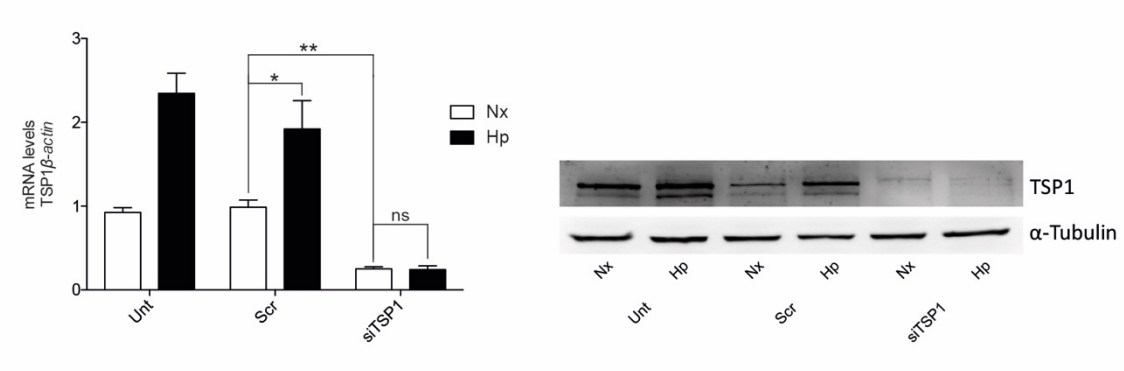

Figure 20: TSP1 silencing in hPAEC. hPAEC were untreated or transfected with scrambled (Scr) or specific TSP1 siRNA (siTSP1) and 24h after transfection cells were exposed to normoxia (Nx) or hypoxia (Hp) -1% O_2-. mRNA and protein levels of TSP1. mRNA expression levels are expressed over normoxic conditions and controlled with *β-Actin* as the housekeeping gene. Average ± SEM of n=4 performed is shown. Statistical comparisons between different conditions were made using two-way ANOVA test followed by Bonferroni's post hoc test, * P<0.05, **P<0.01. n=4. ns (not significant). Western blot is controlled with α-Tubulin. Representative images of four experiments are shown.

As predicted, hPAEC treated with the TSP1 targeting siRNA demonstrated significantly less TSP1 protein following hypoxia compared to cells treated with the scrambled control siRNA or untreated cells (Figure 20). Interestingly, hypoxia and exogenous TSP1 (20 µg/mL) both increased cell permeability. Conversely, knock down of TSP1 blocked the hypoxic-mediated increase in cell permeability (Figure 21A). To test the accuracy of our permeability assays we used hPAEC treated with 1mM EGTA as a control. As expected we observed an increase on permeability after the treatment (Figure 21B). To inquire if this was due to changes in intercellular junctions we performed immunofluorescent staining of an essential constituent of tight junctions, the protein Zonulin-1 (ZO-1) in these cells. Interestingly, hPAEC transfected with the control siRNA under hypoxia displayed an irregular immunofluorescent staining pattern of ZO-1 distribution. However, treating the cells with a TSP1 siRNA ameliorated the hypoxia-mediated dysregulation of ZO-1 (Figure 22).

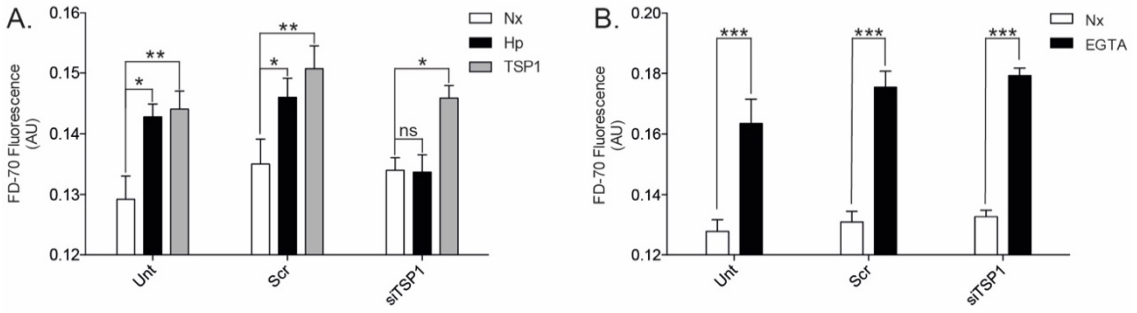

Figure 21: Hypoxia-mediated increase in TSP1 increases paracellular permeability in hPAEC. A. Confluent hPAEC monolayers transfected with scrambled (scr) or specific TSP1 siRNA (siTSP1) were exposed to normoxia (Nx) or hypoxia (Hp) -1% O_2- or treated with TSP1 exogenous (20 ug/ml) for 7h, and flux of FITC-dextran 70kDa (FD-70) across hPAEC monolayers was assessed for 1h. **B.** Permeability control. Confluent hPAEC monolayers were exposed to EGTA (1mM) for 2 minutes and flux of FITC-dextran 70kDa across hPAEC monolayers for 1h. **(A,B)** Fluorescence was quantified with a spectrophotometer at 515 nm. Average ± SEM of n=6 performed is shown. Statistical comparisons between different conditions were made using two-way ANOVA test followed by Bonferroni's post hoc test, * P<0.05, **P<0.01, ***P<0.001. ns (not significant), (AU) arbitrary units.

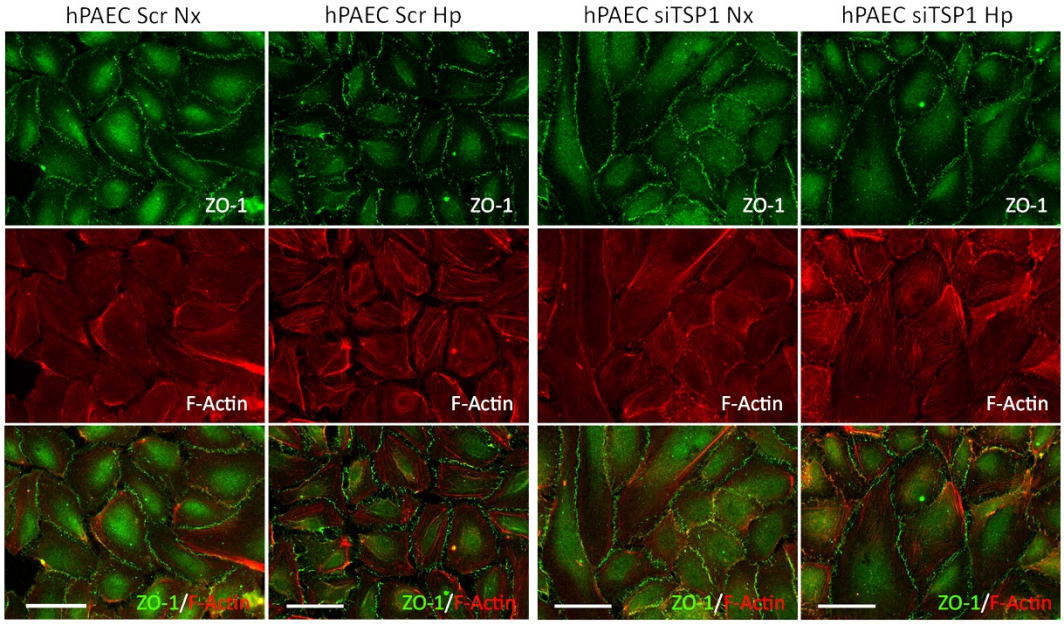

Figure 22: Hypoxia-mediated increase in TSP1 destabilizes hPAEC junctions. Immunofluorescence analysis of ZO-1-Alexa 488 (green) and phalloidin 568 (red) to visualize actin filaments (F-Actin) in hPAEC transfected with scrambled (Scr) or specific TSP1 siRNA (siTSP1). Two days after transfection cells were grown on fibronectin (2 µg/ml)-coated coverslips and cultured under normoxia (Nx) or hypoxia (Hp) -1% O_2- for 24 h. Images shown are representative of three experiments. Bars, 50 µm.

1.08 Hypoxia-mediated increase of TSP1 promotes human PA fibroblast (hPAFIB) differentiation into myofibroblast.

PAFIB contribute to PA remodeling through differentiation into SMC-like phenotype cells, known as myofibroblasts [147, 148]. PAFIB grow and differentiate into myofibroblasts under hypoxic or stress conditions [272], contributing to the tunica media hyperplasia. PAFIB also acquire a contractile phenotype [273], and therefore, aggravate the PAH vasocontraction [274]. Such differentiation drives effective wound healing and is largely regulated by the TGF-β, which on the other hand is a well-known activating target of TSP1 [275, 276]. Therefore, we hypothesized that hypoxia-mediated increase in TSP1 activates latent TGF-β, which in turn triggers PAFIB differentiation. To asses this, we exposed undifferentiated hPAFIB to normoxia or hypoxia alone or in combination with a TSP1 inhibitor (LSKL) or a TGF-β inhibitor (SB 431542) and then observed the number of appearing smooth muscle actin fibers, a stablished smooth muscle cells marker. After four days, we saw that hypoxia clearly increased the number of SMA fibers and that LSKL and SB 431542 treatment abolished this phenomenon (Figure 23).

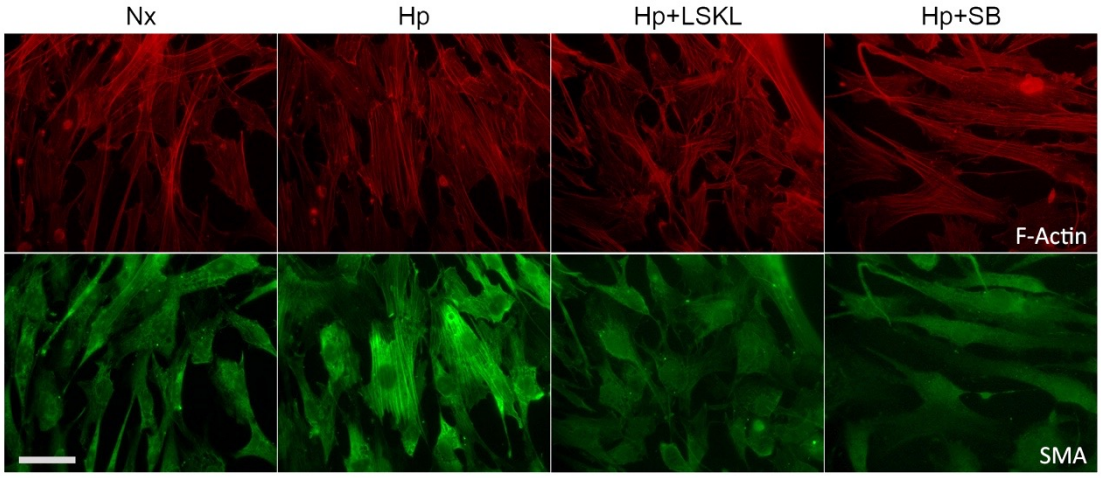

Figure 23: Effect of hypoxia-mediated increase of TSP1 levels in the recruitment of SMA in F-Actin filaments in hPAFIB. Immunofluorescence of hPAFIB with SMA-cy3 (green) and phalloidin 568 (red) to visualize actin filaments (F-Actin). Cells at passage 5 were grown on fibronectin (2 μg/ml)-coated coverslips and treated with TSP1 inhibitor, LSKL (1μM) or TGFβ inhibitor, SB 431542 (10μM), tagged as SB. Afterwards cells were cultured under normoxia (Nx) or hypoxia (Hp) -1% O_2- for 4 days. Images shown are representative of three experiments. Bars, 50 μm.

1.09 TSP1 limits hypoxia-mediated vascular responses in PAs.

Vascular contraction and dilation are oxygen sensitive processes that deteriorate under hypoxic conditions [277]. *In vivo*, hypoxia promotes vasodilation of the systemic circulation and increased tissue perfusion [278], whereas in the pulmonary circulation acute hypoxia promotes vasoconstriction to increase perfusion of parenchyma that is less ventilated [279]. Previous studies have reported that under normoxia, systemic arterial blood flow in skeletal muscles and perfusion of skin flaps is limited by TSP1 basally, and in response to ischemia reperfusion injury [185, 260, 280, 281]. However, it was not clear if endogenous TSP1 limited pulmonary arterial function under hypoxia. To investigate this, we challenged PA from male WT and *tsp1*$^{-/-}$ mice to sodium nitroprusside (SNP), a pro-drug metabolized by smooth muscle cells to nitric oxide (NO), or acetylcholine (Ach), an endothelial cell activator and stimulator of endogenous NO production, and assessed vasodilation under both normoxia and hypoxia (1% O_2). We observed that vasodilation induced by SNP under normoxic or hypoxic conditions was similar among WT and *tsp1*$^{-/-}$ PA (Figure 24).

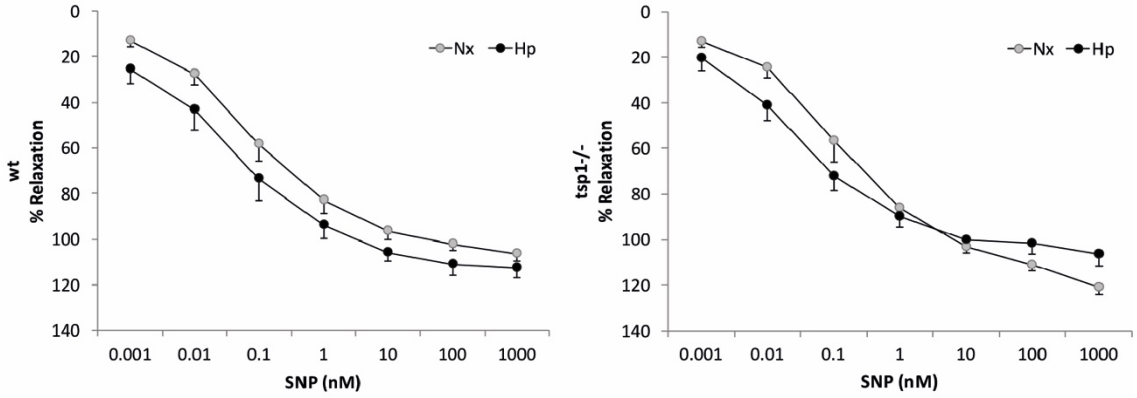

Figure 24: Effect of hypoxia on SNP-induced relaxation in mice PAs. Vascular response to SNP was analyzed in (5-HT)-stimulated endothelium-intact PAs from WT or *tsp1*$^{-/-}$ mice previously incubated for 16 hours under normoxic (Nx) or hypoxic (Hp) -1% O_2- conditions. Statistical comparisons were made using two-way ANOVA, followed by Bonferroni's post hoc test. Results are expressed as means ± SEM (% relaxation), (n=10).

Similarly, under normoxia WT and *tsp1*$^{-/-}$ PAs displayed comparable sensitivity to Ach (Figures 25). However, endothelium-dependent vasodilation induced with Ach was significantly reduced in hypoxic WT PA. In contrast, hypoxic *tsp1*$^{-/-}$ PA maintained Ach sensitivity comparable to normoxic vessels (Figures 25).

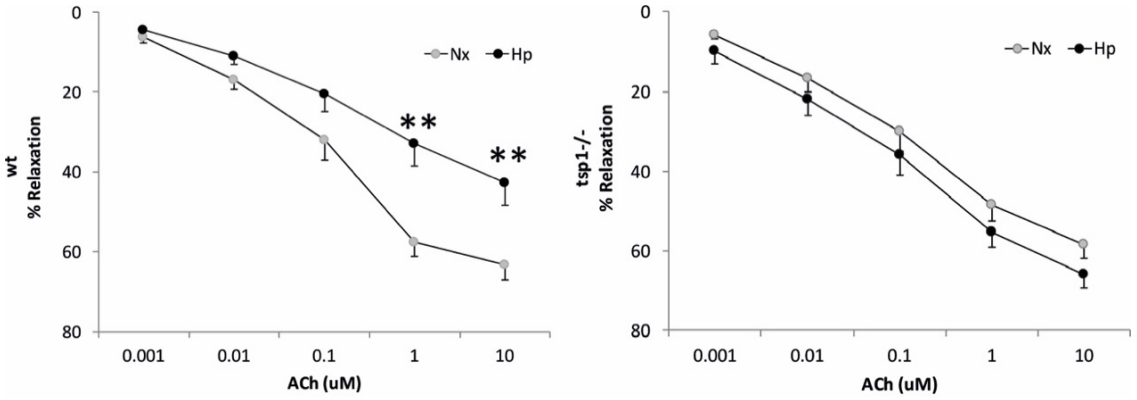

Figure 25: Effect of hypoxia on ACh-induced relaxation in mice PAs Vascular response to ACh was analyzed in (5-HT)-stimulated endothelium-intact PAs from WT or *tsp1*$^{-/-}$ mice previously incubated for 16 hours under normoxic (Nx) or hypoxic (Hp) -1% O_2- conditions. Statistical comparisons were made using two-way ANOVA, followed by Bonferroni's post hoc test, * P<0.05, **P<0.01. Results are expressed as means ± SEM (% relaxation), (n=10).

TSP1 affects hypoxia-mediated dowregulation of Kv1.5. It is reported that hypoxia inhibits the function and expression of several Kv channels in PASMC, which results in membrane depolarization and leads to an increase in intracellular Ca^{2+} concentrations [282]. Therefore, we tested the role of TSP1 on the modulatory effect of hypoxia on Kv channels and whether this affected intracellular calcium concentration. We analyzed the contractile responses induced by Kv1.5 or Kv7 channel inhibitors in PA from WT or *tsp1*$^{-/-}$ mice exposed to normoxia or hypoxia. We found that the Kv7 channel inhibitor XE991 produced a similar degree of contraction under normoxia and hypoxia in both, WT and *tsp1*$^{-/-}$ PA (Figure 26A). Conversely, contraction mediated by the Kv1.5 channel inhibitor DPO1 was markedly diminished in hypoxic, as compared to normoxic, WT PA. Remarkably, hypoxic *tsp1*$^{-/-}$ PA treated with DPO1 had no loss of vasoconstriction (Figure 26B).

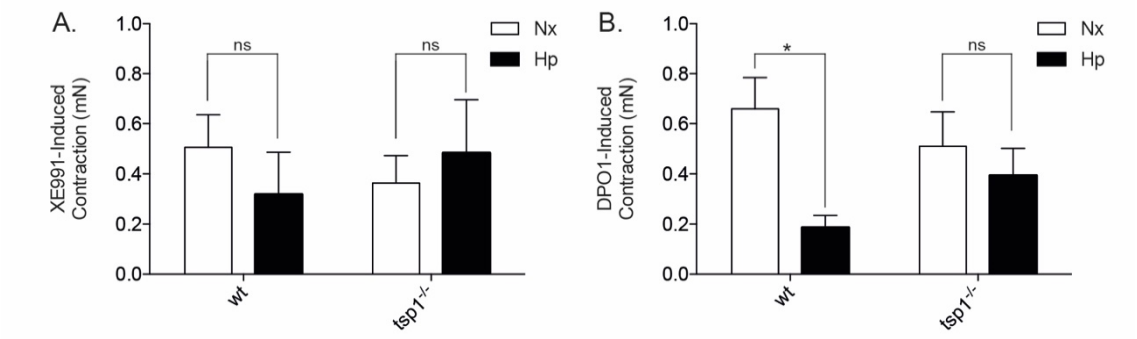

Figure 26: Effect of TSP1 expression on XE991 and DPO1-induced contraction of mice PAs after hypoxia. Vascular responses were analyzed in endothelium-intact PAs from WT or *tsp1*$^{-/-}$ mice previously incubated for 16 hours under normoxic (Nx) or hypoxic (Hp) -1% O_2- conditions. Average values of the contraction induced by XE991 (0.3 µmol/L) **(A)** and DPO1 (1 µmol/L) **(B),** Kv7 and Kv1.5 channels inhibitors respectively. Statistical comparisons were made using two-way ANOVA, followed by Bonferroni's post hoc test, * P<0.05, ns (not significant). Results are expressed as means ± SEM (% contraction), (n=10).

Since we observed a lower response to DPO1 in WT PAs under hypoxia, next, we analyzed the effects of this drug on intracellular Ca^{2+} levels. In agreement with the data in Figure 26, the increase in intracellular Ca^{2+} induced by DPO1 was attenuated in hypoxic as compared to normoxic WT mPASMC. Of note, this difference was not observed in *tsp1*$^{-/-}$ mPASMC (Figure 27A). mPASMC treated with ionomycin, a calcium ionophore, were used as controls (Figure 27B).

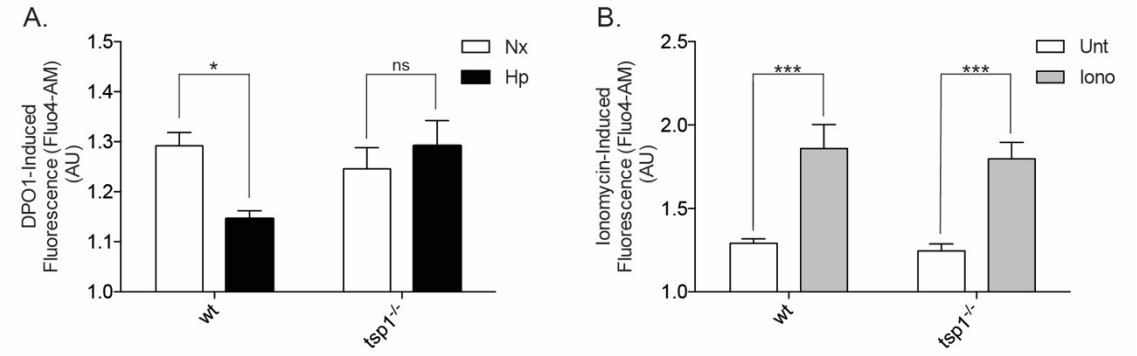

Figure 27: Life cell DPO1-induced calcium measurement in mPASMC. Life cell calcium measurement with cytosolic calcium probe Fluo-4 AM. **A.** Average values of DPO1-induced fluorescence (2 µmol/L) in mPASMC from WT or *tsp1*$^{-/-}$ mice previously incuated for 16 hours under normoxic (Nx) or hypoxic (Hp) -1% O_2- conditions. **B.** Intracellular calcium control: Average values of the ionomycin-induced fluorescence (1 µmol/L) in mPASMC from WT or tsp1$^{-/-}$ mice. Untreated (Unt), treated with ionomycin (Iono). Statistical comparisons were made using two-way ANOVA, followed by Bonferroni's post hoc test; * P<0.05, ***P<0.001, ns (not significant). Results are expressed as means ± SEM, (DPO1 n=10, Ionomycin n=4). AU (arbitrary units).

To assess if these effects were due to changes on Kv1.5 expression, we analyzed Kv1.5 mRNA levels in mPASMC under hypoxia. We observed that hypoxia significantly decreased Kv1.5 mRNA levels in mPASMC harvested from lungs of WT mice. Conversely hypoxia did not alter Kv1.5 mRNA levels in cells from *tsp1*$^{-/-}$ mice (Figure 28).

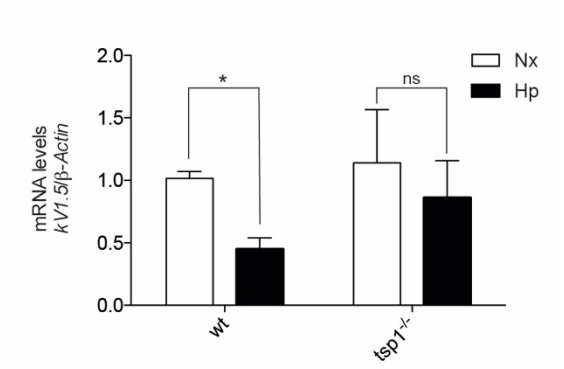

Figure 28 TSP1 null mPASMC are protected from hypoxia-induced inhibition of Kv1.5 mRNA. Quantitative RT-Q-PCR analysis was performed to determine Kv1.5 mRNA expression levels in mPASMC from WT or *tsp1*$^{-/-}$ mice under normoxia (Nx) or hypoxia (Hp) -1% O_2- for 24 h. mRNA levels are expressed as fold change over WT in normoxic conditions and controlled with *β-Actin* as the housekeeping gene. Results are expressed as means ± SEM. Statistical comparisons between different conditions were made using a mouse type stratified Student´s T-test, * $P<0.05$, n=3.

1.10 Implementation of 3D imaging CLARITY technique in mice lungs.

Our previous results gave us new insights into the molecular mechanisms that regulate TSP1 in hypoxic lungs. They also reveal the possible role of hypoxia in the control of cellular functions relevant to PAH. However, there is an important need to understand in detail the structural changes that occur in the lung during this pathology. As we traverse from molecular mechanisms to cellular events, it is crucial to illuminate PAH events at the organ scale. Although immunohistochemistry and immunofluorescence techniques could give us some relevant information about what is happening in the lung architecture under pathologic conditions, these approaches are limited and do not allow us to appreciate changes that affect the integrity or cellular compartmentalization in the whole lung. We aimed to understand the structure-function relationship at cellular and organ level produced under hypoxia using new imaging techniques as CLARITY. It is an innovative technological advance in which intact biological tissue is transformed into a nanoporous hydrogel-hybridized form with markedly improved chemical and optical accessibility [283-285]. With this powerful tool, we can obtain high-resolution structural data in a 3D reconstruction of the organ that allows us to study structural changes at cellular level *in situ* giving us a new perspective of the disease without disrupting tissue cytoarchitecture. We can analyze the general lung structure, bronchus, alveoli and the vasculature zooming in to the

cell and /or organelles level. We performed CLARITY of WT and *tsp1*$^{-/-}$ mice lungs of males exposed to normoxia or hypoxia plus sugen 5416 for 3 weeks following a simplified passive CLARITY protocol from Dr Rinaman [257]. After clarifying process, we performed staining with SMA to validate the technique. In Figure 29, we show a 3D image of WT mice lung staining where it can be appreciated SMA staining in big PAs and main bronchus. Although these results demonstrate that CLARITY can be performed in mice lungs, there is still room for improvement.

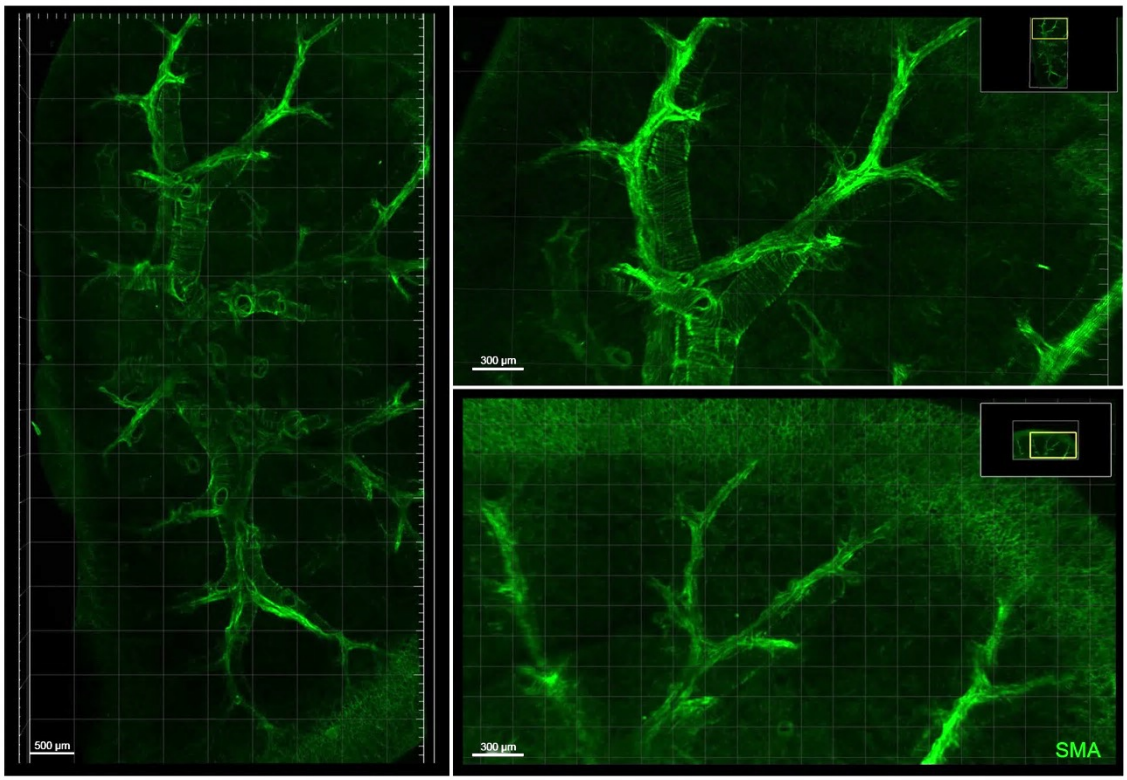

Figure 29: SMA staining in clarified mouse lungs. Images depict a 400 µm z-stack 3D reconstruction of adult (3 months) WT mouse lungs clarified by passive CLARITY and stained for α-SMA with Alexa 488 (green). Big PAs and main bronchus can be appreciated. Scale bar indicates the image size.

Next, we analyzed TSP1 staining in male WT and *tsp1*$^{-/-}$ exposed to normoxia or hypoxia plus sugen 5416 for 3 weeks (Figure 30). We observed that in lungs from WT mice under hypoxia plus sugen 5416 TSP1 staining appears in clusters through the whole parenchyma. Multiple staining with other cell specific markers will allow us to determine the source of TSP1 in the lungs and which cell type is contributing more to increase TSP1 levels under hypoxia or in PAH. At this point we are still working on improving the resolution of our images.

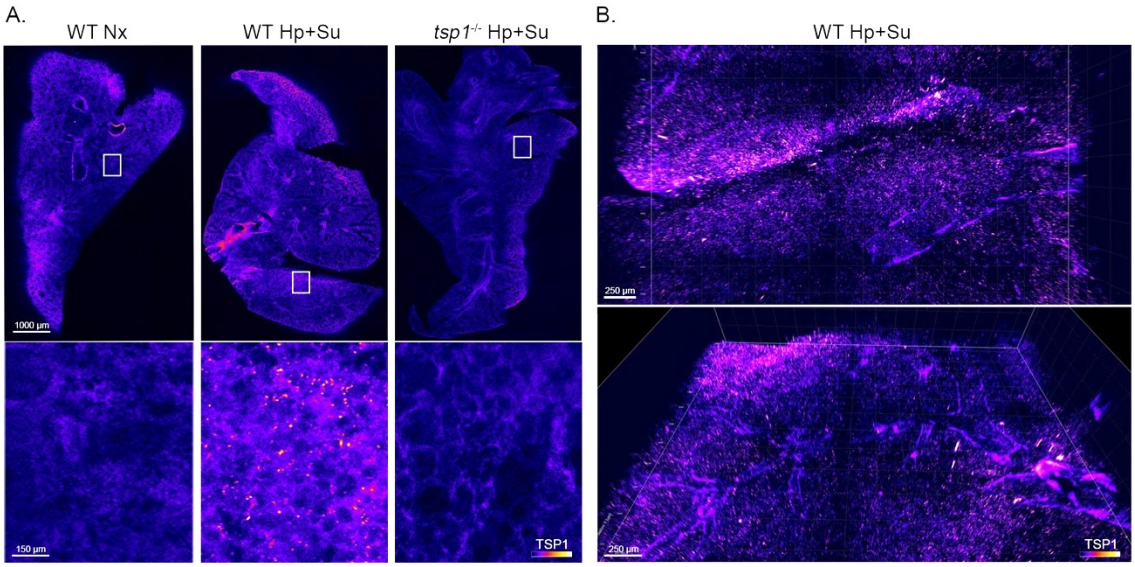

Figure 30: TSP1 staining in clarified mouse lungs under Hp/Sugen treatment. A. Visualization of TSP1 in adults (3 month) mouse lungs of male WT and *tsp1*$^{-/-}$ exposed to normoxia (Nx) or hypoxia (10%) plus sugen 5416 (Hp+Su) for 3 weeks. Mice lung were clarified by passive CLARITY and stained with TSP1 with Alexa 488 (fire). Representative images are shown (n=3). **B.** Images depict a 400 µm z-stack 3D reconstruction. Scale bars indicate image size in each frame.

2. HYPOXIA AND CANCER: IMPACT OF HYPOXIA AND VHL LOSS ON THE REGULATION OF VCAM-1 AND ITS FUNCTIONAL EFFECTS ON THE IMMUNE EVASION OF RCC

2.01 VHL loss and hypoxia regulate VCAM-1 levels in ccRCC cells.

Although previous studies have suggested the significance of VCAM-1 levels in renal carcinomas, little is known about the mechanisms that regulate this adhesion molecule in ccRCC. We aim to study whether VHL loss, the most characteristic event occurring in these tumors, affected VCAM-1 expression. To this aim we first analyzed VCAM-1 mRNA and protein expression levels in ccRCC cell lines that expressed a non-functional or aberrant VHL protein (786-O and RCC4), and were stably transfected with empty vector (786-O-pRv, RCC4-pRv) or with *wild-type* VHL (786-O-VHL, RCC4-VHL) respectively; cells that expressed normal VHL (Caki-1) and cells with a non-functional mutated VHL (Caki-2). Our results proved that VCAM-1 mRNA and protein levels were significantly decreased in cells lacking functional VHL (Figures 31A, B).

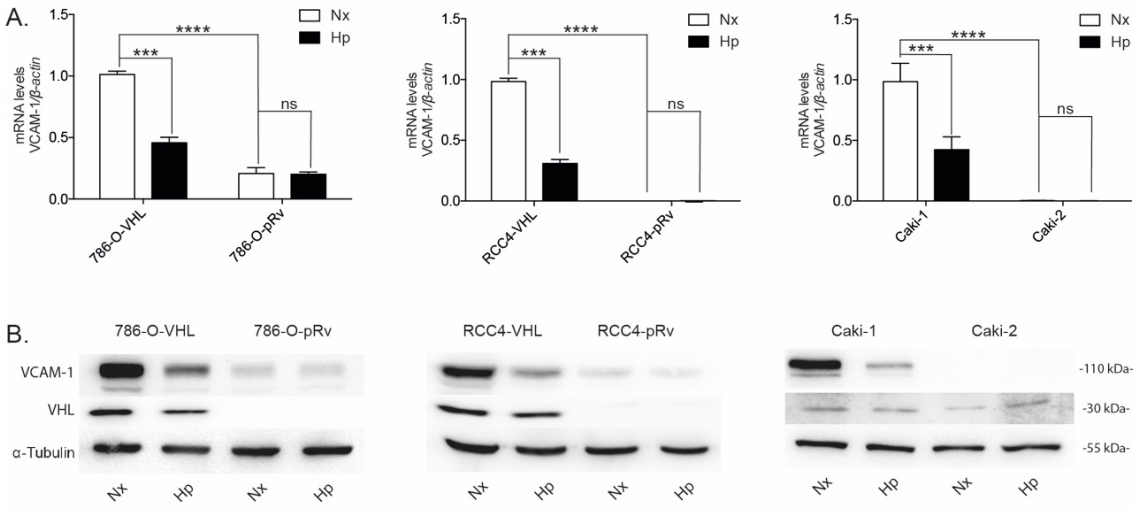

Figure 31: Effect of VHL loss and hypoxia on VCAM-1 levels in ccRCC cell lines. A. VCAM-1 mRNA levels were determined by quantitative RT-Q-PCR in 786-O and RCC4 transfected with empty vector pRv (786-O-pRv and RCC4-pRv) or with pRv-VHL (786-O-VHL and RCC4-VHL), Caki-1 and Caki-2 exposed to normoxia (Nx) or hypoxia 0.5 % O_2 (Hp) for 24 h. mRNA levels are expressed as fold change and normalized over the levels of VHL positive cells in normoxic conditions and controlled with *β-Actin* as the housekeeping gene. Statistical analysis was made using two-way ANOVA test followed by Bonferroni's post hoc test. The values represent the average ± SEM (n=6) experiments with *P<0.05; **P<0.01; ***P<0.001 or ****P<0.0001 were considered significant; ns (not significant). **B.** VCAM-1 and VHL protein levels were analyzed in total cell lysates from 786-O-pRv, 786-O-VHL, RCC4-pRv, RCC4-VHL, Caki-1 and Caki-2 cell lines exposed to normoxia (Nx) or hypoxia 0.5 % O_2 (Hp) for 24 h. A representative Western blot is shown, n=6. As a loading control α-Tubulin was used.

To confirm that this regulation was not a side effect due to the overexpression of VHL we analyzed the effect of VHL loss in the ACHN cell line, which express functional VHL, and knocked down its expression using siRNA. Our results confirmed that VHL loss significantly affected VCAM-1 mRNA levels (Figure 32).

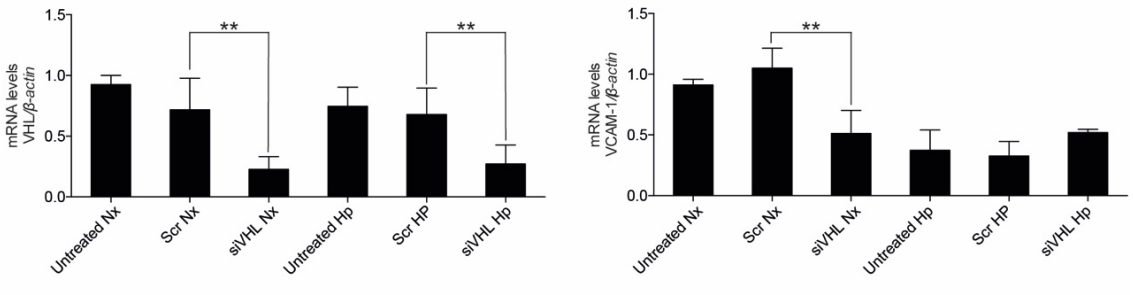

Figure 32: Effect of VHL loss and hypoxia on VCAM-1 mRNA levels in the renal adenocarcinoma cell line ACHN. VHL and VCAM-1 mRNA levels were determined by quantitative RT-Q-PCR in ACHN cells, untreated, transfected with a scrambled siRNA (Scr), or siRNAs specific for VHL, exposed to normoxia (Nx) or hypoxia 0.5 % O_2 (Hp) for 24 h. Gene expression was represented as the fold change against the levels of untreated cells in normoxic conditions and controlled with *β-Actin* gene expression levels. Statistical analysis was made using one-way ANOVA test followed by Bonferroni's post hoc test, the values represent the average ± SEM (n=4) experiments with *P< 0.05, **P<0.01, were considered significant, ns (not significant).

Since hypoxia is considered a hallmark for tumor progression and is associated with disease progression and poor prognosis, we also analyzed the effects of hypoxia in the levels of VCAM-1 in these tumor cells. Similar to VHL loss, hypoxic conditions decreased VCAM-1 mRNA and protein levels (Figure 31). Furthermore, the decrease in mRNA levels was observed at the short time of 6 h while protein changes were observed after 12 h (Figure 33).

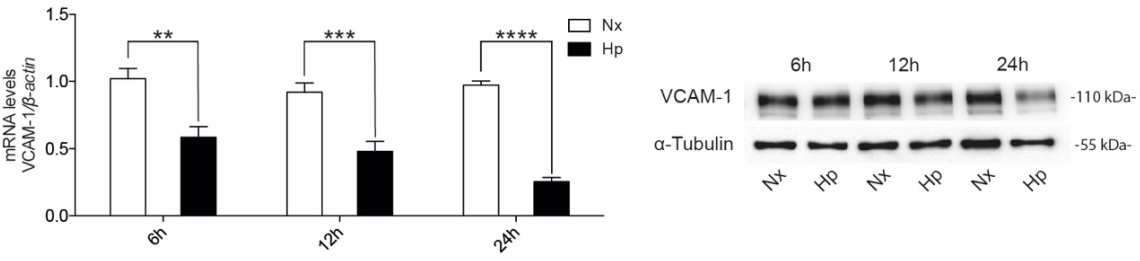

Figure 33: Short time effects of hypoxia on VCAM-1 mRNA and protein levels in 786-O-VHL cell line. VCAM-1 mRNA levels were determined by quantitative RT-Q-PCR in 786-O-VHL cells exposed to normoxia (Nx) or hypoxia 0.5 % O_2 (Hp) for 6, 12 and 24 h. Gene expression was represented as the fold

change against the levels of cells in normoxic conditions and controlled with *β-Actin* gene expression levels. Statistical analysis was made using two-way ANOVA test followed by Bonferroni's post hoc test, the values represent the average ± SEM (n=4) experiments, **P<0.01, ***P<0.001 and ****P<0.0001 were considered significant. VCAM-1 protein levels of the same experiment were analyzed. As a loading control α-Tubulin was used. A representative Western blot is shown, n=3.

Next, we asked whether VCAM-1 decreased mRNA levels were due to transcriptional regulation or mediated by post-transcriptional events (e.g., processing, degradation). To this aim we first analyzed mRNA stability by treating 786-0-VHL cells with the transcriptional inhibitor actinomycin D and then subjected them to normoxia or hypoxia for different times. Our results proved that hypoxia did not affect the stability of VCAM-1 mRNA (Figure 34A). To further confirm that a transcriptional mechanism was involved we analyzed the heterogeneous nuclear RNA (hnRNA), mRNA before splicing modification that proves to be useful to determine gen transcriptional state. We found that hnRNA was similarly decreased under hypoxia or in VHL negative cells (Figure 34B). Therefore, these data provide support for a transcriptional repression of VCAM-1 mediated by VHL loss or hypoxia.

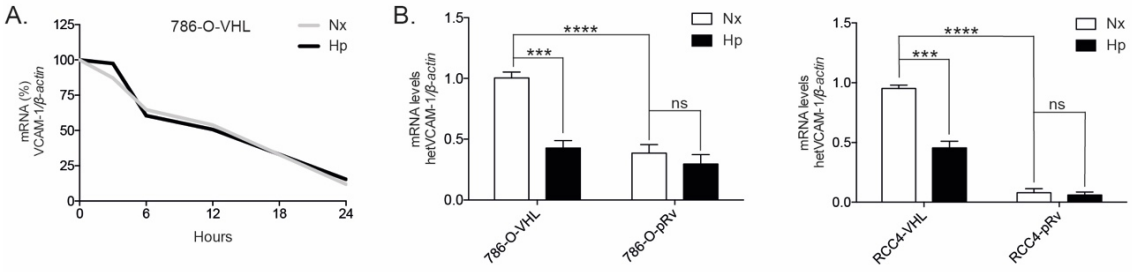

Figure 34: Effect of hypoxia and VHL loss on VCAM-1 mRNA stability and hnRNA in ccRCC lines. **A.** 786-O-VHL cells were treated with actinomycin D (2 μg/ml) and then cultured under normoxia or hypoxia for the indicated times. Gene expression are represented as fold change and normalized over the levels of VHL positive cells in normoxic conditions (considered 100 %) and controlled with *β-Actin* gene expression levels. The values of a representative experiment of n=4 is shown. **B.** VCAM-1 mRNA levels were determined by quantitative RT-Q-PCR before splicing (measuring nuclear heterogeneous RNA, hnRNA) in 786-O-pRv, 786-O-VHL, RCC4-pRv and RCC4-VHL exposed to normoxia (Nx) or hypoxia 0.5 % O_2 (Hp) for 24 h. Gene expression was represented as fold change over the levels of VHL positive cells in normoxic conditions and controlled with *β-Actin* as the housekeeping gene. Statistical analysis between different conditions was made using two-way ANOVA test followed by Bonferroni's post hoc test, the values represent the average ± SEM (n=4) experiments, ***P<0.001, ****P<0.0001 were considered significant, ns (not significant).

Since VCAM-1 is a cell membrane protein, we asked whether a decrease in total protein levels resulted in decreased expression in the cell membrane. Analysis of VCAM-1 membrane protein by flow cytometry revealed a significant decrease in VHL deficient cells compared to their counterparts stably transfected with VHL and in VHL positive cells subjected to hypoxic conditions compared to normoxia (Figure 35). These results indicated that VHL loss or hypoxia affect VCAM-1 exposition in the cell surface which in turn might also have functional effects.

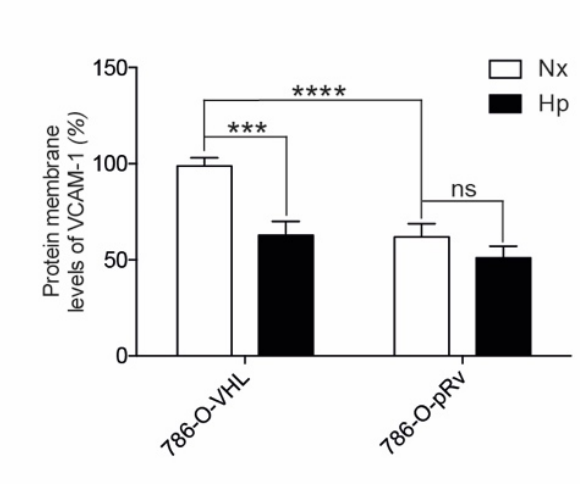

Figure 35: Effect of VHL loss and hypoxia on VCAM-1 membrane levels in ccRCC cell lines. VCAM-1 levels at the cell membrane were determined by flow cytometry in 786-O-VHL and 786-O-pRv cells exposed to normoxia (Nx) or hypoxia 0.5 % O_2 (Hp) for 24 h. Quantification of the fluorescence mean in each condition is shown. Statistical analysis was made using two-way ANOVA test followed by Bonferroni's post hoc test and the values represent the average ± SEM (n=4) experiments. ***P<0.001 was considered significant, ns (not significant).

2.02 Transcriptional regulation of VCAM-1 under hypoxia or in the absence of VHL is not mediated by HIF.

VCAM-1 transcriptional regulation in the absence of VHL or in hypoxia suggested that the hypoxia inducible factors, HIFs, might be involved in downregulating VCAM-1 in ccRCC cell lines. To address this aim, we knockdown their expression by using specific siRNA to HIF1α or HIF2α in these cells. HIF2α interference in 786-O cells, which have lost HIF1α expression [194], did not prevent the decrease in VCAM-1 mRNA levels in VHL negative cells or in hypoxia (Figure 36A, top). However, the expression levels of the HIFα target gene *phd3* were significantly decreased (Figure36A, bottom). Similar results were observed when VCAM-1 protein levels were analyzed in RCC4-VHL cells in which HIF1α or HIF2α had been interfered (Figure 36B).

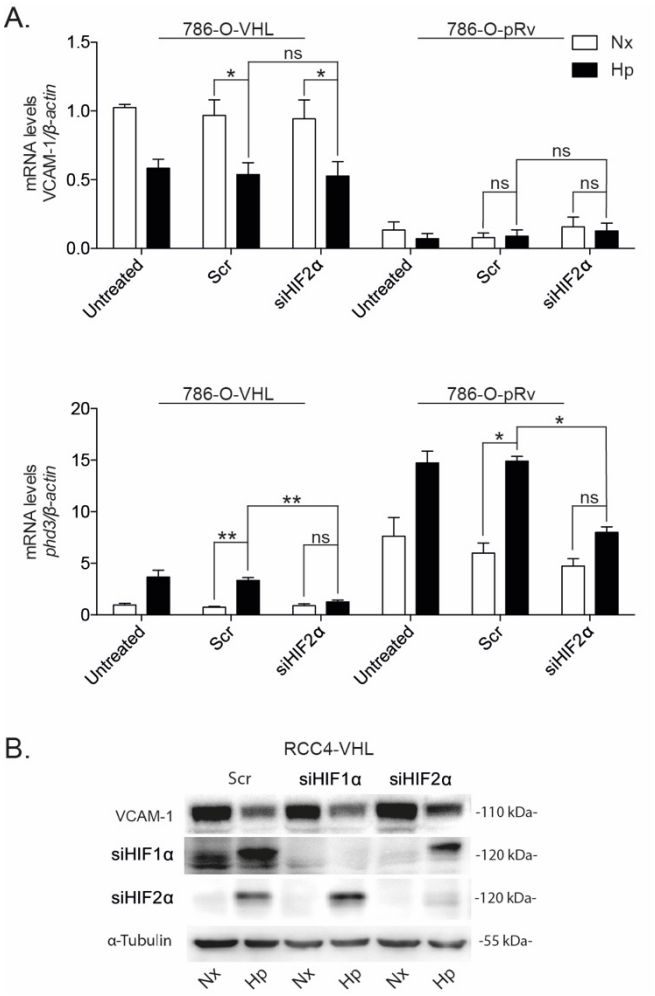

Figure 36: Role of HIFα in VCAM-1 regulation in ccRCC cell lines. A. VCAM-1 and *phd3* mRNA levels in 786-O-VHL or 786-pRv cells untreated, transfected with a scrambled siRNA (Scr), or siRNAs specific for HIF2α (siHIF2α) were analyzed after 24 h under normoxia (Nx) or hypoxia 0.5 % O_2 (Hp). Gene expression was represented as fold change over the levels of VHL positive cells in normoxic conditions and controlled with *β-Actin* as the housekeeping gene. Statistical analysis was made using two-way ANOVA test followed by Bonferroni's post hoc test, the values represent the average ± SEM (n=3) experiments, *P<0.05 and **P<0.01 were considered significant, ns (not significant). **B.** VCAM-1, HIF1α and HIF2α protein levels were analyzed in total cell lysates from RCC4-VHL transfected with a scrambled siRNA (Scr), or siRNAs specific for HIF1α (siHIF1α) or HIF2α (siHIF2α) and then subjected to 24 h under normoxic (Nx) or hypoxic (0.5 % O_2) conditions (Hp). A representative Western blot is shown, n=3.

Additionally, HIF-independent regulation of VCAM-1 in ccRCC cells was also confirmed in cells expressing a mutant form of VHL that has been previously reported to regulate HIF normally but is defective in promoting extracellular fibronectin matrix assembly, the naturally occurring type 2C VHL mutant L188V [286, 287]. Our results demonstrated that VCAM-1 mRNA and protein levels in VHL mutant L188V under normoxic or hypoxic conditions were significantly decreased to levels resembling those in VHL negative cells (Figures 37A, B). Conversely, mRNA levels of a well-known HIF target gene, GLUT-1, were similarly regulated in VHL and VHL mutant L188V (Figure 37A). Taken together these data demonstrate that VCAM-1 transcriptional regulation in ccRCC cell lines is independent of HIF.

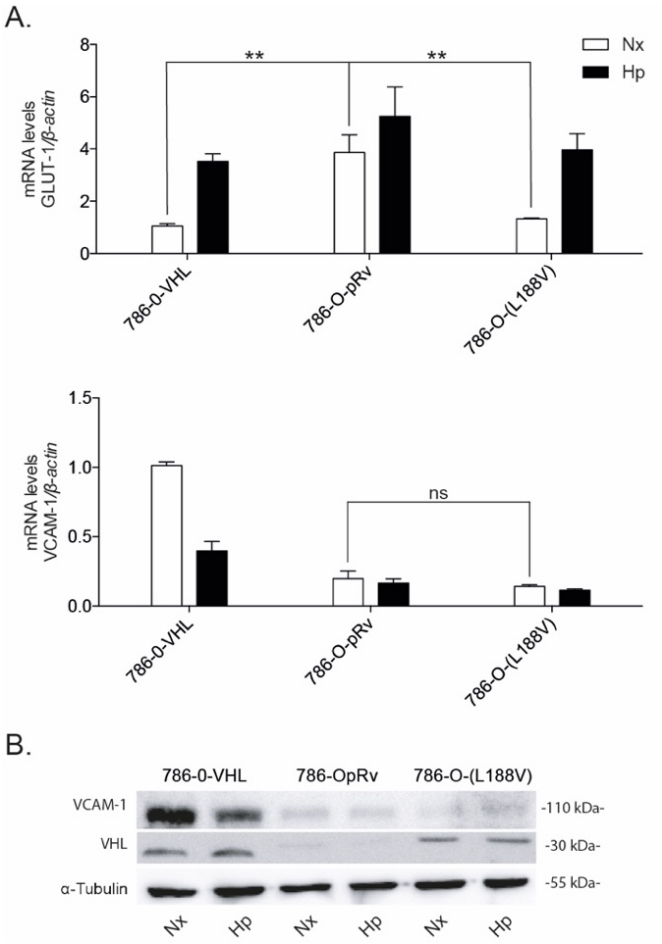

Figure 37: Effect of VHL mutation L188V in VCAM-1 regulation. A. GLUT-1 and VCAM-1 mRNA levels were quantified by RT-Q-PCR in 786-O-VHL, 786-pRv or 786-O-VHL (L188V) (cells stably expressing the VHL mutant L188V) cultured under normoxia (Nx) or hypoxia 0.5 % O_2 (Hp) for 24 h. mRNA levels are represented as fold change over the levels of VHL positive cells in normoxic conditions and controlled with *β-Actin* as the housekeeping gene. Statistical analysis was made using two-way ANOVA test followed by Bonferroni's post hoc test, the values represent the average ± SEM (n=4) experiments. **P<0.01 was considered significant, ns (not significant). **B.** VCAM-1 and VHL protein levels were analyzed in total cell lysates of 786-O-VHL, 786-pRv or 786-O-VHL (L188V) cells. As a loading control α-Tubulin was used. A representative Western blot is shown, n=3.

2.03 VHL and PHDs control VCAM-1 levels in ccRCC cells via NF-κB pathway.

It is well established that nuclear factor-kappa B (NF-κB) pathway regulates VCAM-1 expression [288, 289]. To ascertain how hypoxia or VHL loss affected the NF-κB signaling pathway and whether this was involved in VCAM-1 regulation in ccRCC cells, we cultured the cells under hypoxia and treated them with the NF-κB agonist TNF-α. Our results proved that hypoxia-mediated decrease of VCAM-1 mRNA levels in VHL positive cells were completely recovered with TNF-α treatment and those in normoxia were further increased (Figure 38). Conversely, TNF-dependent induction of VCAM-1 was lost in the absence of VHL (Figure 38).

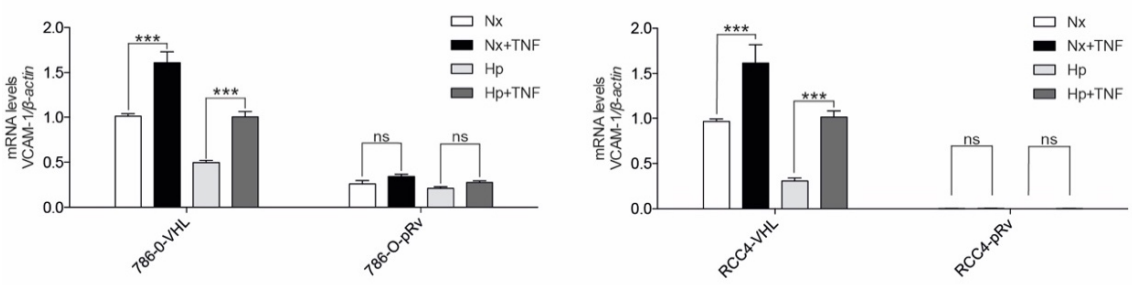

Figure 38: Effect of TNFα in ccRCC cell lines. VCAM-1 mRNA levels were analyzed in 786-O or RCC4 positive or negative cells under different stimulus for 24 h: normoxia (Nx) hypoxia 0.5 % O_2 (Hp), alone or in combination with TNFα (20 ng/ml). Statistical analysis was made using two-way ANOVA test followed by Bonferroni's post hoc test. The values represent the average ± SEM (n=6) experiments, ***P<0.001 was considered significant, ns (not significant).

To further prove that the NF-κB signaling pathway was involved in keeping high levels of VCAM-1 in VHL positive cells, we cultured the cells under hypoxia, with DMOG (a PHD inhibitor) and with an inhibitor of the NF-κB pathway (SM7368), alone or in the presence of TNF-α. Our results demonstrated that SM7368 treatment decreased significantly VCAM-1 mRNA and protein levels (Figure 39). Similarly, VCAM-1 levels remained low in cells treated with DMOG alone or in combination with TNF-α (Figure 39). These results prompted us to think that hypoxic decrease of PHD activity was probably involved in this signaling pathway.

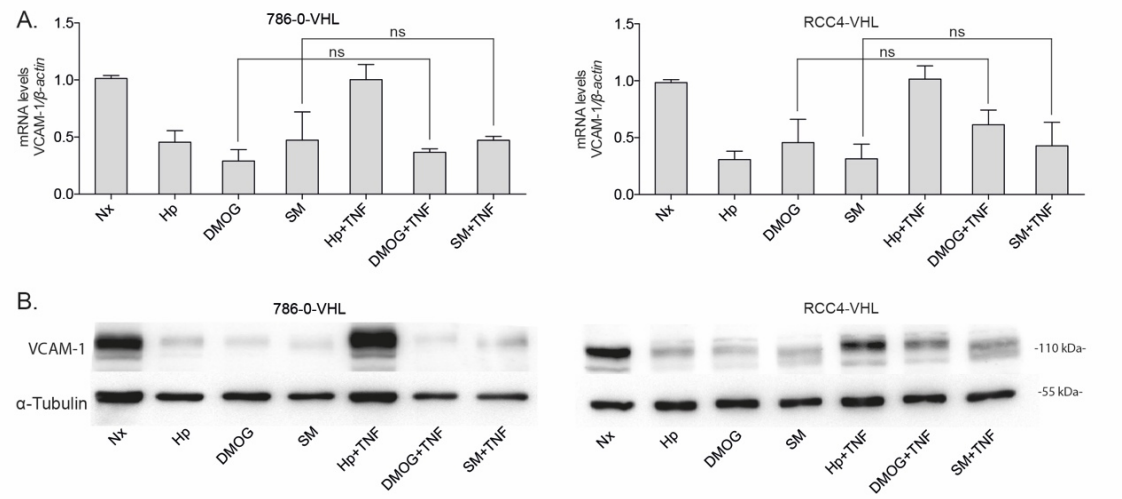

Figure 39: VHL and PHDs limit VCAM-1 regulation via NF-κB in ccRCC cells. VCAM-1 mRNA levels **(A, B)** and protein **(B)** were analyzed in 786-O or RCC4 positive cells under different stimulus for 24 h: normoxia (Nx), hypoxia 0.5 % O_2 (Hp), DMOG (1 mM) or SM7368 at 20 µM (SM) alone or in combination with TNFα (20 ng/ml). Statistical analysis was made using one-way ANOVA test followed by Bonferroni's post hoc test. The values represent the average ± SEM (n=6) experiments, ***P<0.001 was considered significant, ns (not significant). A representative Western blot is shown (n=4). As a loading control α-Tubulin was used.

To ascertain this, we knocked down the three PHDs, PHD1, PHD2 and PHD3 in our VHL positive cells and analyzed VCAM-1 mRNA and protein levels. We observed that VCAM-1 mRNA and protein levels were decreased when specific siRNA for PHD1, 2 or 3 were used, although this regulation only reached significance when PHD2 or PHD3 were interfered (Figure 33). Altogether these results indicated that VHL is an essential component in the NF-κB-mediated regulation of VCAM-1 in these cell lines, and that PHDs might be a switch that enables VHL to increase VCAM-1 levels.

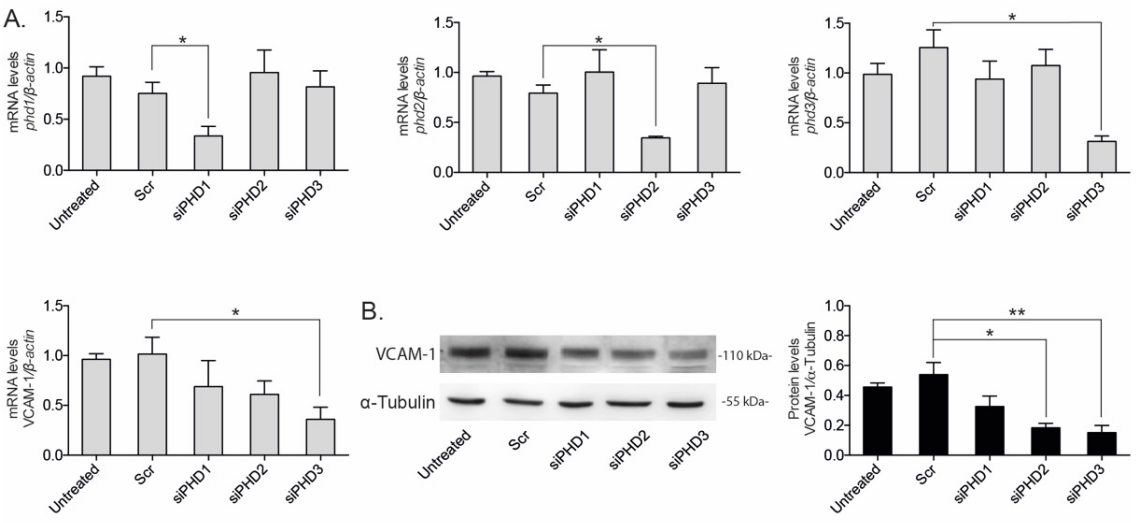

Figure 40: PHDs contributes to maintain VCAM-1 levels in ccRCC cells. A. PHD1, PHD2, PHD3 and VCAM-1 mRNA levels in 786-O-VHL cells untreated, transfected with a scrambled siRNA (Scr), or siRNAs specific for each PHD (siPHD1, siPHD2 or siPHD3) were analyzed. Gene expression is represented as fold change over the levels of untreated cells and controlled with *β-Actin* as the housekeeping gene. Statistical analysis was made using one-way ANOVA test followed by Bonferroni's post hoc test, the values represent the average ± SEM (n=4). *P<0.05 was considered significant. **B.** VCAM-1 protein levels were detected in the same samples and quantification of protein bands controlled with α-Tubulin is represented. Protein levels are expressed as fold change over untreated cells. Statistical analysis was made using one-way ANOVA test followed by Bonferroni's post hoc test, the values represent the average ± SEM (n=4). *P<0.05, **P<0.01 were considered significant, ns (not significant). A representative Western blot is shown, n=3.

2.04 VHL and hypoxia affect non-canonical NF-κB pathways in ccRCC cells.

Our results above indicated that VCAM-1 repression in ccRCC cells might be due to decreased NF-κB signaling in cells lacking VHL or in hypoxia. Conversely, previous results demonstrate that VHL loss or hypoxia activates the canonic NF-κB signaling in RCC cell lines [94, 95, 290]. To reconcile our results with previously published ones we aimed to analyze if changes on

different members of the non-canonical NF-κB pathways were affected in ccRCC cells and these could explain the regulation of VCAM-1 in these cells. Interestingly protein levels of central signaling components of the non-canonical NF-κB pathway, NIK and its downstream kinase, inhibitor of NF-κB kinase α (IKKα), demonstrated a consistent decrease in cells lacking VHL (Figure 41). In addition, protein levels of the transcriptional activator complex Rel B-p52 were significantly decreased in the absence of VHL or in hypoxic conditions, while protein levels of the canonical NF-κB transcription factor p65 (Rel A) remained stable in all conditions (Figure 41).

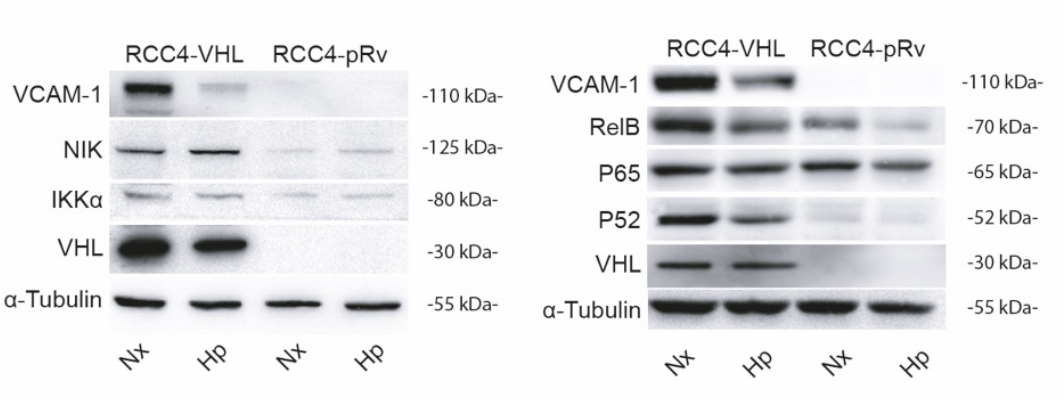

Figure 41: Effects of VHL and hypoxia in the non-canonical NF-κB pathway in ccRCC cells. Western blot of RCC4 VHL positive or negative cells under normoxia (Nx) or hypoxia 0.5 % O_2 (Hp) for 24 h. Images show protein levels of VCAM-1, NIK, IKKα, Rel B, p65, p52, VHL and α-Tubulin as a loading control. A representative Western blot is shown, n=3.

To further confirm that defects on the non-canonical pathway were responsible for the decrease on VCAM-1 levels, we knocked down the expression of several components of this pathway in VHL positive cells. Our results proved that interference of IKKα, NIK or p52 in VHL positive cells resulted in a significant decrease of VCAM-1 levels. Conversely, the interference of the canonic component p50 had only minimal effects on VCAM-1 protein levels (Figure 42). These results clearly prove that in the absence of VHL or in hypoxia the non-canonical NF-κB pathway is affected, and this contributes to the regulation of VCAM-1 in these conditions.

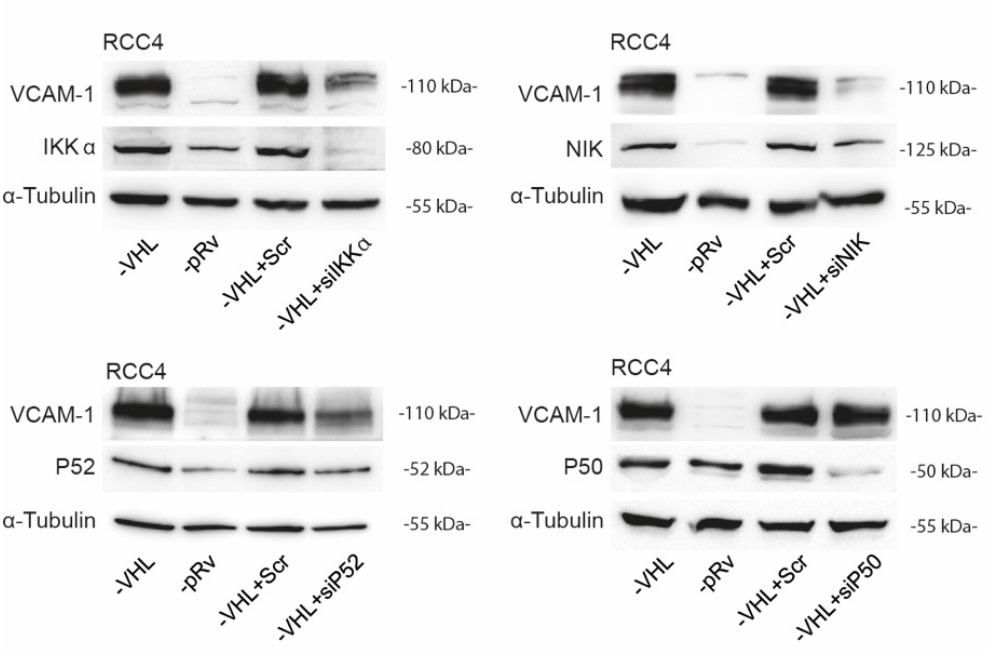

Figure 42: Effects of the interference of the non-canonical NF-κB pathway on VCAM-1 levels. Western blot of RCC4 VHL positive or negative cells transfected with a scrambled siRNA (Scr), or siRNAs specific for IKKα, NIK, p52, p50. Images show protein levels of VCAM-1, NIK, IKKα, p52, p50, and α-Tubulin as a loading control. A representative Western blot is shown, n=3.

2.05 TNFα effects on VHL mutant ccRCC cell lines.

Each tumor sample is a mixture of many different cell types and that they may be expressing unique and different VCAM-1 messengers. Furthermore, there is a wide range of VHL mutations that determine the tumor's own characteristics as well as the contribution of other factors that may be affected and have synergistic or antagonistic effects on gene regulation. Our previous results demonstrate the dependence of VHL on the regulation of VCAM-1 in 786-O and RCC4 cells, even so we wanted to know whether other VHL mutations could interfere in the TNF-α-mediated induction of VCAM-1. To this aim, we used 786-O cells expressing the naturally occurring type 2C VHL mutant L188V, a non neddylateable version of VHL termed RRR or another version of VHL (KRR) which does not interfere with the normal function of VHL. ccRCC cells were treated with TNF-α for 24 h and VCAM-1 protein and mRNA levels were analyzed (Figure 43), Our results demonstrated that each VHL mutation had different sensibilities for TNF-α-mediated induction of VCAM-1. Of note, 786-O-RRR cells had low basal levels of VCAM-1, although it preserved sensibility to TNF-α treatment. In addition, these results proved to be interesting in that different VHL mutations affected VCAM-1 levels and regulation differently.

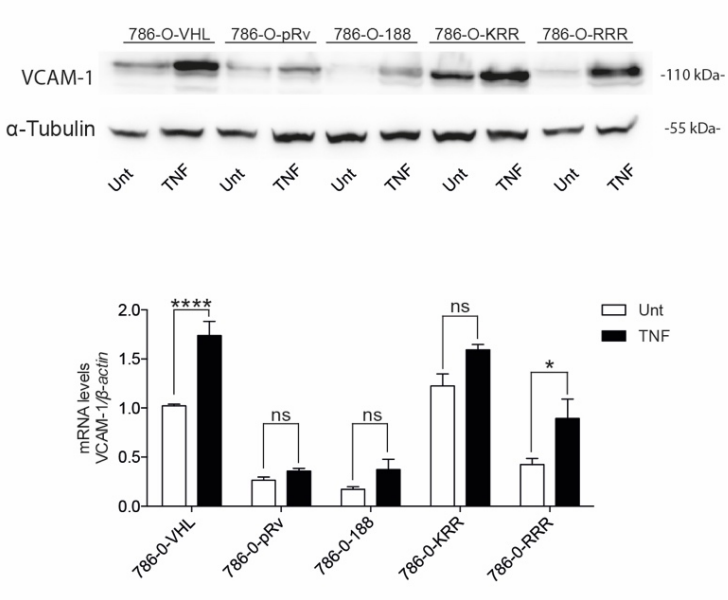

Figure 43: Analysis of VCAM-1 levels in VHL mutants. VCAM-1 mRNA and protein levels were determined in 786-O transfected with empty vector pRv (786-O-pRv), with pRv-VHL (786-O-VHL) or with type 2C mutants L188V (786-O-188), RRR (786-O-RRR) and its control KRR (786-O-KRR). Statistical analysis was made using two-ways ANOVA test followed by Bonferroni's post hoc test. The values represent the average ± SEM (n=6) experiments, *P<0.05 and ****P<0.0001 were considered significant. A representative Western blot of n=4 is shown. As a loading control α-Tubulin levels were analyzed.

2.06 VHL and PHDs control VCAM-1 levels in human umbilical vein endothelial cells (HUVECS).

VCAM-1 is very relevant in activated endothelium specially in the context of tumor migration and immune cell trafficking. Several reports in the literature have investigated the effects of hypoxia and/or TNF-α on endothelial VCAM-1 levels, however those studies prove a lack of consensus in the pattern of regulation. Some of them report a hypoxia-mediated increase on VCAM-1 levels [291, 292] while others observe a decrease on endothelial VCAM-1 mRNA and protein levels under hypoxic conditions [293]. Since the studies were performed with different endothelial cell types, we believe that the differences observed are due to a cell type dependent regulation. Although those studies analyzed the effects of hypoxia on VCAM-1 levels, none of them tested the effects of VHL loss in the levels of endothelial VCAM-1. Therefore, we tested the effects of hypoxia and VHL loss on VCAM-1 levels in HUVEC. We found that TNF-α-induced VCAM-1 levels were significantly decreased in HUVEC treated under hypoxia, or treated with PHD or NF-κB inhibitors (Figure 44A), as well as in cells treated with VHL siRNA (Figure 44B). Therefore, these results clearly prove that a VHL/and or hypoxia-dependent regulation of VCAM-1 is not unique to ccRCC, but it can also be extended to not tumoral cells.

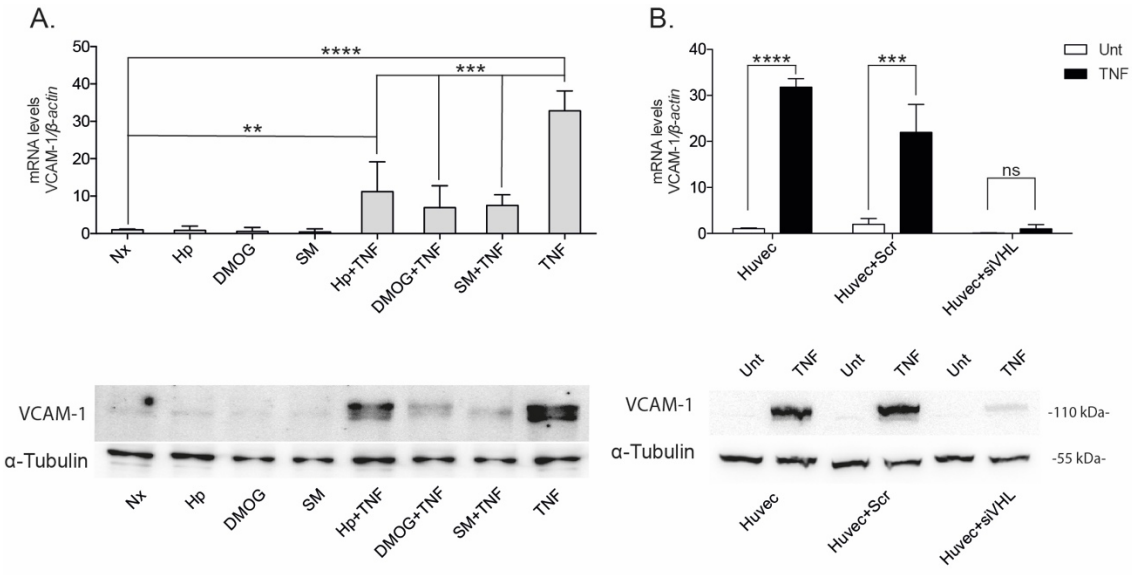

Figure 44: Effect of VHL loss, hypoxia and NF-κB inhibitors on VCAM-1 levels in HUVEC. A. VCAM-1 mRNA and protein levels were determined in HUVEC under different stimulus for 24 h: normoxia (Nx), hypoxia 0.5 % O_2 (Hp), DMOG (1 mM) or SM7368 at 20 µM (SM) alone or in combination with TNFα (20 ng/ml). Gene expression was represented as fold change over the levels of cells in normoxic conditions and controlled with *β-Actin* as the housekeeping gene. Statistical analysis was made using one-way ANOVA test followed by Bonferroni's post hoc test, the values represent the average ± SEM (n=5) experiments, **P<0.01, ***P<0.001 and ****P<0.0001 were considered significant. A representative Western blot is shown (n=5). **B.** VCAM-1 mRNA and protein levels were determined in HUVEC untreated or transfected with a scrambled siRNA (Scr), or siRNAs specific for VHL in the presence or absence of TNFα (20 ng/ml). Gene expression was represented as fold change over the levels of cells untreated and controlled with *β-Actin* gene expression levels. Statistical analysis was made using two-ways ANOVA test followed by Bonferroni's post hoc test. The values represent the average ± SEM (n=4) experiments, ***P<0.001 and ****P<0.0001 were considered significant. A representative Western blot, n=4 is shown. As a loading control α-Tubulin levels were analyzed.

2.07 VHL loss or hypoxia diminish monocytic cell adhesion to ccRCC cells.

It is well known that VCAM-1 through its binding to the integrins α4β1 and α4β7 mediates binding of circulating monocytes and lymphocytes to the endothelium [219]. Similarly, VCAM-1 expression on the surface of tumor cells mediates interaction of several cell types of the hematopoietic lineage that express α4 integrin [294]. To study whether VCAM-1 decrease in ccRCC cells played any functional role in the biology of these tumor cells, we analyzed their capacity to mediate monocytic cell adhesion. To this aim we used two monocytic cell lines labeled with fluorescent markers. We incubated them with our ccRCC cell lines and let them interact for 20 min and afterwards we quantified cell-cell adhesion by counting fluorescent cells. Our results proved that monocytes binding to ccRCC cells was VHL-dependent since adhesion to VHL negative cells was significantly lower compared to the adhesion to VHL expressing cells (Figure

45A, B). Similarly, hypoxia significantly decreased monocytes binding to ccRCC cells (Figure 45C).

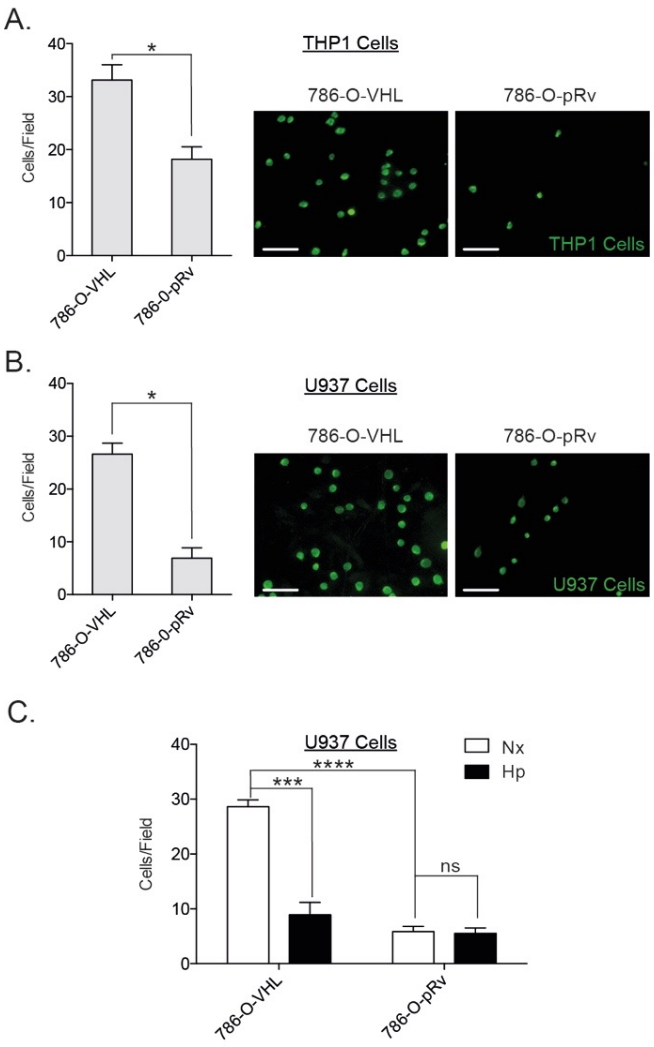

Figure 45: Effects of VHL loss and hypoxia on monocytic cell adhesion to ccRCC cells. 786-O-VHL or 786-pRv cells were grown at confluence in a 24-multiwell plate and cultured under normoxic conditions. Then THP1 **A.** or U937 **B.** monocytic cell lines ($60x10^3$ cells/well) previously labelled with 10 mM calcein-AM (green) were added. Cell adhesion was performed for 20 min at 37ºC and afterwards attached fluorescent cells were counted under the microscope. Data is represented as number of cells ± SEM (n=5). Ten random fields were analyzed per condition and two-tailed Student's t-test was performed, *P<0.05, was considered significant. Representative images of attached THP1 or U937 monocytic cell (green) are shown. **(C)** U937-calcein-AM labelled cell adhesion on 786-O-VHL or 786-pRv cells previously cultured under normoxia (Nx) or hypoxia 0.5 % O_2 (Hp) for 24 h. Cell adhesion was performed for 20 min at 37ºC and afterwards fluorescent cells were counted under the microscope. Data is represented as number of cells ± SEM (n=5), ten random fields were analyzed per condition. Statistical analysis was made using two-way ANOVA test followed by Bonferroni's post hoc test, ***P<0.001, ****P<0.0001 was considered significant, ns (not significant). Scale bars 50 nm

2.08 Monocytic-ccRCC cell adhesion through VCAM-1-α4β1 interaction promotes a cytotoxic immune response.

Given that VHL loss or hypoxia regulated the adhesion of monocytic cells to ccRCC, we asked whether this was mediated by VCAM-1 interaction with its cognate receptor the integrin α4β1 (VLA4). To this aim we knocked down VCAM-1 expression in VHL positive cells and then tested ccRCC-monocytes cell adhesion. We observed that cell adhesion was significantly decreased

when VCAM-1 levels were decreased (Figures 46). Interestingly this adhesion was similar to that observed in VHL-negative cells, which might be explained by the fact that VCAM-1 levels after siRNA interference, and those in VHL negative cells were comparable (Figure 46).

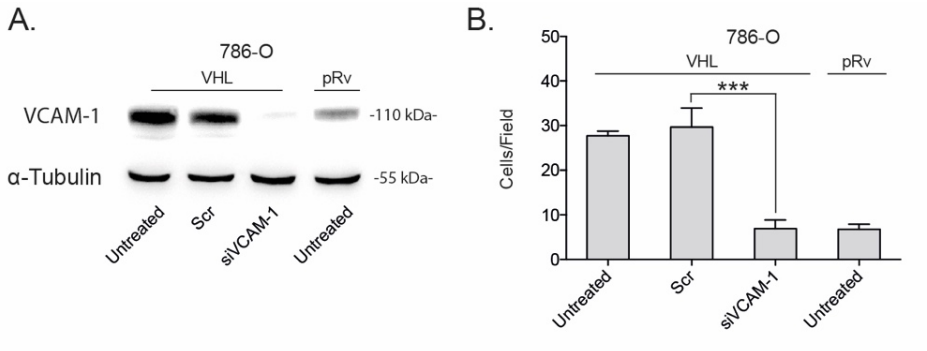

Figure 46: Role of VCAM-1 regulation in monocyte adhesion to ccRCC. A. Analysis of VCAM-1 protein levels in 786-O-pRv or 786-O-VHL cells untreated, or transfected with a scrambled siRNA (Scr), or siRNAs specific for VCAM-1. α-Tubulin was used as a loading control. Western blot representative of three experiments is shown. **B.** U937-calcein-AM labelled cell adhesion on 786-O-pRv or 786-O-VHL cells untreated, or transfected with a scrambled siRNA (Scr), or siRNAs specific for VCAM-1. Cell adhesion was performed for 20 min at 37ºC and afterwards fluorescent cells were counted under the microscope. Data is represented as number of cells ± SEM (n=5), and ten random fields were analyzed per condition. Statistical analysis was made using one-way ANOVA test followed by Bonferroni's post hoc test, ***P<0.001 was considered significant.

More importantly, monocytic cell adhesion to VHL positive cells was also inhibited in the presence of VCAM-1 receptor blocking antibodies, like those blocking the α4 or β1 subunits of the integrin α4β1, while no effects were observed with an αL blocking antibody as a control (Figure 47). However, cell adhesion to VHL negative cells was not further decreased in the presence of these blocking antibodies (Figure 47). These results demonstrate that ccRCC cells are able to elicit immune cell binding and this is specifically mediated by VCAM-1 interaction with the integrin α4β1.

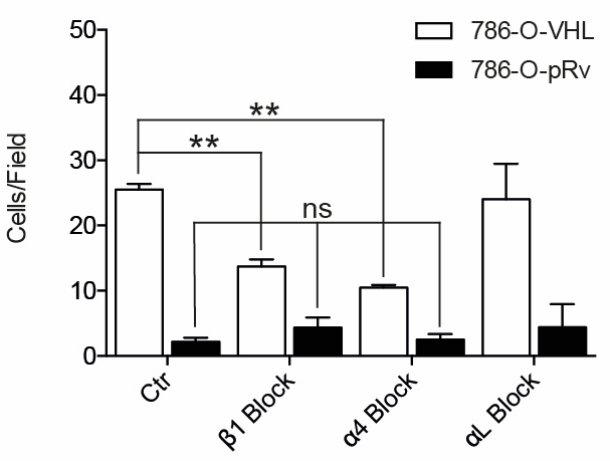

Figure 47: Role of VCAM-1/α4β1 interaction in monocyte adhesion to ccRCC. U937-calcein-AM labelled adhesion experiment on 786-O-pRv or 786-O-VHL untreated (Control) or treated with 10 µg/mL of blocking antibodies against β1, α4, or αL integrin subunits. Cell adhesion was performed for 20 min at 37ºC and afterwards fluorescent cells were counted under the microscope. Data is represented as number of cells ± SEM (n=4), ten random fields were analyzed per condition. Statistical analysis was made using two-way ANOVA test followed by Bonferroni's post hoc test, **P<0.01 significant, ns (not significant).

U937 cells have been widely used as a model to investigate a variety of biological processes related to monocyte and macrophage function. Our results indicating that VCAM-1 expression on the surface of ccRCC cells allowed interaction with monocytic cells made conceivable that this interaction might trigger an immune response against tumor cells. Therefore, we assessed cytotoxicity assays in co-cultures of ccRCC with human monocytic cells activated towards a M1 phenotype. We observed that loss of VHL conferred a cell advantage against the cytotoxic effects of activated monocytic cells since it reduced ccRCC death (Figure 48). These results indicate that VCAM-1 decrease in tumor cells lacking VHL or in hypoxia adversely affect the antitumor immune response.

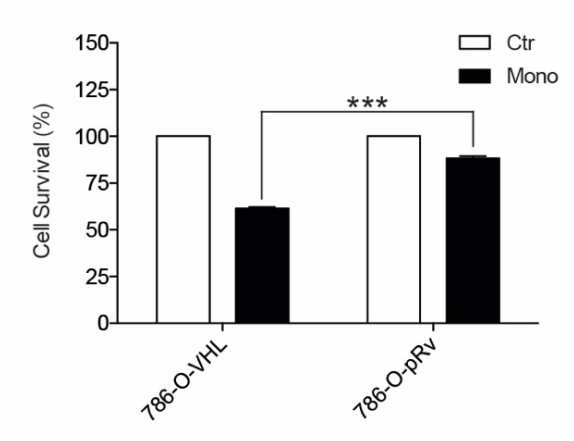

Figure 48: Effects of VHL loss in monocytic cell-mediated cytotoxicity against ccRCC cells. 786-O-pRv or 786-O-VHL target cells were seeded into 16-well sensor plates and activated human monocytes treated with INF-γ and LPS were directly added into wells at a 60/1 ratio monocytes/ccRCCs. Cell survival measurements were automatically collected every 5 min by the by the analyzer RT-CES system (xCELLigence System, Roche) for up to 96 h. Cellular index results were expressed as cell survival percentage at 96 h. Data are representative of three different experiments. Statistical analysis between different conditions was made using two-way ANOVA test followed by Bonferroni's post hoc test, ***P< 0.001 was considered significant.

2.09 Analysis of VCAM-1 levels in human ccRCC.

To address a possible clinical value of our data we analyzed VCAM-1 expression levels in nephrectomy samples from patients with ccRCC. We analyzed a cohort with a total of 127 tumor samples that were divided into two groups according to the type of VHL mutation. One group included missense mutations and the other one non-missense mutations, these including nonsense, insertions, deletions and methylations. In these two groups, we analyzed the association between VCAM-1 expression levels and several clinicopathologic variables.

Table 6: Effects of VHL mutations on VCAM-1 expression levels and its association with clinicopathologic characteristics in human ccRCCs.

VHL alteration	N	VCAM-1 levels	P	Clinicopathologic characteristics		N	VCAM-1 levels	p*
Missense	32	2.622	0.739	Tumor stage	I+II	12	2.943	0.613
					III+IV	20	1.933	
				Tumor grade	1+2	22	2.943	0.223
					3+4	10	1.484	
				Tumor size	≤7	19	3.042	0.173
					7.1≥	13	1.775	
				Microvascular invasion	neg	19	2.846	0.863
					pos	13	1.775	
				Symptom presentation	neg	12	3.577	0.018
					pos	20	1.225	
Non-missense	95	2.099		Tumor stage	I+II	55	2.481	0.01
					III+IV	40	1.562	
				Tumor grade	1+2	70	2.309	0.001
					3+4	25	1.336	
				Tumor size	≤7	77	2.250	0.118
					7.1≥	18	1.492	
				Microvascular invasion	neg	57	2.524	0.009
					pos	38	1.650	
				Symptom presentation	neg	57	2.481	0.004
					pos	38	1.588	

*Mann-Whitney U test

Our results indicated that VCAM-1 levels were higher in samples included in the group of VHL missense mutations compared with non-missense mutations, although this difference did not reach statistical significance. However, we observed a negative association between VCAM-1 levels and ccRCC stage and microvascular invasion that was statistically significant in the group with non-missense mutations ($p \leq 0.05$ Mann-Whitney U test, Table 6). Overall, our results point out the clinical value of VCAM-1 levels as a marker of ccRCC progression. In addition, they also point to effects on the regulation of VCAM-1 that appear to be dependent on the type of VHL mutation.

DISCUSSION

DISCUSSION

In this thesis, we have addressed the role of hypoxia in physiopathology, and in particular we have treated two different topics; pulmonary arterial hypertension and clear cell renal cell carcinoma. Since these topics were presented as well in two experimental sections of results, we decided to discuss them separately to develop a deeper argumentation of each pathology. Nonetheless, we have included a final remark section trying to stablish a relationship between these two diseases. Both are related with hypoxia and with some of its molecular pathways. Hypoxia activates the molecular acute mechanism to adapt the organism, which is essential in acute onset, but harmful in prolonged or chronic hypoxia. In the case of PAH prolonged exposure to low levels of oxygen is the cause of the disease, while in the case of clear cell renal cell carcinoma, local hypoxia is a consequence of an uncontrolled proliferation, characteristic of cancer growth, and the stabilization of HIF due to the loss of VHL. Although both pathologies have converging points, the molecular mechanisms are different.

1. TSP1, THE NEW HYPOXIO-SPONDIN AND ITS EMERGING ROLE IN PAH.

Oxygen is essential for mammalian life and cells are well designed to rapidly alter gene expression profiles in response to changes in the partial pressure of oxygen. Hypoxia activates cellular sensing mechanisms focused on restoring oxygen to the hypoxic regions and maintain cell viability. Previous studies from human and animal models point to HIF1α and HIF2α as important regulators in pulmonary vascular responses to both acute and chronic hypoxia [160-163, 295]. However, results from human subjects and mice models highlight the relevance of HIF2α in PAH [164]. Individuals with Chuvash polycythemia, which is caused by a mutation in VHL, are found to develop PAH [296]. In addition, pulmonary HIF2α activity was found to be increased in a murine model of Chuvash polycythemia, whereas loss of one copy of the HIF2α gene was associated with less pulmonary hypertension in these animals [165]. Not unexpectedly, HIF2α gain-of-function mutations are associated with pulmonary arterial hypertension [162, 164, 297]. Moreover, EPO, a downstream target of HIF2α [298], is increased in the peripheral blood and endothelial cells from explanted lungs of end-stage PAH patients [299, 300]. In hPASMC hypoxia, via HIF2α, increases expression of the transcription factor forkhead box M1 (FoxM1) to promote cell proliferation [301], and the downstream gene target octamer-binding transcription factor 4 (Oct4) [302].

We now find that HIF2α induces TSP1 levels in hypoxic murine lungs. Furthermore, in animals lacking HIF2α, hypoxic upregulation of pulmonary TSP1 was completely abrogated. In addition, TSP1 induction in *vhl*$^{-/-}$ mice, that have constitutive HIF activity and mimic chronic hypoxia, was only reverted in the absence of HIF2α, but not when HIF1α was eliminated, suggesting that HIF2α is necessary for hypoxic-mediated pulmonary induction of TSP1. Moreover, we have seen that the arterial remodeling phenotype of *vhl*$^{-/-}$ was partially decreased in the *vhl*$^{-/-}$/*hif2α*$^{-/-}$ double null mice (unpublished data). Likewise, in both human and murine pulmonary vascular and non-vascular cells hypoxia stimulated an increase in TSP1 mRNA and protein levels. This was due to a transcriptional mechanism mediated by HIF2α-binding to hypoxia-response elements close to the *tsp1* promoter.

Curiously, in mPASMC, hypoxic challenge resulted in a modest and non-significant increase in TSP1 transcript. Although the reasons for this remain to be determined, it is possible that cell viability was adversely altered under the serum restricted conditions of the experiment. However, we cannot exclude that other HIF-independent events could also affect TSP1 protein levels in hypoxic PASMC. Finally, preliminary results in a cohort of human PAH and non-PAH samples suggests that both HIF1α and HIF2α might be involved in the regulation of TSP1 in human lungs in the pulmonary vasculature. However, a more extensive investigation in human PAH will be required to confirm these initial findings.

Migration of PA fibroblasts and PASMC contribute to PA remodeling and luminal narrowing in PAH [303]. Previous studies from our group found *tsp1*$^{-/-}$ systemic arterial smooth muscle cells deficient in platelet-derived growth factor-driven migration compared to WT cells [304]. Consistent with this, we observed that under hypoxia mFIB and mPASMC from *tsp1*$^{-/-}$ mice had decreased migration compared with cells from WT mice. These *in vitro* data predict an effect in vessel remodeling in hypoxic lungs, in keeping with our previous results demonstrating decreased PA remodeling in *tsp1*$^{-/-}$ mice following chronic hypoxia [169]. In cells from TSP1 wild type mice hypoxia-mediated increase in pulmonary TSP1 likely stimulated mFIB and mPASMC migration, in part, through decreasing cell-matrix adhesion. In contrast, the expression of focal adhesion (FA) contacts in hypoxic *tsp1*$^{-/-}$ mFIB and mPASMC was not significantly affected. These results support previous findings from Dr. Murphy Ulrich laboratory regarding the role of TSP1 in the regulation of FA. In their studies, they observe that TSP1 activates focal adhesion kinase (FAK), and this mediates the activation of PI3K and ERK, which culminate with the inactivation of the small GTPase protein Rho A and FA disassembly [269]. The pathogenesis of PAH also involves endothelial cell dysfunction that plays an integral role in mediating the structural changes in the pulmonary vasculature. Our new findings herein demonstrate that hypoxia-mediated induction of TSP1 levels contributed to increase endothelial permeability, this mediated in part by changes in

cell-cell adhesion. This in fact may facilitate PASMC migration through the endothelial barrier and may be an initial cause of endothelial dysfunction, which in turn might contribute to vessel remodeling during PAH. In addition, we also showed that hypoxia-mediated induction of TSP1 may induce human adventitial fibroblast differentiation into cells with SMC-like phenotype expressing SMA decorated F-Actin filaments. These cells could also contribute to the hyperplasia of the tunica media. This *in vitro* differentiation was reverted in the presence of TSP1 and TGF-β inhibitors, indicating that TSP1 through the activation of TGF-β can be involved in this process.

These results give new insights into the molecular mechanisms that regulate TSP1 in hypoxic lungs. They also reveal the possible role of hypoxia in the control of cellular functions relevant to PAH, but most of our studies have been performed in cultured cells and we believe that it is crucial to illuminate PAH events at the organ scale. We performed passive CLARITY in mice lungs to create a pulmonary transparent structure, which allowed us to do immunofluorescence and take high-resolution 3D images without disrupting the organ. Although the technique still needs to be improved, we obtained some considerable achievements. Staining with SMA was observed in big arteries and bronchus, although small arteries labeling still needs further improvements. Regarding TSP1 immunofluorescences on clarified lungs exposed to Hp/Sugen for 3 weeks we observed a big increment of TSP1 protein levels that appeared like aggregates in the parenchyma, with a higher density in the peripheral area of the lung. This is still puzzeling to us and raised more questions than answers to our research project. We do not know exactly the origin of TSP1 and which cells are contributing to its increase under hypoxia. However, our hypothesis is that it could be an additive increment from cells in the PA, cells from the parenchyma, or it could also be released from blood cells, circulating TSP1 released from the α-granules in platelets. In this respect Kaiser et *al* 2016 [172] showed that patients with chronic thromboembolic PH (CTEPH) have a 20-fold increase on TSP-1 circulating concentration compared to healthy controls and that this TSP1 increment correlates with bad hemodynamic parameters as PA pressure mean (PAPm) and systolic PA pressure (PAPsys). In addition, they show a correlation of TSP1 levels with patient survival in that high levels of TSP1 are associated with an increase in mortality. Due the role of TSP1 in platelet aggregation [305, 306] and the results from Kaiser et al [172] we believe that the aggregates we observed in our hypoxic lungs are little thrombus created by a high increase of TSP1. Therefore, TSP1 secreted from platelets may have a new and unsuspected function during PAH. This is interesting and further experimental work needs to be done to confirm our hypothesis.

Together these data provide genetic evidence that TSP1 drives hypoxic pulmonary vascular remodeling. These findings also provide possible mechanistic insight into the previously reported

finding that HIFs stimulate pulmonary fibroblast migration [307], which based on our results herein, is mediated to some degree through the induction of TSP1.

At a functional level, we found that endothelial-dependent vasodilation elicited by ACh was impaired in hypoxic PA from WT mice. In contrast, hypoxic *tsp1*$^{-/-}$ PA retained sensitivity to Ach, indicating a decrease in NO release which supports previously published results from our group in collaboration with Dr Isenberg´s group (University of Pittsburgh)[169, 280]. In addition, arterial contraction and the increase in intracellular calcium induced by the Kv1.5 channel inhibitor DPO1 were markedly decreased in hypoxic versus normoxic WT PA whereas *tsp1*$^{-/-}$ PA were resistant to these DPO1 effects. The reduced contraction in response to DPO1 in hypoxic WT PAs is consistent with the downregulation of Kv1.5 mRNA levels and with the decreased accumulation of intracellular calcium observed in mPASMC. These results are in agreement with studies showing reduced Kv1.5 channel activity and expression in cultured mPASMC [308-310] and intact animals [311, 312] exposed to chronic hypoxia. Downregulation of Kv1.5 and other oxygen-sensitive Kv channels is associated with loss of acute hypoxia-mediated pulmonary vasoconstriction [312, 313]. As Kv1.5 channel expression is preserved in *tsp1*$^{-/-}$ mice, it is expected that hypoxic pulmonary vasoconstriction would be preserved rather than lost when these mice are exposed to chronic hypoxia. However, the mechanisms underlying the preservation of Kv1.5 channel activity in isolated PA from *tsp1*$^{-/-}$ mice remain unknown. Of some possible importance in this regard, it was previously reported that endothelin receptor protein levels were downregulated in lungs from *tsp1*$^{-/-}$ compared to WT mice [280]. As ET-1 is known to inhibit Kv1.5 channels [314, 315], this raises the possibility that the TSP1 effects on Kv channel-mediated contraction in hypoxic PA could be mediated through ET-1. We have recently unraveled in collaboration with Dr Isenberg´s group a new mechanism of the TSP1/CD47 axis in PAH. TSP1 through binding to its CD47 membrane receptor inhibits c-myc activity increasing the synthesis of ET-1, one of the most relevant hallmarks of PAH [316].

Alternatively, the resistance of *tsp1*$^{-/-}$ PA to hypoxia may be due to effects on other signaling moieties including ROS that are increased in hypoxia [317] and promote vasoconstriction. Previous reports indicate that TSP1 can directly activate NADPH oxidases in aortic vascular smooth muscle cells [318] and renal tubular epithelial cells [319] to increase superoxide production. In addition, our previous results obtained in Bauer *et al* 2012 [169] suggest a mechanism by which TSP1 signaling via CD47 could influence PAH by promoting an increase in ROS due to decoupling of endothelial nitric oxide synthase (eNOS) in PAEC. However, it remains to be seen if TSP1 directly stimulates enzymatic ROS production in the pulmonary vasculature.

The present results show that hypoxia, in a HIF2α-dependent manner, elicits an increase on TSP1 levels in tissues and PA cells mediating structural changes in the pulmonary vasculature (summarized in Figure 49). Together these new findings suggest multiple mechanisms through which TSP1 may promote PAH. While its original identification as a thrombin-sensitive protein coined its name "thrombospondin" [177], its induction by hypoxia and its role in PAH may, in fact, lead us to think of TSP1 rather as the new "hypoxio-spondin", as suggested by Shimoda and Kuebler [320]. As TSP1 has been found to be increased in several pulmonary diseases associated with excessive fibrosis [321-323], asthma [324] and COPD [325] our present findings likely have implications beyond PAH.

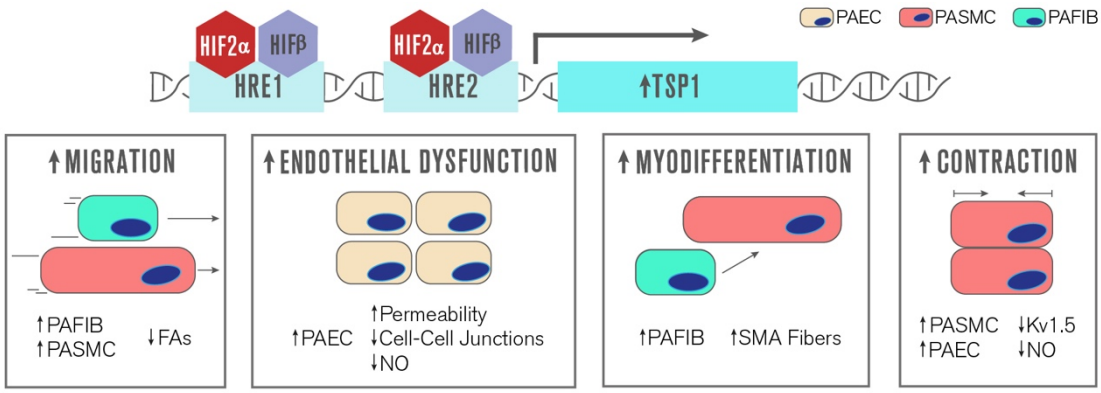

Figure 49: Hypoxia, in a HIF2α-dependent manner, elicits an increase on TSP1 levels in PA cells mediating changes in their cellular behavior. Graphical abstract showing HIF2α binding to *tsp1* HREs and effects of TSP1 on PA cells (migration, endothelial dysfunction, myodifferentiation and contraction).

2. REGULATION OF VCAM-1 LEVELS THROUGH A VHL-PHD-NFκB-DEPENDENT PATHWAY AND ITS ROLE IN THE IMMUNE RESPONSE AGAINST CLEAR-CELL RENAL CELL CARCINOMA.

Clear cell renal cell carcinoma is one of the most abundant cancers in the world [198]**.** Remarkably, 50–80% of sporadic renal cell carcinomas (RCC) and the most frequent form with clear cell histologic feature (ccRCC) present inactivating mutations or epigenetic silencing of VHL [203]. Although the role of VHL in the regulation of HIF prove to be important for tumor growth, other VHL functions independent of HIF have been reported and help to explain why loss of VHL leads to renal cancer [207]. Previous studies report the relevance of VHL expression on VCAM-1 levels in renal carcinoma [326, 327] and other studies correlate higher levels of VCAM-1 expression in ccRCC with a better prognosis [209-211], however the mechanism underneath VCAM-1 regulation in these tumors remains unknown.

Our studies demonstrate that VHL loss or hypoxia down-regulate VCAM-1 mRNA and protein levels in ccRCC cells. This regulation was at the transcriptional level but independent of HIF. Interestingly ccRCC cells treatment with TNF-α reverted VCAM-1 decrease in VHL positive cells under hypoxia, although this was not reproduced in VHL negative cells. In agreement with these results previous findings demonstrate a VHL-dependent sensitization of RCC cells to TNFα-mediated effects [328]. This regulation does not appear to be exclusive to tumor cells, since TNF-α-induced expression of VCAM-1 in HUVEC was significantly decreased under hypoxia, or when treated with PHD or NF-κB inhibitors, as well as in cells treated with VHL siRNA. This is of especial relevance in the setting of tumor migration and immune cell trafficking.

Although VHL most accepted function is as an ubiquitin ligase that targets various proteins for degradation by the proteasome, it has also been observed that VHL has an opposite role promoting protein half-life of several proteins such as BIMEL [77], p53 [78] and Jade-1 [79]. Previous results demonstrate a constitutive activation of the NF-κB pathway in RCC cell lines. On the other hand, VHL expression abolishes the canonical NF-κB pathway and the induction of anti-apoptotic genes in those cells [92-94]. Furthermore, other authors have shown that PHD2 controls TNF-α effects by positively regulating NF-κB signaling [103], and PHD3 serves as a co-activator of NF-κB signaling activity [104]. Our results demonstrate that both VHL and PHD activity are required to maintain VCAM-1 levels in ccRCC cells and they are essential for TNFα-mediated induction of VCAM-1 through a NF-κB non-canonical pathway. These results are relevant considering the results published by Cummins et al. [95] in which they show that kinases of the NF-κB signaling pathway, IKKα and IKKβ, contain the LXXLAP motif for proline hydroxylation. These authors demonstrate that IKKs co-immunoprecipitate with PHD1 and with VHL. Interestingly, this interaction does not result in ubiquitination or proteasomal degradation of IKKs. Although we were unable to demonstrate a direct interaction of VHL with IKKs in ccRCC cell lines, probably due to the lability of this interaction, our results clearly prove that in the absence of VHL or in hypoxia the non-canonical NF-κB pathway is affected and this contributes to decrease VCAM-1 levels.

NF-κB non-canonical pathway requires IKKα-dependent NF-κB2 (p100) processing in the proteasome to generate the binding subunit p52. This subunit is then associated to the transcriptional activator Rel B, enters the nucleus and binds to DNA-NF-κB binding sites in certain NF-κB-responsive genes [329-331]. In our ccRCC cell lines we observed that IKKα and the upstream activator NIK [332] were decreased in the absence of VHL. Furthermore, Rel B and p52 were notably decreased under hypoxia or in the absence of VHL, while no changes in the canonic binding subunit p65 were observed. The possibility exists that PHD-mediated hydroxylation of the non-canonical activator IKKα promotes VHL binding or an intermediate

protein that is also regulated by VHL. This interaction activates the non-canonical pathway while its interaction with IKKβ represses the canonical pathway. Alternatively, an upstream regulation of the non-canonical pathway might occur after direct hydroxylation of NIK by PHDs. In this respect, NIK contains an LXXXLAP sequence that is similar to the LXXLAP consensus hydroxylation sequence present in IKKs [95]. Although these results demonstrated that the non-canonical pathway was involved in VCAM-1 regulation in these cells, we cannot discard that the canonical NF-κB pathway might also contribute.

NF-κB signaling pathways have a diverse spectrum of effects and the NF-κB canonical pathway represents only a fraction of the whole range of genes that are regulated by this family of transcription factors. Despite it is well established that canonical NF-κB regulates VCAM-1 in many different cell types [236], the binding of non-canonical dimers to the VCAM-1 NF-κB described binding sites is highly probable due to the high similarity among these sequences. Our model proposes that VHL-PHD signaling promotes NF-κB non-canonical pathway that increases VCAM-1 levels while downregulating the NF-κB canonical pathway (Figure 50). Future studies will be required to clarify whether canonical and non-canonical NF-κB pathways are interconnected or differentially activated in ccRCCs contributing to tumor growth and progression. Although the two pathways usually cooperate in their biological functions, negative interplays have also been identified. The positive and negative interplays between the two NF-κB pathways may serve to modulate the kinetics and magnitude of expression of NFκB target genes.

The biological roles of the non-canonical NF-κB pathway have been extensively studied [333-335], however how this pathway functions in specific cell types is still unclear. VCAM-1 has been generally correlated with activated endothelium; although its expression has also been detected in tumor models in which the function attributed to VCAM-1 depends on the type of tumor. Thus, recent studies in breast cancer and gastric carcinoma have shown that increased expression of VCAM-1 in these tumors favors metastasis to organs such as lung and bone [336, 337]. Conversely, other studies have highlighted the important role of VCAM-1 in the development of kidney tumors, in which an inverse correlation between the expression of VCAM-1 and tumor malignancy has been observed [209-211]. In agreement with these results we have shown that VCAM-1 expression levels were decreased in a cohort of human ccRCC carrying VHL non-missense mutations compared to those with missense mutations. In addition, a negative correlation between VCAM-1 levels and ccRCC stage and microvascular invasion was only statistically significant in the group with non-missense mutations. These results suggest the existence of differential effects on VCAM-1 regulation and functions that might depend on the type of mutation affecting VHL. This is also supported by our in vitro results in which we observed that TNF-α-mediated regulation of VCAM-1 levels was differentially affected in

various VHL mutants. In addition, our results demonstrated that VCAM-1 expression in VHL positive ccRCC cell promotes adhesion to monocytic cells through its interaction with the integrin α4β1 and elicits an M1 cytotoxic response. Conversely, VHL loss or hypoxia disrupts this interaction probably due to the decrease in VCAM-1 levels.

Taken together these findings reveal pathways that may be critical in ccRCC tumorigenicity, and identify novel candidates that could serve as targets for future therapeutic intervention or as diagnostic/prognostic biomarkers for patients with advanced ccRCC. In addition, the findings described herein may help to understand how VHL acts as a gatekeeper gene in the kidney and provide an insight into the existence of VHL-regulated functions through HIF-independent mechanisms. A better understanding of the molecular mechanisms that allow tumors to escape immune response will be a great benefit on the development of strategies for cancer treatment

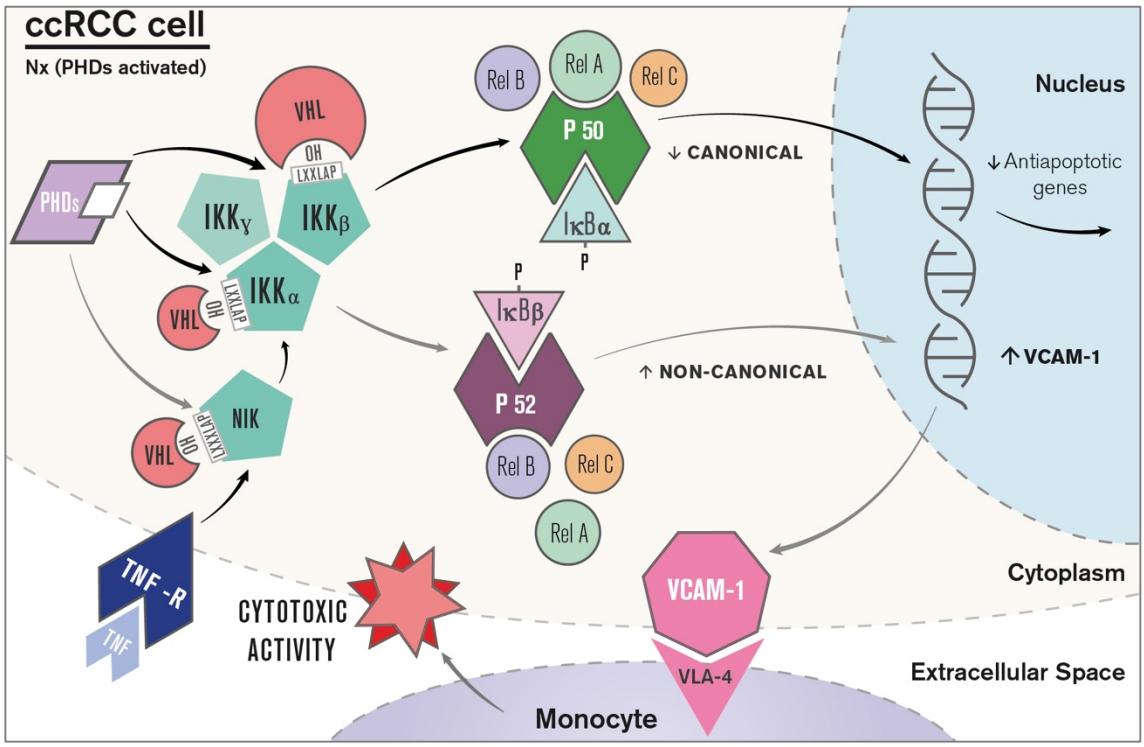

Figure 50: Proposed molecular model of VCAM-1 regulation in ccRCC-VHL expressing cells. IKKα and IKKβ hydroxylation by active PHDs in normoxic conditions allows VHL binding to IKKs. VHL-dependent regulation of IKKα promotes the non-canonical pathway while regulation of IKKβ represses the canonical pathway. Alternatively, an upstream regulation of the non-canonical pathway might occur after PHD direct hydroxylation of NIK. These events regulate transcriptional effectors of the non-canonical pathway (p52-RelB) that ultimately lead to the upregulation of VCAM-1 in Nx. VCAM-1 increase in the ccRCC cell membrane promotes binding to monocytes VLA-4 (α4β1 integrin) and activates their antitumoral effects. In the absence of VHL or in hypoxia this pathway is nonfunctional and VCAM-1 transcriptional induction is repressed. Black arrows indicate previously published data. Grey arrows indicate the proposed model based on results from this thesis.

3. FINAL REMARKS.

In this thesis work we have addressed the role of hypoxia in physiopathology, in particular in lung disease such as PAH, and in ccRCC. We have shown how low oxygen is the cause of a pathological phenotype in hypoxic PAH, leading to processes that are orchestrated by HIF2α. Under hypoxic condition HIF2*α* is stabilized and upregulates the expression of *tsp1*. In a chronic setting, this matricellular protein, far from its homeostatic role becomes a great destabilizer triggering some important PAH events.

In ccRCC we have a very different scenario; conversely to what we observed in our PAH model, in which the canonical pathway in hypoxia, after VHL loss triggered the induction of TSP1 in a HIF-dependent manner, in our ccRCC cell lines the loss of VHL or the inactivation of PHDs under hypoxia repressed the induction of VCAM-1 through HIF-independent mechanisms. Interestingly, in this case VHL and PHDs functions do not involve ubiquitination and proteasome degradation. In fact, the presence of VHL and activated PHDs seem to have a protective role increasing activity of the non-canonic NF-κB pathway. Surprisingly, these effects are probably not unique to this tumor model, as demonstrated in our experiments with HUVEC, which share the same regulation of VCAM-1 observed in tumor cells. This suggests that VHL is crucial for NF-κB pathway beyond cancer, but this is especially relevant in the setting of immune cell trafficking and tumor migration.

Overall, we have found two molecular mechanisms affected by hypoxia in two pathologic contexts in which VHL plays a pivotal role together with PHDs. These results are relevant in that they help to understand the mechanisms behind disease and will benefit the development of new therapies.

CONCLUSIONS

CONCLUSIONS

The findings presented herein support the following conclusions, which have been classified in two sections:

TSP1, the new "hypoxio-spondin" and its emerging role in PAH.

1. HIF2α regulates TSP1 induction under hypoxia in lungs, through its binding to HREs in the proximal promoter region of *tsp1* both in human and mouse.
2. Hypoxic-induced TSP1 in mouse PASMC and pulmonary fibroblasts increases cell migration through focal adhesion disassembly, and in human PAEC promotes disassembly of cell-cell mediated tight junctions and increases endothelial permeability.
3. Hypoxic-induced TSP1 in human PAFIB leads to fibroblast differentiation into a SMC-like phenotype increasing the number of SMA-decorated actin filaments through a process dependent of TFG-β.
4. Hypoxic-induced TSP1 decreases vascular relaxation of PASMC, in part mediated by a reduction in the levels of Kv1.5 channel.
5. The increase of TSP1 in pulmonary arteries of patients with PAH versus healthy controls could be considered as a diagnostic marker of the pathology as well as a new target for the development of new therapeutic strategies in PAH.

Regulation of VCAM-1 levels through a VHL-PHD-NFκB-dependent pathway and its role in the immune response against clear-cell renal cell carcinoma.

6. VHL loss, hypoxia and PHD inhibition or silencing inhibit VCAM-1 transcription in ccRCC cell lines in a HIF-independent manner.
7. VCAM-1 regulation after VHL loss, hypoxia and PHD inhibition is mediated by a noncanonic NF-kB pathway.
8. VCAM-1 decreased expression in ccRCC membrane decreases monocyte binding through its receptor, the α4β1 integrin.
9. Monocytic-ccRCC cell adhesion through VCAM-1-α4β1 interaction promotes an immune response against tumor cells.
10. Human ccRCC carrying non-missense mutations of VHL express lower levels of VCAM-1 compared to those with missense mutations. Moreover, a negative correlation between VCAM-1 levels and ccRCC stage and microvascular invasion was only statistically significant in the group with non-missense mutations.

CONCLUSIONES

CONLCUSIONES

Los hallazgos presentados en esta tesis apoyan las siguientes conclusiones, que se han clasificado en dos secciones:

TSP1, la nueva "hipoxia-espondina" y su papel emergente en la HAP.

1. HIF2α regula la inducción de TSP1 en hipoxia en el pulmón mediante su unión a HREs en la región promotora proximal de TSP1 tanto en humano como en ratón.
2. La inducción de TSP1 por hipoxia aumenta la migración de PASMC y fibroblastos de pulmón murinos a través del desensamblaje de adhesiones focales, y en PAEC humanas promueve el desensamblaje de adhesiones intercelulares estrechas aumentando así la permeabilidad endotelial.
3. La inducción de TSP1 por hipoxia induce la diferenciación de PAFIB humanos a un fenotipo tipo SMC con un aumento en el número de filamentos de actina decorados con SMA a través de un proceso dependiente de TFG-β.
4. La TSP1 inducida por hipoxia disminuye la relajación vascular de PASMC, en parte mediada por una reducción en los niveles del canal de potasio Kv1.5.
5. El aumento de la TSP1 en arterias pulmonares de pacientes con HAP versus controles sanos podría ser considerados como marcador diagnóstico de la patología, así como una nueva diana para el desarrollo de nuevas estrategias terapéuticas en HAP.

Regulación de los niveles de VCAM-1 a través de una vía VHL-PHD-NFκB-dependiente y su papel en la respuesta inmune contra carcinoma renal de célula clara.

6. La pérdida de VHL, la hipoxia y la inhibición o silenciamiento de las PHDs inhiben la transcripción de VCAM-1 en líneas celulares de ccRCC de manera independiente de HIF.
7. La regulación de VCAM-1 por VHL, hipoxia o inhibición de las PHDs está mediada por la vía no-canónica de NF-*κ*B.
8. La expresión disminuida de VCAM-1 en la membrana de células ccRCC disminuye la unión de monocitos a través de su receptor, la integrina α4β1.
9. La adhesión célula ccRCC-monocito mediante la interacción VCAM-1-α4β1 promueve una respuesta inmune anti-tumoral.
10. El ccRCC humano con mutaciones sin sentido en *vhl* expresa niveles más bajos de VCAM-1 en comparación con aquellos con mutaciones con cambio de sentido. Además, se demuestra una correlación negativa entre los niveles de VCAM-1 y el estadio del ccRCC y la invasión microvascular que es estadísticamente significativa en el grupo con mutaciones sin sentido.

REFERENCES

REFERENCES

1. Dunwoodie, S.L., *The role of hypoxia in development of the Mammalian embryo.* Dev Cell, 2009. **17**(6): p. 755-73.

2. Casey, D.P. and M.J. Joyner, *Compensatory vasodilatation during hypoxic exercise: mechanisms responsible for matching oxygen supply to demand.* J Physiol, 2012. **590**(24): p. 6321-6.

3. Buizer, A.T., et al., *The balance between proliferation and transcription of angiogenic factors of mesenchymal stem cells in hypoxia.* Connect Tissue Res, 2017.

4. Fernandez-Aguera, M.C., et al., *Oxygen Sensing by Arterial Chemoreceptors Depends on Mitochondrial Complex I Signaling.* Cell Metab, 2015. **22**(5): p. 825-37.

5. Lopez-Barneo, J., et al., *Oxygen sensing by the carotid body: mechanisms and role in adaptation to hypoxia.* Am J Physiol Cell Physiol, 2016. **310**(8): p. C629-42.

6. Lopez-Barneo, J., R. Pardal, and P. Ortega-Saenz, *Cellular mechanism of oxygen sensing.* Annu Rev Physiol, 2001. **63**: p. 259-87.

7. Kapitsinou, P.P., et al., *Hepatic HIF-2 regulates erythropoietic responses to hypoxia in renal anemia.* Blood, 2010. **116**(16): p. 3039-48.

8. Percy, M.J., et al., *Two new mutations in the HIF2A gene associated with erythrocytosis.* Am J Hematol, 2012. **87**(4): p. 439-42.

9. Jelkmann, W., *Regulation of erythropoietin production.* J Physiol, 2011. **589**(Pt 6): p. 1251-8.

10. Zhu, L., et al., *Mitochondrial transplantation attenuates hypoxic pulmonary hypertension.* Oncotarget, 2016. **7**(31): p. 48925-48940.

11. Ardanaz, N., W.H. Beierwaltes, and P.J. Pagano, *Comparison of H2O2-induced vasoconstriction in the abdominal aorta and mesenteric artery of the mouse.* Vascul Pharmacol, 2007. **47**(5-6): p. 288-94.

12. Webb, R.C., *Smooth muscle contraction and relaxation.* Adv Physiol Educ, 2003. **27**(1-4): p. 201-6.

13. Grassie, M.E., et al., *Cross-talk between Rho-associated kinase and cyclic nucleotide-dependent kinase signaling pathways in the regulation of smooth muscle myosin light chain phosphatase.* J Biol Chem, 2012. **287**(43): p. 36356-69.

14. Hedegaard, E.R., et al., *Non-endothelial endothelin counteracts hypoxic vasodilation in porcine large coronary arteries.* BMC Physiol, 2011. **11**(1): p. 8.

15. Inserte, J., et al., *Activation of cGMP/protein kinase G pathway in postconditioned myocardium depends on reduced oxidative stress and preserved endothelial nitric oxide synthase coupling.* J Am Heart Assoc, 2013. **2**(1): p. e005975.

16. Francis, S.H., et al., *cGMP-dependent protein kinases and cGMP phosphodiesterases in nitric oxide and cGMP action.* Pharmacol Rev, 2010. **62**(3): p. 525-63.

17. Yamakage, M. and A. Namiki, *Calcium channels--basic aspects of their structure, function and gene encoding; anesthetic action on the channels--a review.* Can J Anaesth, 2002. **49**(2): p. 151-64.

18. Miller, J.R., P.J. Silver, and J.T. Stull, *The role of myosin light chain kinase phosphorylation in beta-adrenergic relaxation of tracheal smooth muscle.* Mol Pharmacol, 1983. **24**(2): p. 235-42.

19. Cooke, R., *The sliding filament model: 1972-2004.* J Gen Physiol, 2004. **123**(6): p. 643-56.

20. Houdusse, A. and H.L. Sweeney, *How Myosin Generates Force on Actin Filaments.* Trends Biochem Sci, 2016. **41**(12): p. 989-997.

21. Madden, J.A., M.S. Vadula, and V.P. Kurup, *Effects of hypoxia and other vasoactive agents on pulmonary and cerebral artery smooth muscle cells.* Am J Physiol, 1992. **263**(3 Pt 1): p. L384-93.

22. Marshall, C. and B.E. Marshall, *Hypoxic pulmonary vasoconstriction is not endothelium dependent.* Proc Soc Exp Biol Med, 1992. **201**(3): p. 267-70.

23. Kuhr, F.K., et al., *New mechanisms of pulmonary arterial hypertension: role of Ca(2)(+) signaling.* Am J Physiol Heart Circ Physiol, 2012. **302**(8): p. H1546-62.

24. Sommer, N., et al., *Regulation of hypoxic pulmonary vasoconstriction: basic mechanisms.* Eur Respir J, 2008. **32**(6): p. 1639-51.

25. Moral-Sanz, J., et al., *AMP-activated protein kinase inhibits Kv 1.5 channel currents of pulmonary arterial myocytes in response to hypoxia and inhibition of mitochondrial oxidative phosphorylation.* J Physiol, 2016. **594**(17): p. 4901-15.

26. Gu, Y.Z., et al., *Molecular characterization and chromosomal localization of a third alpha-class hypoxia inducible factor subunit, HIF3alpha.* Gene Expr, 1998. **7**(3): p. 205-13.

27. Tian, H., S.L. McKnight, and D.W. Russell, *Endothelial PAS domain protein 1 (EPAS1), a transcription factor selectively expressed in endothelial cells.* Genes Dev, 1997. **11**(1): p. 72-82.

28. Wang, G.L., et al., *Hypoxia-inducible factor 1 is a basic-helix-loop-helix-PAS heterodimer regulated by cellular O2 tension.* Proc Natl Acad Sci U S A, 1995. **92**(12): p. 5510-4.

29. Semenza, G.L. and G.L. Wang, *A nuclear factor induced by hypoxia via de novo protein synthesis binds to the human erythropoietin gene enhancer at a site required for transcriptional activation.* Mol Cell Biol, 1992. **12**(12): p. 5447-54.

30. Freedman, S.J., et al., *Structural basis for recruitment of CBP/p300 by hypoxia-inducible factor-1 alpha.* Proc Natl Acad Sci U S A, 2002. **99**(8): p. 5367-72.

31. Lendahl, U., et al., *Generating specificity and diversity in the transcriptional response to hypoxia.* Nat Rev Genet, 2009. **10**(12): p. 821-32.

32. O'Rourke, J.F., et al., *Oxygen-regulated and transactivating domains in endothelial PAS protein 1: comparison with hypoxia-inducible factor-1alpha.* J Biol Chem, 1999. **274**(4): p. 2060-71.

33. Huang, L.E., et al., *Regulation of hypoxia-inducible factor 1alpha is mediated by an O2-dependent degradation domain via the ubiquitin-proteasome pathway.* Proc Natl Acad Sci U S A, 1998. **95**(14): p. 7987-92.

34. Jiang, B.H., et al., *Transactivation and inhibitory domains of hypoxia-inducible factor 1alpha. Modulation of transcriptional activity by oxygen tension.* J Biol Chem, 1997. **272**(31): p. 19253-60.

35. Jiang, B.H., et al., *Dimerization, DNA binding, and transactivation properties of hypoxia-inducible factor 1.* J Biol Chem, 1996. **271**(30): p. 17771-8.

36. Wang, G.L. and G.L. Semenza, *Characterization of hypoxia-inducible factor 1 and regulation of DNA binding activity by hypoxia.* J Biol Chem, 1993. **268**(29): p. 21513-8.

37. Dengler, V.L., M.D. Galbraith, and J.M. Espinosa, *Transcriptional regulation by hypoxia inducible factors.* Crit Rev Biochem Mol Biol, 2014. **49**(1): p. 1-15.

38. Maynard, M.A., et al., *Multiple splice variants of the human HIF-3 alpha locus are targets of the von Hippel-Lindau E3 ubiquitin ligase complex.* J Biol Chem, 2003. **278**(13): p. 11032-40.

39. Kaelin, W.G., Jr. and P.J. Ratcliffe, *Oxygen sensing by metazoans: the central role of the HIF hydroxylase pathway.* Mol Cell, 2008. **30**(4): p. 393-402.

40. Koh, M.Y. and G. Powis, *Passing the baton: the HIF switch.* Trends Biochem Sci, 2012. **37**(9): p. 364-72.

41. Villar, D., et al., *Cooperativity of stress-responsive transcription factors in core hypoxia-inducible factor binding regions.* PLoS One, 2012. **7**(9): p. e45708.

42. Semenza, G.L., *Hypoxia-inducible factors in physiology and medicine.* Cell, 2012. **148**(3): p. 399-408.

43. Tian, H., S.L. McKnight, and D.W. Russell, *Endothelial PAS domain protein 1 (EPAS1), a transcription factor selectively expressed in endothelial cells.* Genes Dev., 1997. **11**(1): p. 72-82.

44. Ema, M., et al., *A novel bHLH-PAS factor with close sequence similarity to hypoxia-inducible factor 1alpha regulates the VEGF expression and is potentially involved in lung and vascular development.* Proc Natl Acad Sci U S A, 1997. **94**(9): p. 4273-8.

45. Koh, M.Y., et al., *The hypoxia-associated factor switches cells from HIF-1alpha- to HIF-2alpha-dependent signaling promoting stem cell characteristics, aggressive tumor growth and invasion.* Cancer Res, 2011. **71**(11): p. 4015-27.

46. Takagi, H., G.L. King, and L.P. Aiello, *Hypoxia upregulates glucose transport activity through an adenosine-mediated increase of GLUT1 expression in retinal capillary endothelial cells.* Diabetes, 1998. **47**(9): p. 1480-8.

47. Firth, J.D., B.L. Ebert, and P.J. Ratcliffe, *Hypoxic regulation of lactate dehydrogenase A. Interaction between hypoxia-inducible factor 1 and cAMP response elements.* J Biol Chem, 1995. **270**(36): p. 21021-7.

48. McDonald, P.C. and S. Dedhar, *Carbonic anhydrase IX (CAIX) as a mediator of hypoxia-induced stress response in cancer cells.* Subcell Biochem, 2014. **75**: p. 255-69.

49. Pelletier, J., et al., *Glycogen Synthesis is Induced in Hypoxia by the Hypoxia-Inducible Factor and Promotes Cancer Cell Survival.* Front Oncol, 2012. **2**: p. 18.

50. Pescador, N., et al., *Hypoxia promotes glycogen accumulation through hypoxia inducible factor (HIF)-mediated induction of glycogen synthase 1.* PLoS One, 2010. **5**(3): p. e9644.

51. Tello, D., et al., *Induction of the mitochondrial NDUFA4L2 protein by HIF-1alpha decreases oxygen consumption by inhibiting Complex I activity.* Cell Metab, 2011. **14**(6): p. 768-79.

52. Forristal, C.E., et al., *Hypoxia inducible factors regulate pluripotency and proliferation in human embryonic stem cells cultured at reduced oxygen tensions.* Reproduction, 2010. **139**(1): p. 85-97.

53. Mimeault, M. and S.K. Batra, *Hypoxia-inducing factors as master regulators of stemness properties and altered metabolism of cancer- and metastasis-initiating cells.* J Cell Mol Med, 2013. **17**(1): p. 30-54.

54. Takeda, N., et al., *Endothelial PAS domain protein 1 gene promotes angiogenesis through the transactivation of both vascular endothelial growth factor and its receptor, Flt-1.* Circ Res., 2004. **95**(2): p. 146-53. Epub 2004 Jun 10.

55. Hu, C.J., et al., *Differential roles of hypoxia-inducible factor 1alpha (HIF-1alpha) and HIF-2alpha in hypoxic gene regulation.* Mol Cell Biol, 2003. **23**(24): p. 9361-74.

56. Wenger, R.H., *Cellular adaptation to hypoxia: O2-sensing protein hydroxylases, hypoxia-inducible transcription factors, and O2-regulated gene expression.* Faseb J, 2002. **16**(10): p. 1151-62.

57. Calzada, M.J. and L. del Peso, *Hypoxia-inducible factors and cancer.* Clin Transl Oncol, 2007. **9**(5): p. 278-89.

58. Jaakkola, P., et al., *Targeting of HIF-alpha to the von Hippel-Lindau ubiquitylation complex by O2-regulated prolyl hydroxylation.* Science, 2001. **292**(5516): p. 468-72.

59. Masson, N., et al., *Independent function of two destruction domains in hypoxia-inducible factor-alpha chains activated by prolyl hydroxylation.* Embo J, 2001. **20**(18): p. 5197-206.

60. Bruick, R.K. and S.L. McKnight, *A conserved family of prolyl-4-hydroxylases that modify HIF.* Science, 2001. **294**(5545): p. 1337-40.

61. Appelhoff, R.J., et al., *Differential function of the prolyl hydroxylases PHD1, PHD2, and PHD3 in the regulation of hypoxia-inducible factor.* J Biol Chem, 2004. **279**(37): p. 38458-65.

62. Richard, S., et al., *Von Hippel-Lindau: how a rare disease illuminates cancer biology.* Semin Cancer Biol, 2013. **23**(1): p. 26-37.

63. Maxwell, P.H., et al., *The tumour suppressor protein VHL targets hypoxia-inducible factors for oxygen-dependent proteolysis.* Nature, 1999. **399**(6733): p. 271-5.

64. Tanimoto, K., et al., *Mechanism of regulation of the hypoxia-inducible factor-1 alpha by the von Hippel-Lindau tumor suppressor protein.* Embo J, 2000. **19**(16): p. 4298-309.

65. Semenza, G.L., *Targeting HIF-1 for cancer therapy.* Nat Rev Cancer, 2003. **3**(10): p. 721-32.

66. Gossage, L., T. Eisen, and E.R. Maher, *VHL, the story of a tumour suppressor gene.* Nat Rev Cancer, 2015. **15**(1): p. 55-64.

67. Iliopoulos, O., M. Ohh, and W.G. Kaelin, Jr., *pVHL19 is a biologically active product of the von Hippel-Lindau gene arising from internal translation initiation.* Proc Natl Acad Sci U S A, 1998. **95**(20): p. 11661-6.

68. Maher, E.R., H.P. Neumann, and S. Richard, *von Hippel-Lindau disease: a clinical and scientific review.* Eur J Hum Genet, 2011. **19**(6): p. 617-23.

69. Franke, G., et al., *Alu-Alu recombination underlies the vast majority of large VHL germline deletions: Molecular characterization and genotype-phenotype correlations in VHL patients.* Hum Mutat, 2009. **30**(5): p. 776-86.

70. Kaelin, W.G., Jr., *Molecular basis of the VHL hereditary cancer syndrome.* Nat Rev Cancer, 2002. **2**(9): p. 673-82.

71. Hickey, M.M., et al., *von Hippel-Lindau mutation in mice recapitulates Chuvash polycythemia via hypoxia-inducible factor-2alpha signaling and splenic erythropoiesis.* J Clin Invest, 2007. **117**(12): p. 3879-89.

72. Sufan, R.I., M.A. Jewett, and M. Ohh, *The role of von Hippel-Lindau tumor suppressor protein and hypoxia in renal clear cell carcinoma.* Am J Physiol Renal Physiol, 2004. **287**(1): p. F1-6.

73. Hes, F.J., et al., *Von hippel-lindau disease.* Hered Cancer Clin Pract, 2005. **3**(4): p. 171-8.

74. Nguyen, H.C., et al., *Insights into Cullin-RING E3 ubiquitin ligase recruitment: structure of the VHL-EloBC-Cul2 complex.* Structure, 2015. **23**(3): p. 441-9.

75. Cai, W. and H. Yang, *The structure and regulation of Cullin 2 based E3 ubiquitin ligases and their biological functions.* Cell Div, 2016. **11**: p. 7.

76. Arias-Gonzalez, L., et al., *ERK5/BMK1 is a novel target of the tumor suppressor VHL: implication in clear cell renal carcinoma.* Neoplasia, 2013. **15**(6): p. 649-59.

77. Guo, Y., M.C. Schoell, and R.S. Freeman, *The von Hippel-Lindau protein sensitizes renal carcinoma cells to apoptotic stimuli through stabilization of BIM(EL).* Oncogene, 2009. **28**(16): p. 1864-74.

78. Roe, J.S., et al., *p53 stabilization and transactivation by a von Hippel-Lindau protein.* Mol Cell., 2006. **22**(3): p. 395-405.

79. Zhou, M.I., et al., *Tumor suppressor von Hippel-Lindau (VHL) stabilization of Jade-1 protein occurs through plant homeodomains and is VHL mutation dependent.* Cancer Res, 2004. **64**(4): p. 1278-86.

80. Panchenko, M.V., *Structure, function and regulation of jade family PHD finger 1 (JADE1).* Gene, 2016. **589**(1): p. 1-11.

81. Ordonez-Navadijo, A., et al., *Mutant versions of von Hippel-Lindau (VHL) can protect HIF1alpha from SART1-mediated degradation in clear-cell renal cell carcinoma.* Oncogene, 2016. **35**(5): p. 587-94.

82. Davidowitz, E.J., A.R. Schoenfeld, and R.D. Burk, *VHL induces renal cell differentiation and growth arrest through integration of cell-cell and cell-extracellular matrix signaling.* Mol Cell Biol, 2001. **21**(3): p. 865-74.

83. Esteban-Barragan, M.A., et al., *Role of the von Hippel-Lindau tumor suppressor gene in the formation of beta1-integrin fibrillar adhesions.* Cancer Res, 2002. **62**(10): p. 2929-36.

84. Esteban, M.A., et al., *Formation of primary cilia in the renal epithelium is regulated by the von hippel-lindau tumor suppressor protein.* J Am Soc Nephrol., 2006. **17**(7): p. 1801-6.

85. Evans, A.J., et al., *VHL promotes E2 box-dependent E-cadherin transcription by HIF-mediated regulation of SIP1 and snail.* Mol Cell Biol., 2007. **27**(1): p. 157-69. Epub 2006 Oct 23.

86. Calzada, M.J., et al., *von Hippel-Lindau tumor suppressor protein regulates the assembly of intercellular junctions in renal cancer cells through hypoxia-inducible factor-independent mechanisms.* Cancer Res, 2006. **66**(3): p. 1553-60.

87. Li, L., et al., *Hypoxia-inducible factor linked to differential kidney cancer risk seen with type 2A and type 2B VHL mutations.* Mol Cell Biol, 2007. **27**(15): p. 5381-92.

88. Knauth, K., et al., *Renal cell carcinoma risk in type 2 von Hippel-Lindau disease correlates with defects in pVHL stability and HIF-1alpha interactions.* Oncogene, 2006. **25**(3): p. 370-7.

89. Harten, S.K., et al., *Regulation of renal epithelial tight junctions by the von Hippel-Lindau tumor suppressor gene involves occludin and claudin 1 and is independent of E-cadherin.* Mol Biol Cell, 2009. **20**(3): p. 1089-101.

90. Feijoo-Cuaresma, M., et al., *Inadequate activation of the GTPase RhoA contributes to the lack of fibronectin matrix assembly in von Hippel-Lindau protein-defective renal cancer cells.* J Biol Chem, 2008. **283**(36): p. 24982-90.

91. Lieubeau-Teillet, B., et al., *von Hippel-Lindau gene-mediated growth suppression and induction of differentiation in renal cell carcinoma cells grown as multicellular tumor spheroids.* Cancer Res, 1998. **58**(21): p. 4957-62.

92. Oya, M., et al., *Constitutive activation of nuclear factor-kappaB prevents TRAIL-induced apoptosis in renal cancer cells.* Oncogene, 2001. **20**(29): p. 3888-96.

93. An, J., M. Fisher, and M.B. Rettig, *VHL expression in renal cell carcinoma sensitizes to bortezomib (PS-341) through an NF-kappaB-dependent mechanism.* Oncogene, 2005. **24**(9): p. 1563-70.

94. Qi, H. and M. Ohh, *The von Hippel-Lindau tumor suppressor protein sensitizes renal cell carcinoma cells to tumor necrosis factor-induced cytotoxicity by suppressing the nuclear factor-kappaB-dependent antiapoptotic pathway.* Cancer Res, 2003. **63**(21): p. 7076-80.

95. Cummins, E.P., et al., *Prolyl hydroxylase-1 negatively regulates IkappaB kinase-beta, giving insight into hypoxia-induced NFkappaB activity.* Proc Natl Acad Sci U S A, 2006. **103**(48): p. 18154-9.

96. Berra, E., et al., *HIF prolyl-hydroxylase 2 is the key oxygen sensor setting low steady-state levels of HIF-1alpha in normoxia.* Embo J, 2003. **22**(16): p. 4082-90.

97. McNeill, L.A., et al., *The use of dioxygen by HIF prolyl hydroxylase (PHD1).* Bioorg Med Chem Lett, 2002. **12**(12): p. 1547-50.

98. Chowdhury, R., et al., *Structural basis for binding of hypoxia-inducible factor to the oxygen-sensing prolyl hydroxylases.* Structure, 2009. **17**(7): p. 981-9.

99. Gorres, K.L. and R.T. Raines, *Prolyl 4-hydroxylase.* Crit Rev Biochem Mol Biol, 2010. **45**(2): p. 106-24.

100. Xie, L., et al., *PHD3-dependent hydroxylation of HCLK2 promotes the DNA damage response.* J Clin Invest, 2012. **122**(8): p. 2827-36.

101. Luo, W., et al., *Pyruvate kinase M2 is a PHD3-stimulated coactivator for hypoxia-inducible factor 1.* Cell, 2011. **145**(5): p. 732-44.

102. Xie, L., et al., *Oxygen-regulated beta(2)-adrenergic receptor hydroxylation by EGLN3 and ubiquitylation by pVHL.* Sci Signal, 2009. **2**(78): p. ra33.

103. Li, J., et al., *Prolyl-4-hydroxylase domain protein 2 controls NF-kappaB/p65 transactivation and enhances the catabolic effects of inflammatory cytokines on cells of the nucleus pulposus.* J Biol Chem, 2015. **290**(11): p. 7195-207.

104. Fujita, N., et al., *Prolyl hydroxylase 3 (PHD3) modulates catabolic effects of tumor necrosis factor-alpha (TNF-alpha) on cells of the nucleus pulposus through co-activation of nuclear factor kappaB (NF-kappaB)/p65 signaling.* J Biol Chem, 2012. **287**(47): p. 39942-53.

105. Koditz, J., et al., *Oxygen-dependent ATF-4 stability is mediated by the PHD3 oxygen sensor.* Blood, 2007. **110**(10): p. 3610-7.

106. Ehrismann, D., et al., *Studies on the activity of the hypoxia-inducible-factor hydroxylases using an oxygen consumption assay.* Biochem J, 2007. **401**(1): p. 227-34.

107. Waypa, G.B., K.A. Smith, and P.T. Schumacker, *O2 sensing, mitochondria and ROS signaling: The fog is lifting.* Mol Aspects Med, 2016. **47-48**: p. 76-89.

108. Klimova, T. and N.S. Chandel, *Mitochondrial complex III regulates hypoxic activation of HIF.* Cell Death Differ, 2008. **15**(4): p. 660-6.

109. Zorov, D.B., M. Juhaszova, and S.J. Sollott, *Mitochondrial reactive oxygen species (ROS) and ROS-induced ROS release.* Physiol Rev, 2014. **94**(3): p. 909-50.

110. Mahon, P.C., K. Hirota, and G.L. Semenza, *FIH-1: a novel protein that interacts with HIF-1alpha and VHL to mediate repression of HIF-1 transcriptional activity.* Genes Dev, 2001. **15**(20): p. 2675-86.

111. Lando, D., et al., *FIH-1 is an asparaginyl hydroxylase enzyme that regulates the transcriptional activity of hypoxia-inducible factor.* Genes Dev, 2002. **16**(12): p. 1466-71.

112. Jeong, J.W., et al., *Regulation and destabilization of HIF-1alpha by ARD1-mediated acetylation.* Cell, 2002. **111**(5): p. 709-20.

113. Brahimi-Horn, C., N. Mazure, and J. Pouyssegur, *Signalling via the hypoxia-inducible factor-1alpha requires multiple posttranslational modifications.* Cell Signal, 2005. **17**(1): p. 1-9.

114. Knippschild, U., et al., *The role of the casein kinase 1 (CK1) family in different signaling pathways linked to cancer development.* Onkologie, 2005. **28**(10): p. 508-14.

115. Kalousi, A., et al., *Casein kinase 1 regulates human hypoxia-inducible factor HIF-1.* J Cell Sci, 2010. **123**(Pt 17): p. 2976-86.

116. Pangou, E., et al., *HIF-2alpha phosphorylation by CK1delta promotes erythropoietin secretion in liver cancer cells under hypoxia.* J Cell Sci, 2016. **129**(22): p. 4213-4226.

117. Kietzmann, T., D. Mennerich, and E.Y. Dimova, *Hypoxia-Inducible Factors (HIFs) and Phosphorylation: Impact on Stability, Localization, and Transactivity.* Front Cell Dev Biol, 2016. **4**: p. 11.

118. Wang, F., et al., *Roles of coactivators in hypoxic induction of the erythropoietin gene.* PLoS One, 2010. **5**(4): p. e10002.

119. Christofk, H.R., et al., *The M2 splice isoform of pyruvate kinase is important for cancer metabolism and tumour growth.* Nature, 2008. **452**(7184): p. 230-3.

120. Galbraith, M.D., et al., *HIF1A employs CDK8-mediator to stimulate RNAPII elongation in response to hypoxia.* Cell, 2013. **153**(6): p. 1327-39.

121. Zhong, L. and R. Mostoslavsky, *Fine tuning our cellular factories: sirtuins in mitochondrial biology.* Cell Metab, 2011. **13**(6): p. 621-6.

122. Belaiba, R.S., et al., *Hypoxia up-regulates hypoxia-inducible factor-1alpha transcription by involving phosphatidylinositol 3-kinase and nuclear factor kappaB in pulmonary artery smooth muscle cells.* Mol Biol Cell, 2007. **18**(12): p. 4691-7.

123. Sperandio, S., et al., *The transcription factor Egr1 regulates the HIF-1alpha gene during hypoxia.* Mol Carcinog, 2009. **48**(1): p. 38-44.

124. Galban, S. and M. Gorospe, *Factors interacting with HIF-1alpha mRNA: novel therapeutic targets.* Curr Pharm Des, 2009. **15**(33): p. 3853-60.

125. Culver, C., et al., *Mechanism of hypoxia-induced NF-kappaB.* Mol Cell Biol, 2010. **30**(20): p. 4901-21.

126. Mabjeesh, N.J., et al., *Androgens stimulate hypoxia-inducible factor 1 activation via autocrine loop of tyrosine kinase receptor/phosphatidylinositol 3'-kinase/protein kinase B in prostate cancer cells.* Clin Cancer Res, 2003. **9**(7): p. 2416-25.

127. Masoud, G.N. and W. Li, *HIF-1alpha pathway: role, regulation and intervention for cancer therapy.* Acta Pharm Sin B, 2015. **5**(5): p. 378-89.

128. Semenza, G.L., *Hypoxia-inducible factors: mediators of cancer progression and targets for cancer therapy.* Trends Pharmacol Sci, 2012. **33**(4): p. 207-14.

129. Semenza, G.L., *Hypoxia-inducible factors: coupling glucose metabolism and redox regulation with induction of the breast cancer stem cell phenotype.* EMBO J, 2017. **36**(3): p. 252-259.

130. Manoochehri Khoshinani, H., S. Afshar, and R. Najafi, *Hypoxia: A Double-Edged Sword in Cancer Therapy.* Cancer Invest, 2016. **34**(10): p. 536-545.

131. Fishman, A.P., *Primary pulmonary arterial hypertension: a look back.* J Am Coll Cardiol, 2004. **43**(12 Suppl S): p. 2S-4S.

132. Galie, N., et al., *2015 ESC/ERS Guidelines for the diagnosis and treatment of pulmonary hypertension: The Joint Task Force for the Diagnosis and Treatment of Pulmonary Hypertension of the European Society of Cardiology (ESC) and the European Respiratory Society (ERS): Endorsed by: Association for European Paediatric and Congenital Cardiology (AEPC),*

International Society for Heart and Lung Transplantation (ISHLT). Eur Heart J, 2016. **37**(1): p. 67-119.

133. Lammers, A.E., et al., *Functional classification of pulmonary hypertension in children: Report from the PVRI pediatric taskforce, Panama 2011.* Pulm Circ, 2011. **1**(2): p. 280-285.

134. Saglam, M., et al., *Functional exercise capacity, physical activity, and respiratory and peripheral muscle strength in pulmonary hypertension according to disease severity.* J Phys Ther Sci, 2015. **27**(5): p. 1309-12.

135. MacKenzie, A.M. and A.J. Peacock, *Medical Therapies for the Treatment of Pulmonary Arterial Hypertension: How Do We Choose?* Curr Hypertens Rep, 2015. **17**(7): p. 56.

136. Mair, K.M., et al., *Sex-dependent influence of endogenous estrogen in pulmonary hypertension.* Am J Respir Crit Care Med, 2014. **190**(4): p. 456-67.

137. Best, D.H., et al., *Genetics of pulmonary hypertension.* Curr Opin Cardiol, 2014. **29**(6): p. 520-7.

138. Klinger, J.R., S.H. Abman, and M.T. Gladwin, *Nitric oxide deficiency and endothelial dysfunction in pulmonary arterial hypertension.* Am J Respir Crit Care Med, 2013. **188**(6): p. 639-46.

139. Rabinovitch, M., *Molecular pathogenesis of pulmonary arterial hypertension.* J Clin Invest, 2012. **122**(12): p. 4306-13.

140. Cogolludo, A., et al., *The dietary flavonoid quercetin activates BKCa currents in coronary arteries via production of H2O2. Role in vasodilatation.* Cardiovasc Res, 2007. **73**(2): p. 424-31.

141. Wilkins, M.R., *Pulmonary hypertension: the science behind the disease spectrum.* Eur Respir Rev, 2012. **21**(123): p. 19-26.

142. Cogolludo, A. and F. Perez-Vizcaino, *5-HT receptors and K(V) channel internalization.* Adv Exp Med Biol, 2010. **661**: p. 391-401.

143. Remillard, C.V., et al., *Function of Kv1.5 channels and genetic variations of KCNA5 in patients with idiopathic pulmonary arterial hypertension.* Am J Physiol Cell Physiol, 2007. **292**(5): p. C1837-53.

144. Yuan, J.X., et al., *Dysfunctional voltage-gated K+ channels in pulmonary artery smooth muscle cells of patients with primary pulmonary hypertension.* Circulation, 1998. **98**(14): p. 1400-6.

145. Firth, A.L., et al., *Hypoxia selectively inhibits KCNA5 channels in pulmonary artery smooth muscle cells.* Ann N Y Acad Sci, 2009. **1177**: p. 101-11.

146. Clapp, L.H. and R. Gurung, *The mechanistic basis of prostacyclin and its stable analogues in pulmonary arterial hypertension: Role of membrane versus nuclear receptors.* Prostaglandins Other Lipid Mediat, 2015. **120**: p. 56-71.

147. Midgley, A.C., et al., *Transforming growth factor-beta1 (TGF-beta1)-stimulated fibroblast to myofibroblast differentiation is mediated by hyaluronan (HA)-facilitated epidermal growth factor receptor (EGFR) and CD44 co-localization in lipid rafts.* J Biol Chem, 2013. **288**(21): p. 14824-38.

148. Scharenberg, M.A., et al., *TGF-beta-induced differentiation into myofibroblasts involves specific regulation of two MKL1 isoforms.* J Cell Sci, 2014. **127**(Pt 5): p. 1079-91.

149. Pugliese, S.C., et al., *The role of inflammation in hypoxic pulmonary hypertension: from cellular mechanisms to clinical phenotypes.* Am J Physiol Lung Cell Mol Physiol, 2015. **308**(3): p. L229-52.

150. Rabinovitch, M., et al., *Inflammation and immunity in the pathogenesis of pulmonary arterial hypertension.* Circ Res, 2014. **115**(1): p. 165-75.

151. Bertero, T., et al., *Matrix Remodeling Promotes Pulmonary Hypertension through Feedback Mechanoactivation of the YAP/TAZ-miR-130/301 Circuit.* Cell Rep, 2015. **13**(5): p. 1016-32.

152. Nogueira-Ferreira, R., R. Ferreira, and T. Henriques-Coelho, *Cellular interplay in pulmonary arterial hypertension: implications for new therapies.* Biochim Biophys Acta, 2014. **1843**(5): p. 885-93.

153. Lai, Y.C., et al., *Pulmonary arterial hypertension: the clinical syndrome.* Circ Res, 2014. **115**(1): p. 115-30.

154. Grunig, E., et al., *Enhanced hypoxic pulmonary vasoconstriction in families of adults or children with idiopathic pulmonary arterial hypertension.* Chest, 2005. **128**(6 Suppl): p. 630S-633S.

155. Crosswhite, P. and Z. Sun, *Nitric oxide, oxidative stress and inflammation in pulmonary arterial hypertension.* J Hypertens, 2010. **28**(2): p. 201-12.

156. Lakshminrusimha, S., et al., *The role of nitric oxide synthase-derived reactive oxygen species in the altered relaxation of pulmonary arteries from lambs with increased pulmonary blood flow.* Am J Physiol Heart Circ Physiol, 2007. **293**(3): p. H1491-7.

157. Malenfant, S., et al., *Signal transduction in the development of pulmonary arterial hypertension.* Pulm Circ, 2013. **3**(2): p. 278-93.

158. Antezana, A.M., et al., *Pulmonary hypertension in high-altitude chronic hypoxia: response to nifedipine.* Eur Respir J, 1998. **12**(5): p. 1181-5.

159. Compernolle, V., et al., *Loss of HIF-2alpha and inhibition of VEGF impair fetal lung maturation, whereas treatment with VEGF prevents fatal respiratory distress in premature mice.* Nat Med., 2002. **8**(7): p. 702-10. Epub 2002 Jun 10.

160. Yu, A.Y., et al., *Impaired physiological responses to chronic hypoxia in mice partially deficient for hypoxia-inducible factor 1alpha.* J Clin Invest, 1999. **103**(5): p. 691-6.

161. Brusselmans, K., et al., *Heterozygous deficiency of hypoxia-inducible factor-2alpha protects mice against pulmonary hypertension and right ventricular dysfunction during prolonged hypoxia.* J Clin Invest, 2003. **111**(10): p. 1519-27.

162. Tan, Q., et al., *Erythrocytosis and pulmonary hypertension in a mouse model of human HIF2A gain of function mutation.* J Biol Chem, 2013. **288**(24): p. 17134-44.

163. Shan, F., J. Li, and Q.Y. Huang, *HIF-1 alpha-induced up-regulation of miR-9 contributes to phenotypic modulation in pulmonary artery smooth muscle cells during hypoxia.* J Cell Physiol, 2014. **229**(10): p. 1511-20.

164. Gale, D.P., et al., *Autosomal dominant erythrocytosis and pulmonary arterial hypertension associated with an activating HIF2 alpha mutation.* Blood, 2008. **112**(3): p. 919-21.

165. Hickey, M.M., et al., *The von Hippel-Lindau Chuvash mutation promotes pulmonary hypertension and fibrosis in mice.* J Clin Invest, 2010. **120**(3): p. 827-39.

166. Lawler, J., et al., *Thrombospondin-1 is required for normal murine pulmonary homeostasis and its absence causes pneumonia.* J Clin Invest, 1998. **101**(5): p. 982-92.

167. Chen, Y., et al., *A TSP-1 functional fragment inhibits activation of latent transforming growth factor-beta1 derived from rat alveolar macrophage after bleomycin treatment.* Exp Toxicol Pathol, 2009. **61**(1): p. 67-73.

168. Phelan, M.W., et al., *Hypoxia increases thrombospondin-1 transcript and protein in cultured endothelial cells.* J Lab Clin Med, 1998. **132**(6): p. 519-29.

169. Bauer, P.M., et al., *Activated CD47 promotes pulmonary arterial hypertension through targeting caveolin-1.* Cardiovasc Res, 2012. **93**(4): p. 682-93.

170. Isenberg, J.S., et al., *Thrombospondin-1 limits ischemic tissue survival by inhibiting nitric oxide-mediated vascular smooth muscle relaxation.* Blood, 2007. **109**(5): p. 1945-52.

171. Isenberg, J.S., et al., *Thrombospondin-1 and CD47 regulate blood pressure and cardiac responses to vasoactive stress.* Matrix Biol, 2009. **28**(2): p. 110-9.

172. Kaiser, R., et al., *The role of circulating thrombospondin-1 in patients with precapillary pulmonary hypertension.* Respir Res, 2016. **17**(1): p. 96.

173. Adams, J.C. and J. Lawler, *The thrombospondins.* Cold Spring Harb Perspect Biol, 2011. **3**(10): p. a009712.

174. Resovi, A., et al., *Current understanding of the thrombospondin-1 interactome.* Matrix Biol, 2014. **37**: p. 83-91.

175. Adams, J.C. and J. Lawler, *The thrombospondins.* Int J Biochem Cell Biol., 2004. **36**(6): p. 961-8.

176. Adams, J.C., *Thrombospondins: multifunctional regulators of cell interactions.* Annu Rev Cell Dev Biol., 2001. **17**: p. 25-51.

177. Baenziger, N.L., G.N. Brodie, and P.W. Majerus, *A thrombin-sensitive protein of human platelet membranes.* Proc Natl Acad Sci U S A, 1971. **68**(1): p. 240-3.

178. Baenziger, N.L., G.N. Brodie, and P.W. Majerus, *Isolation and properties of a thrombin-sensitive protein of human platelets.* J Biol Chem, 1972. **247**(9): p. 2723-31.

179. Poczatek, M.H., et al., *Glucose stimulation of transforming growth factor-beta bioactivity in mesangial cells is mediated by thrombospondin-1.* Am J Pathol, 2000. **157**(4): p. 1353-63.

180. Sweetwyne, M.T. and J.E. Murphy-Ullrich, *Thrombospondin1 in tissue repair and fibrosis: TGF-beta-dependent and independent mechanisms.* Matrix Biol, 2012. **31**(3): p. 178-86.

181. Daniel, C., et al., *Thrombospondin-1 is an endogenous activator of TGF-beta in experimental diabetic nephropathy in vivo.* Diabetes, 2007. **56**(12): p. 2982-9.

182. Good, D.J., et al., *A tumor suppressor-dependent inhibitor of angiogenesis is immunologically and functionally indistinguishable from a fragment of thrombospondin.* Proc Natl Acad Sci U S A, 1990. **87**(17): p. 6624-8.

183. Jimenez, B., et al., *Signals leading to apoptosis-dependent inhibition of neovascularization by thrombospondin-1.* Nat Med, 2000. **6**(1): p. 41-8.

184. Crawford, S.E., et al., *Thrombospondin-1 is a major activator of TGF-beta1 in vivo.* Cell, 1998. **93**(7): p. 1159-70.

185. Isenberg, J.S., et al., *Blocking thrombospondin-1/CD47 signaling alleviates deleterious effects of aging on tissue responses to ischemia.* Arterioscler Thromb Vasc Biol, 2007. **27**(12): p. 2582-8.

186. Stenina, O.I., et al., *Increased expression of thrombospondin-1 in vessel wall of diabetic Zucker rat.* Circulation, 2003. **107**(25): p. 3209-15.

187. Roth, J.J., et al., *Thrombospondin-1 is elevated with both intimal hyperplasia and hypercholesterolemia.* J Surg Res, 1998. **74**(1): p. 11-6.

188. Yamaguchi, M., et al., *Reduced expression of thrombospondin-1 correlates with a poor prognosis in patients with non-small cell lung cancer.* Lung Cancer, 2002. **36**(2): p. 143-50.

189. Lee, Y.J., et al., *Variable inhibition of thrombospondin 1 against liver and lung metastases through differential activation of metalloproteinase ADAMTS1.* Cancer Res, 2010. **70**(3): p. 948-56.

190. Ochoa, C.D., et al., *Thrombospondin-1 null mice are resistant to hypoxia-induced pulmonary hypertension.* J Cardiothorac Surg, 2010. **5**: p. 32.

191. Carmeliet, P., et al., *Role of HIF-1alpha in hypoxia-mediated apoptosis, cell proliferation and tumour angiogenesis.* Nature., 1998. **394**(6692): p. 485-90.

192. Scortegagna, M., et al., *Multiple organ pathology, metabolic abnormalities and impaired homeostasis of reactive oxygen species in Epas1-/- mice.* Nat Genet., 2003. **35**(4): p. 331-40. Epub 2003 Nov 9.

193. Kondo, K., et al., *Inhibition of HIF2alpha is sufficient to suppress pVHL-defective tumor growth.* PLoS Biol, 2003. **1**(3): p. E83.

194. Raval, R.R., et al., *Contrasting properties of hypoxia-inducible factor 1 (HIF-1) and HIF-2 in von Hippel-Lindau-associated renal cell carcinoma.* Mol Cell Biol, 2005. **25**(13): p. 5675-86.

195. Shen, C., et al., *Genetic and functional studies implicate HIF1alpha as a 14q kidney cancer suppressor gene.* Cancer Discov, 2011. **1**(3): p. 222-35.

196. Gordan, J.D., et al., *HIF-2alpha promotes hypoxic cell proliferation by enhancing c-myc transcriptional activity.* Cancer Cell, 2007. **11**(4): p. 335-47.

197. Raval, R.R., et al., *Contrasting properties of hypoxia-inducible factor 1 (HIF-1) and HIF-2 in von Hippel-Lindau-associated renal cell carcinoma.* Mol Cell Biol., 2005. **25**(13): p. 5675-86.

198. Kabaria, R., Z. Klaassen, and M.K. Terris, *Renal cell carcinoma: links and risks.* Int J Nephrol Renovasc Dis, 2016. **9**: p. 45-52.

199. Garcia, J.A. and B.I. Rini, *Recent progress in the management of advanced renal cell carcinoma.* CA Cancer J Clin, 2007. **57**(2): p. 112-25.

200. Hartmann, J.T. and C. Bokemeyer, *Chemotherapy for renal cell carcinoma.* Anticancer Res, 1999. **19**(2C): p. 1541-3.

201. Blanco, A.I., B.S. Teh, and R.J. Amato, *Role of radiation therapy in the management of renal cell cancer.* Cancers (Basel), 2011. **3**(4): p. 4010-23.

202. Linehan, W.M., M.I. Lerman, and B. Zbar, *Identification of the von Hippel-Lindau (VHL) gene. Its role in renal cancer.* JAMA, 1995. **273**(7): p. 564-70.

203. Kaelin, W.G., Jr., *Molecular basis of the VHL hereditary cancer syndrome.* Nat Rev Cancer, 2002. **2**(9): p. 673-82.

204. Pritchett, T.L., et al., *Conditional inactivation of the mouse von Hippel-Lindau tumor suppressor gene results in wide-spread hyperplastic, inflammatory and fibrotic lesions in the kidney.* Oncogene, 2015. **34**(20): p. 2631-9.

205. Gebhard, R.L., et al., *Abnormal cholesterol metabolism in renal clear cell carcinoma.* J Lipid Res, 1987. **28**(10): p. 1177-84.

206. Clark, P.E., *The role of VHL in clear-cell renal cell carcinoma and its relation to targeted therapy.* Kidney Int, 2009. **76**(9): p. 939-45.

207. Calzada, M.J., *Von Hippel-Lindau syndrome: molecular mechanisms of the disease.* Clin Transl Oncol, 2010. **12**(3): p. 160-5.

208. Kurban, G., et al., *Characterization of a von Hippel Lindau pathway involved in extracellular matrix remodeling, cell invasion, and angiogenesis.* Cancer Res., 2006. **66**(3): p. 1313-9.

209. Shioi, K., et al., *Vascular cell adhesion molecule 1 predicts cancer-free survival in clear cell renal carcinoma patients.* Clin Cancer Res, 2006. **12**(24): p. 7339-46.

210. Vasselli, J.R., et al., *Predicting survival in patients with metastatic kidney cancer by gene-expression profiling in the primary tumor.* Proc Natl Acad Sci U S A, 2003. **100**(12): p. 6958-63.

211. Yao, M., et al., *A three-gene expression signature model to predict clinical outcome of clear cell renal carcinoma.* Int J Cancer, 2008. **123**(5): p. 1126-32.

212. Wai Wong, C., D.E. Dye, and D.R. Coombe, *The role of immunoglobulin superfamily cell adhesion molecules in cancer metastasis.* Int J Cell Biol, 2012. **2012**: p. 340296.

213. Osborn, L., et al., *Direct expression cloning of vascular cell adhesion molecule 1, a cytokine-induced endothelial protein that binds to lymphocytes.* Cell, 1989. **59**(6): p. 1203-11.

214. Carlos, T.M., et al., *Vascular cell adhesion molecule-1 mediates lymphocyte adherence to cytokine-activated cultured human endothelial cells.* Blood, 1990. **76**(5): p. 965-70.

215. Wittchen, E.S., *Endothelial signaling in paracellular and transcellular leukocyte transmigration.* Front Biosci (Landmark Ed), 2009. **14**: p. 2522-45.

216. Ley, K., et al., *Getting to the site of inflammation: the leukocyte adhesion cascade updated.* Nat Rev Immunol, 2007. **7**(9): p. 678-89.

217. Freedman, A.S., et al., *Adhesion of human B cells to germinal centers in vitro involves VLA-4 and INCAM-110.* Science, 1990. **249**(4972): p. 1030-3.

218. Gonzalez-Amaro, R. and F. Sanchez-Madrid, *Cell adhesion molecules: selectins and integrins.* Crit Rev Immunol, 1999. **19**(5-6): p. 389-429.

219. Elices, M.J., et al., *VCAM-1 on activated endothelium interacts with the leukocyte integrin VLA-4 at a site distinct from the VLA-4/fibronectin binding site.* Cell, 1990. **60**(4): p. 577-84.

220. Hemler, M.E., *Tetraspanin functions and associated microdomains.* Nat Rev Mol Cell Biol, 2005. **6**(10): p. 801-11.

221. Barreiro, O., et al., *Endothelial tetraspanin microdomains regulate leukocyte firm adhesion during extravasation.* Blood, 2005. **105**(7): p. 2852-61.

222. Cook-Mills, J.M., M.E. Marchese, and H. Abdala-Valencia, *Vascular cell adhesion molecule-1 expression and signaling during disease: regulation by reactive oxygen species and antioxidants.* Antioxid Redox Signal, 2011. **15**(6): p. 1607-38.

223. Osborn, L., C. Vassallo, and C.D. Benjamin, *Activated endothelium binds lymphocytes through a novel binding site in the alternately spliced domain of vascular cell adhesion molecule-1.* J Exp Med, 1992. **176**(1): p. 99-107.

224. Yamada, Y., et al., *Plasma concentrations of VCAM-1 and PAI-1: a predictive biomarker for post-operative recurrence in colorectal cancer.* Cancer Sci, 2010. **101**(8): p. 1886-90.

225. Barreiro, O., et al., *Dynamic interaction of VCAM-1 and ICAM-1 with moesin and ezrin in a novel endothelial docking structure for adherent leukocytes.* J Cell Biol, 2002. **157**(7): p. 1233-45.

226. Rice, G.E., et al., *Vascular and nonvascular expression of INCAM-110. A target for mononuclear leukocyte adhesion in normal and inflamed human tissues.* Am J Pathol, 1991. **138**(2): p. 385-93.

227. Stanley, A.C., et al., *VCAM-1 and VLA-4 modulate dendritic cell IL-12p40 production in experimental visceral leishmaniasis.* PLoS Pathog, 2008. **4**(9): p. e1000158.

228. Juneja, H.S., et al., *Vascular cell adhesion molecule-1 and VLA-4 are obligatory adhesion proteins in the heterotypic adherence between human leukemia/lymphoma cells and marrow stromal cells.* Exp Hematol, 1993. **21**(3): p. 444-50.

229. Langley, R.R., et al., *Endothelial expression of vascular cell adhesion molecule-1 correlates with metastatic pattern in spontaneous melanoma.* Microcirculation, 2001. **8**(5): p. 335-45.

230. Gil-Bernabe, A.M., et al., *Recruitment of monocytes/macrophages by tissue factor-mediated coagulation is essential for metastatic cell survival and premetastatic niche establishment in mice.* Blood, 2012. **119**(13): p. 3164-75.

231. Qian, B.Z. and J.W. Pollard, *Macrophage diversity enhances tumor progression and metastasis.* Cell, 2010. **141**(1): p. 39-51.

232. Griffioen, A.W., et al., *Tumor angiogenesis is accompanied by a decreased inflammatory response of tumor-associated endothelium.* Blood, 1996. **88**(2): p. 667-73.

233. Griffioen, A.W., S.C. Tromp, and H.F. Hillen, *Angiogenesis modulates the tumour immune response.* Int J Exp Pathol, 1998. **79**(6): p. 363-8.

234. Seron, D., J.S. Cameron, and D.O. Haskard, *Expression of VCAM-1 in the normal and diseased kidney.* Nephrol Dial Transplant, 1991. **6**(12): p. 917-22.

235. Mackay, F., et al., *Tumor necrosis factor alpha (TNF-alpha)-induced cell adhesion to human endothelial cells is under dominant control of one TNF receptor type, TNF-R55.* J Exp Med, 1993. **177**(5): p. 1277-86.

236. Lin, C.C., et al., *Tumor necrosis factor-alpha induces VCAM-1-mediated inflammation via c-Src-dependent transactivation of EGF receptors in human cardiac fibroblasts.* J Biomed Sci, 2015. **22**: p. 53.

237. Dempsey, P.W., et al., *The signaling adaptors and pathways activated by TNF superfamily.* Cytokine Growth Factor Rev, 2003. **14**(3-4): p. 193-209.

238. Krappmann, D. and M. Vincendeau, *Mechanisms of NF-kappaB deregulation in lymphoid malignancies.* Semin Cancer Biol, 2016. **39**: p. 3-14.

239. Cildir, G., K.C. Low, and V. Tergaonkar, *Noncanonical NF-kappaB Signaling in Health and Disease.* Trends Mol Med, 2016. **22**(5): p. 414-29.

240. Weniger, M.A. and R. Kuppers, *NF-kappaB deregulation in Hodgkin lymphoma.* Semin Cancer Biol, 2016. **39**: p. 32-9.

241. Rosebeck, S., et al., *API2-MALT1 oncoprotein promotes lymphomagenesis via unique program of substrate ubiquitination and proteolysis.* World J Biol Chem, 2016. **7**(1): p. 128-37.

242. Liu, H., et al., *Resistance of t(11;18) positive gastric mucosa-associated lymphoid tissue lymphoma to Helicobacter pylori eradication therapy.* Lancet, 2001. **357**(9249): p. 39-40.

243. Zhou, H., M.Q. Du, and V.M. Dixit, *Constitutive NF-kappaB activation by the t(11;18)(q21;q21) product in MALT lymphoma is linked to deregulated ubiquitin ligase activity.* Cancer Cell, 2005. **7**(5): p. 425-31.

244. Kim, J.Y., et al., *TNFalpha induced noncanonical NF-kappaB activation is attenuated by RIP1 through stabilization of TRAF2.* J Cell Sci, 2011. **124**(Pt 4): p. 647-56.

245. Qiu, J., et al., *TNFalpha up-regulates COX-2 in chronic progressive nephropathy through nuclear accumulation of RelB and NF-kappaB2.* Arch Physiol Biochem, 2016. **122**(2): p. 88-93.

246. Varfolomeev, E. and D. Vucic, *Intracellular regulation of TNF activity in health and disease.* Cytokine, 2016.

247. McDaniel, D.K., et al., *Emerging Roles for Noncanonical NF-kappaB Signaling in the Modulation of Inflammatory Bowel Disease Pathobiology.* Inflamm Bowel Dis, 2016. **22**(9): p. 2265-79.

248. Elorza, A., et al., *HIF2alpha acts as an mTORC1 activator through the amino acid carrier SLC7A5.* Mol Cell, 2012. **48**(5): p. 681-91.

249. Miro-Murillo, M., et al., *Acute Vhl gene inactivation induces cardiac HIF-dependent erythropoietin gene expression.* PLoS One, 2011. **6**(7): p. e22589.

250. Stickle, N.H., et al., *pVHL modification by NEDD8 is required for fibronectin matrix assembly and suppression of tumor development.* Mol Cell Biol, 2004. **24**(8): p. 3251-61.

251. Aragones, J., et al., *Evidence for the involvement of diacylglycerol kinase in the activation of hypoxia-inducible transcription factor 1 by low oxygen tension.* J Biol Chem, 2001. **276**(13): p. 10548-55.

252. Storkel, S., et al., *Classification of renal cell carcinoma: Workgroup No. 1. Union Internationale Contre le Cancer (UICC) and the American Joint Committee on Cancer (AJCC).* Cancer, 1997. **80**(5): p. 987-9.

253. Horzum, U., B. Ozdil, and D. Pesen-Okvur, *Step-by-step quantitative analysis of focal adhesions.* MethodsX, 2014: p. 56-59.

254. Sanchez-Madrid, F., et al., *VLA-3: a novel polypeptide association within the VLA molecular complex: cell distribution and biochemical characterization.* Eur J Immunol, 1986. **16**(11): p. 1343-9.

255. Yanez-Mo, M., et al., *Regulation of endothelial cell motility by complexes of tetraspan molecules CD81/TAPA-1 and CD151/PETA-3 with alpha3 beta1 integrin localized at endothelial lateral junctions.* J Cell Biol, 1998. **141**(3): p. 791-804.

256. Sanchez-Madrid, F., et al., *Three distinct antigens associated with human T-lymphocyte-mediated cytolysis: LFA-1, LFA-2, and LFA-3.* Proc Natl Acad Sci U S A, 1982. **79**(23): p. 7489-93.

257. Zheng, H. and L. Rinaman, *Simplified CLARITY for visualizing immunofluorescence labeling in the developing rat brain.* Brain Struct Funct, 2016. **221**(4): p. 2375-83.

258. Staudt, T., et al., *2,2'-thiodiethanol: a new water soluble mounting medium for high resolution optical microscopy.* Microsc Res Tech, 2007. **70**(1): p. 1-9.

259. Marxsen, J.H., et al., *Hypoxia-inducible factor-1 (HIF-1) promotes its degradation by induction of HIF-alpha-prolyl-4-hydroxylases.* Biochem J, 2004. **381**(Pt 3): p. 761-7.

260. Yao, M., D.D. Roberts, and J.S. Isenberg, *Thrombospondin-1 inhibition of vascular smooth muscle cell responses occurs via modulation of both cAMP and cGMP.* Pharmacol Res, 2011. **63**(1): p. 13-22.

261. Mumby, S.M., et al., *Regulation of thrombospondin secretion by cells in culture.* J Cell Physiol, 1984. **120**(3): p. 280-8.

262. Ortiz-Barahona, A., et al., *Genome-wide identification of hypoxia-inducible factor binding sites and target genes by a probabilistic model integrating transcription-profiling data and in silico binding site prediction.* Nucleic Acids Res, 2010. **38**(7): p. 2332-45.

263. Sartore, S., et al., *Contribution of adventitial fibroblasts to neointima formation and vascular remodeling: from innocent bystander to active participant.* Circ Res, 2001. **89**(12): p. 1111-21.

264. Stenmark, K.R., et al., *Hypoxia-induced pulmonary vascular remodeling: contribution of the adventitial fibroblasts.* Physiol Res, 2000. **49**(5): p. 503-17.

265. Chandrasekaran, L., et al., *Cell contact-dependent activation of alpha3beta1 integrin modulates endothelial cell responses to thrombospondin-1.* Mol Biol Cell., 2000. **11**(9): p. 2885-900.

266. Gahtan, V., et al., *Thrombospondin-1 induces activation of focal adhesion kinase in vascular smooth muscle cells.* J Vasc Surg, 1999. **29**(6): p. 1031-6.

267. Higuchi, M., et al., *Akt1 promotes focal adhesion disassembly and cell motility through phosphorylation of FAK in growth factor-stimulated cells.* J Cell Sci, 2013. **126**(Pt 3): p. 745-55.

268. Murphy-Ullrich, J.E., *The de-adhesive activity of matricellular proteins: is intermediate cell adhesion an adaptive state?* J Clin Invest, 2001. **107**(7): p. 785-90.

269. Orr, A.W., et al., *Thrombospondin induces RhoA inactivation through FAK-dependent signaling to stimulate focal adhesion disassembly.* J Biol Chem, 2004. **279**(47): p. 48983-92.

270. Goldblum, S.E., et al., *Thrombospondin-1 induces tyrosine phosphorylation of adherens junction proteins and regulates an endothelial paracellular pathway.* Mol Biol Cell, 1999. **10**(5): p. 1537-51.

271. Budhiraja, R., R.M. Tuder, and P.M. Hassoun, *Endothelial dysfunction in pulmonary hypertension.* Circulation, 2004. **109**(2): p. 159-65.

272. Short, M., et al., *Hypoxia induces differentiation of pulmonary artery adventitial fibroblasts into myofibroblasts.* Am J Physiol Cell Physiol, 2004. **286**(2): p. C416-25.

273. Hinz, B., et al., *Alpha-smooth muscle actin expression upregulates fibroblast contractile activity.* Mol Biol Cell, 2001. **12**(9): p. 2730-41.

274. Morrell, N.W., et al., *Cellular and molecular basis of pulmonary arterial hypertension.* J Am Coll Cardiol, 2009. **54**(1 Suppl): p. S20-31.

275. Daniel, C., et al., *Thrombospondin-1 is a major activator of TGF-beta in fibrotic renal disease in the rat in vivo.* Kidney Int, 2004. **65**(2): p. 459-68.

276. Nor, J.E., et al., *Activation of Latent TGF-beta1 by Thrombospondin-1 is a Major Component of Wound Repair.* Oral Biosci Med, 2005. **2**(2): p. 153-161.

277. Leach, R.M., et al., *Hypoxic vasoconstriction in rat pulmonary and mesenteric arteries.* Am J Physiol, 1994. **266**(3 Pt 1): p. L223-31.

278. Casey, D.P. and M.J. Joyner, *Compensatory vasodilatation during hypoxic exercise: mechanisms responsible for matching oxygen supply to demand.* J Physiol, 2012. **590**(Pt 24): p. 6321-6.

279. Naeije, R. and C. Dedobbeleer, *Pulmonary hypertension and the right ventricle in hypoxia.* Exp Physiol, 2013. **98**(8): p. 1247-56.

280. Bauer, E.M., et al., *Thrombospondin-1 supports blood pressure by limiting eNOS activation and endothelial-dependent vasorelaxation.* Cardiovasc Res, 2010. **88**(3): p. 471-81.

281. Isenberg, J.S., et al., *Gene silencing of CD47 and antibody ligation of thrombospondin-1 enhance ischemic tissue survival in a porcine model: implications for human disease.* Ann Surg, 2008. **247**(5): p. 860-8.

282. Park, W.S., et al., *Patho-, physiological roles of voltage-dependent K+ channels in pulmonary arterial smooth muscle cells.* J Smooth Muscle Res, 2010. **46**(2): p. 89-105.

283. Yang, B., et al., *Single-cell phenotyping within transparent intact tissue through whole-body clearing.* Cell, 2014. **158**(4): p. 945-58.

284. Epp, J.R., et al., *Optimization of CLARITY for Clearing Whole-Brain and Other Intact Organs(1,2,3).* eNeuro, 2015. **2**(3).

285. Chung, K., et al., *Structural and molecular interrogation of intact biological systems.* Nature, 2013. **497**(7449): p. 332-7.

286. Ohh, M., et al., *Synthetic peptides define critical contacts between elongin C, elongin B, and the von Hippel-Lindau protein.* J Clin Invest, 1999. **104**(11): p. 1583-91.

287. Hoffman, M.A., et al., *von Hippel-Lindau protein mutants linked to type 2C VHL disease preserve the ability to downregulate HIF.* Hum Mol Genet, 2001. **10**(10): p. 1019-27.

288. Iademarco, M.F., et al., *Characterization of the promoter for vascular cell adhesion molecule-1 (VCAM-1).* J Biol Chem, 1992. **267**(23): p. 16323-9.

289. Zerfaoui, M., et al., *Nuclear translocation of p65 NF-kappaB is sufficient for VCAM-1, but not ICAM-1, expression in TNF-stimulated smooth muscle cells: Differential requirement for PARP-1 expression and interaction.* Cell Signal, 2008. **20**(1): p. 186-94.

290. Taylor, C.T. and E.P. Cummins, *The role of NF-kappaB in hypoxia-induced gene expression.* Ann N Y Acad Sci, 2009. **1177**: p. 178-84.

291. Yamashita, T., et al., *The microenvironment for erythropoiesis is regulated by HIF-2alpha through VCAM-1 in endothelial cells.* Blood, 2008. **112**(4): p. 1482-92.

292. Setty, B.N. and M.J. Stuart, *Vascular cell adhesion molecule-1 is involved in mediating hypoxia-induced sickle red blood cell adherence to endothelium: potential role in sickle cell disease.* Blood, 1996. **88**(6): p. 2311-20.

293. Willam, C., et al., *Increases in oxygen tension stimulate expression of ICAM-1 and VCAM-1 on human endothelial cells.* Am J Physiol, 1999. **276**(6 Pt 2): p. H2044-52.

294. Fogler, W.E., et al., *NK cell infiltration into lung, liver, and subcutaneous B16 melanoma is mediated by VCAM-1/VLA-4 interaction.* J Immunol, 1996. **156**(12): p. 4707-14.

295. Yao, L., et al., *Reciprocal regulation of HIF-1alpha and 15-LO/15-HETE promotes anti-apoptosis process in pulmonary artery smooth muscle cells during hypoxia.* Prostaglandins Other Lipid Mediat, 2012. **99**(3-4): p. 96-106.

296. Smith, T.G., et al., *Mutation of von Hippel-Lindau tumour suppressor and human cardiopulmonary physiology.* PLoS Med, 2006. **3**(7): p. e290.

297. Formenti, F., et al., *Cardiopulmonary function in two human disorders of the hypoxia-inducible factor (HIF) pathway: von Hippel-Lindau disease and HIF-2alpha gain-of-function mutation.* FASEB J, 2011. **25**(6): p. 2001-11.

298. Rankin, E.B., et al., *Hypoxia-inducible factor-2 (HIF-2) regulates hepatic erythropoietin in vivo.* J Clin Invest, 2007. **117**(4): p. 1068-77.

299. Farha, S., et al., *Hypoxia-inducible factors in human pulmonary arterial hypertension: a link to the intrinsic myeloid abnormalities.* Blood, 2011. **117**(13): p. 3485-93.

300. Fijalkowska, I., et al., *Hypoxia inducible-factor1alpha regulates the metabolic shift of pulmonary hypertensive endothelial cells.* Am J Pathol, 2010. **176**(3): p. 1130-8.

301. Raghavan, A., et al., *Hypoxia-induced pulmonary arterial smooth muscle cell proliferation is controlled by forkhead box M1.* Am J Respir Cell Mol Biol, 2012. **46**(4): p. 431-6.

302. Firth, A.L., et al., *Upregulation of Oct-4 isoforms in pulmonary artery smooth muscle cells from patients with pulmonary arterial hypertension.* Am J Physiol Lung Cell Mol Physiol, 2010. **298**(4): p. L548-57.

303. Barlassina, C., et al., *Genetics of essential hypertension: from families to genes.* J Am Soc Nephrol, 2002. **13 Suppl 3**: p. S155-64.

304. Isenberg, J.S., et al., *Endogenous thrombospondin-1 is not necessary for proliferation but is permissive for vascular smooth muscle cell responses to platelet-derived growth factor.* Matrix Biol., 2005. **24**(2): p. 110-23.

305. Bonnefoy, A., et al., *Thrombospondin-1 controls vascular platelet recruitment and thrombus adherence in mice by protecting (sub)endothelial VWF from cleavage by ADAMTS13.* Blood, 2006. **107**(3): p. 955-64.

306. Isenberg, J.S., et al., *Thrombospondin-1 stimulates platelet aggregation by blocking the antithrombotic activity of nitric oxide/cGMP signaling.* Blood, 2008. **111**(2): p. 613-23.

307. Eul, B., et al., *Impact of HIF-1alpha and HIF-2alpha on proliferation and migration of human pulmonary artery fibroblasts in hypoxia.* FASEB J, 2006. **20**(1): p. 163-5.

308. Platoshyn, O., et al., *Chronic hypoxia decreases K(V) channel expression and function in pulmonary artery myocytes.* Am J Physiol Lung Cell Mol Physiol, 2001. **280**(4): p. L801-12.

309. Wang, J., et al., *Hypoxia inhibits gene expression of voltage-gated K+ channel alpha subunits in pulmonary artery smooth muscle cells.* J Clin Invest, 1997. **100**(9): p. 2347-53.

310. Wang, J., et al., *Chronic hypoxia inhibits Kv channel gene expression in rat distal pulmonary artery.* Am J Physiol Lung Cell Mol Physiol, 2005. **288**(6): p. L1049-58.

311. Hong, Z., et al., *Subacute hypoxia decreases voltage-activated potassium channel expression and function in pulmonary artery myocytes.* Am J Respir Cell Mol Biol, 2004. **31**(3): p. 337-43.

312. Pozeg, Z.I., et al., *In vivo gene transfer of the O2-sensitive potassium channel Kv1.5 reduces pulmonary hypertension and restores hypoxic pulmonary vasoconstriction in chronically hypoxic rats.* Circulation, 2003. **107**(15): p. 2037-44.

313. Reeve, H.L., et al., *Alterations in a redox oxygen sensing mechanism in chronic hypoxia.* J Appl Physiol (1985), 2001. **90**(6): p. 2249-56.

314. Rainbow, R.D., et al., *Endothelin-I and angiotensin II inhibit arterial voltage-gated K+ channels through different protein kinase C isoenzymes.* Cardiovasc Res, 2009. **83**(3): p. 493-500.

315. Whitman, E.M., et al., *Endothelin-1 mediates hypoxia-induced inhibition of voltage-gated K+ channel expression in pulmonary arterial myocytes.* Am J Physiol Lung Cell Mol Physiol, 2008. **294**(2): p. L309-18.

316. Rogers, N.M., et al., *TSP1-CD47 signaling is upregulated in clinical pulmonary hypertension and contributes to pulmonary arterial vasculopathy and dysfunction.* Cardiovasc Res, 2017. **113**(1): p. 15-29.

317. Guzy, R.D. and P.T. Schumacker, *Oxygen sensing by mitochondria at complex III: the paradox of increased reactive oxygen species during hypoxia.* Exp Physiol, 2006. **91**(5): p. 807-19.

318. Csanyi, G., et al., *Thrombospondin-1 regulates blood flow via CD47 receptor-mediated activation of NADPH oxidase 1.* Arterioscler Thromb Vasc Biol, 2012. **32**(12): p. 2966-73.

319. Yao, M., et al., *Thrombospondin-1 activation of signal-regulatory protein-alpha stimulates reactive oxygen species production and promotes renal ischemia reperfusion injury.* J Am Soc Nephrol, 2014. **25**(6): p. 1171-86.

320. Shimoda, L.A. and W.M. Kuebler, *'Hypoxio-spondin': thrombospondin and its emerging role in pulmonary hypertension.* Cardiovasc Res, 2016. **109**(1): p. 1-3.

321. Agarwal, A.R., J. Mih, and S.C. George, *Expression of matrix proteins in an in vitro model of airway remodeling in asthma.* Allergy Asthma Proc, 2003. **24**(1): p. 35-42.

322. Ide, M., et al., *High serum levels of thrombospondin-1 in patients with idiopathic interstitial pneumonia.* Respir Med, 2008. **102**(11): p. 1625-30.

323. Smadja, D.M., et al., *Increase in both angiogenic and angiostatic mediators in patients with idiopathic pulmonary fibrosis.* Pathol Biol (Paris), 2014.

324. Freishtat, R.J., et al., *Delineation of a gene network underlying the pulmonary response to oxidative stress in asthma.* J Investig Med, 2009. **57**(7): p. 756-64.

325. Wang, I.M., et al., *Gene expression profiling in patients with chronic obstructive pulmonary disease and lung cancer.* Am J Respir Crit Care Med, 2008. **177**(4): p. 402-11.

326. Staller, P., et al., *Chemokine receptor CXCR4 downregulated by von Hippel-Lindau tumour suppressor pVHL.* Nature, 2003. **425**(6955): p. 307-11.

327. Vanharanta, S., et al., *Epigenetic expansion of VHL-HIF signal output drives multiorgan metastasis in renal cancer.* Nat Med, 2013. **19**(1): p. 50-6.

328. Caldwell, M.C., et al., *Serial analysis of gene expression in renal carcinoma cells reveals VHL-dependent sensitivity to TNFalpha cytotoxicity.* Oncogene, 2002. **21**(6): p. 929-36.

329. Dejardin, E., et al., *The lymphotoxin-beta receptor induces different patterns of gene expression via two NF-kappaB pathways.* Immunity, 2002. **17**(4): p. 525-35.

330. Senftleben, U., et al., *Activation by IKKalpha of a second, evolutionary conserved, NF-kappa B signaling pathway.* Science, 2001. **293**(5534): p. 1495-9.

331. Xiao, G., E.W. Harhaj, and S.C. Sun, *NF-kappaB-inducing kinase regulates the processing of NF-kappaB2 p100.* Mol Cell, 2001. **7**(2): p. 401-9.

332. Ling, L., Z. Cao, and D.V. Goeddel, *NF-kappaB-inducing kinase activates IKK-alpha by phosphorylation of Ser-176.* Proc Natl Acad Sci U S A, 1998. **95**(7): p. 3792-7.

333. Dejardin, E., *The alternative NF-kappaB pathway from biochemistry to biology: pitfalls and promises for future drug development.* Biochem Pharmacol, 2006. **72**(9): p. 1161-79.

334. Zhu, M. and Y. Fu, *The complicated role of NF-kappaB in T-cell selection.* Cell Mol Immunol, 2010. **7**(2): p. 89-93.

335. Novack, D.V., *Role of NF-kappaB in the skeleton.* Cell Res, 2011. **21**(1): p. 169-82.

336. Chen, Q., X.H. Zhang, and J. Massague, *Macrophage binding to receptor VCAM-1 transmits survival signals in breast cancer cells that invade the lungs.* Cancer Cell, 2011. **20**(4): p. 538-49.

337. Lu, X., et al., *VCAM-1 promotes osteolytic expansion of indolent bone micrometastasis of breast cancer by engaging alpha4beta1-positive osteoclast progenitors.* Cancer Cell, 2011. **20**(6): p. 701-14.

ANNEXES

ANNEXES

1.1 Supplementary information

Supplementary Movie 1. From figure 29 (SMA staining in clarified mouse lungs). Video depict a 400 µm z-stack 3D reconstruction of adult (3 months) WT mouse lungs clarified by passive CLARITY and stained for α-SMA with Alexa 488 (green). Big PAs and main bronchus can be appreciated. Scale bar indicates the image size. Movie was mounted at 12 fps.

Supplementary Movie 2. From figure 30 (TSP1 staining in clarified mouse lungs under Hp/Sugen treatment). Visualization of TSP1 in adult (3 month) mouse lung of male WT exposed to hypoxia (10%) plus sugen 5416 (Hp+Su) for 3 weeks. Mice lung were clarified by passive CLARITY and stained with TSP1 with Alexa 488 (fire). Video depict a 400 µm z-stack 3D reconstruction. Scale bars indicate image size in each frame. Movie was mounted at 12 fps

Supplementary Movie 3. Visualization of SMA in adult (3 month) mouse lung of male WT exposed to hypoxia (10%) plus sugen 5416 (Hp+Su) Sor 3 weeks. Video depict a 400 µm z-stack 3D reconstruction of adult (3 months). Lungs were clarified by passive CLARITY and stained for α-SMA with Alexa 488 (green). Big PAs and main bronchus can be appreciated. Scale bar indicates the image size. Movie was mounted at 12 fps.

Supplementary Movie 4. CNN1 staining in clarified mouse lungs. Video depict a 400 µm z-stack 3D reconstruction of adult (3 months) WT mouse lungs clarified by passive CLARITY and stained for CNN.1 with Alexa 488 (green). Main bronchus can be appreciated. Scale bar indicates the image size. Movie was mounted at 12 fps.

1.2 Publications related to this thesis

Labrousse-Arias, D., R. Castillo-Gonzalez, N. M. Rogers, M. Torres-Capelli, B. Barreira, J. Aragones, A. Cogolludo, J. S. Isenberg and M. J. Calzada (2016). "HIF2alpha-Mediated Induction of Pulmonary Thrombospondin-1 Contributes to Hypoxia-Driven Vascular Remodeling and Vasoconstriction." Cardiovasc Res.

David Labrousse-Arias*, Emma Martínez-Alonso*, María Corral-Escariz, Raquel Bienes-Martínez, Jaime Berridy, Leticia Serrano-Oviedo, Elisa Conde, Laura García Bermejo, José Miguel Giménez-Bachs, Antonio S. Salinas-Sánchez, Ricardo Sánchez-Prieto, Masahiro Yao, Marina Lasa and María J. Calzada (2017). "VHL promotes immune response against renal cell carcinoma via NF-κB-dependent regulation of VCAM-1". Journal of Cell Biology (accepted January 2017). DOI: 10.1083

1.3 Other publications

Rogers, N. M., M. Sharifi-Sanjani, M. Yao, K. Ghimire, R. Bienes-Martinez, S. M. Mutchler, H. E. Knupp, J. Baust, E. M. Novelli, M. Ross, C. St Croix, J. C. Kutten, C. A. Czajka, J. C. Sembrat, M. Rojas, **D. Labrousse-Arias**, T. N. Bachman, R. R. Vanderpool, B. S. Zuckerbraun, H. C. Champion, A. L. Mora, A. C. Straub, R. A. Bilonick, M. J. Calzada and J. S. Isenberg (2017). "TSP1-CD47 signaling is upregulated in clinical pulmonary hypertension and contributes to pulmonary arterial vasculopathy and dysfunction." Cardiovasc Res **113**(1): 15-29.